9-24-2018

Comparative Analysis of the Machinability of Various Titanium Alloys

Tanny Tran
University of Windsor

Follow this and additional works at: https://scholar.uwindsor.ca/etd

Comparative Analysis of the Machinability of Various Titanium Alloys

By

Tanny Tran

A Thesis

Submitted to the Faculty of Graduate Studies through the

Department of Mechanical, Automotive and Materials Engineering in

Partial Fulfillment of the Requirements for the

Degree of Master of Applied Science

at the University of Windsor

Windsor, Ontario, Canada

2018

Comparative Analysis of the Machinability of Various Titanium Alloys

By

Tanny Tran

APPROVED BY:

_____

J. Ahamed

Department of Mechanical, Automotive and Materials Engineering

_____

H. Hu

Department of Mechanical, Automotive and Materials Engineering

_____

A.R. Riahi, Advisor

Department of Mechanical, Automotive and Materials Engineering

September 17, 2018

Declaration of Originality

I hereby certify that I am the sole author of this thesis and that no part of this thesis has been published or submitted for publication.

I certify that, to the best of my knowledge, my thesis does not infringe upon anyone's copyright nor violate any proprietary rights and that any ideas, techniques, quotations, or any other material from the work of other people included in my thesis, published or otherwise, are fully acknowledged in accordance with the standard referencing practices. Furthermore, to the extent that I have included copyrighted material that surpasses the bounds of fair dealing within the meaning of the Canada Copyright Act, I certify that I have obtained a written permission from the copyright owner(s) to include such material(s) in my thesis and have included copies of such copyright clearances to my appendix.

I declare that this is a true copy of my thesis, including any final revisions, as approved by my thesis committee and the Graduate Studies office, and that this thesis has not been submitted for a higher degree to any other University or Institution.

Abstract

Titanium alloys have a good strength to weight ratio, amazing corrosion resistance. These alloys are mostly used in the aerospace, biomedical and automotive industries. However, titanium alloys are difficult to machine since they are chemically reactive and have low thermal conductivity. Drilling is an important machining process with titanium alloys since it is used is most titanium applications. The machinability of titanium alloys varies depending on the method the titanium alloy was manufactured. There is a lack of knowledge for drilling additive manufactured titanium and powdered metallurgy titanium. This study will investigate and compare the wear of various drill bits with various manufactured titanium alloys using a constant feed rate and cutting speed. The titanium alloys used include the reference alloy of Ti-6Al-4V, powder metallurgy titanium and additive manufactured titanium. The drill bits used include high speed steel drill bits, three flute carbide drill bits and coated carbide drill bits. Additionally, the torque is recorded to analyze the drilling performance for each experiment. The drill bit tips, the drilled holes, and the drilled in the workpiece, and the drilled chips were studied microscopically to determine the wear rate of the drill bits, the material transfer, the quality of the drilled surfaces, and the ease of chip dejection. The additive manufactured titanium showed promising material properties but the machinability aspect showed that the wear was poor compared to the reference Ti-6Al-4V alloy.

Dedication

This study is wholeheartedly dedicated to my beloved parents, Hue Tran and Thanh Nguyen, who have been my source of inspiration and continually provide moral, spiritual, emotional, and financial support.

Acknowledgements

I would like to thank my advisor Dr. A. R. Riahi for his supervision, guidance and assistance throughout the entirety of this project. Additionally, Dr. O.A Gali for beneficial feedback and assistance through the evaluation process.

I would also like to thank my committee members Dr. A. Jalal and Dr. H. Hu for attending my presentations and reviewing my thesis. Additionally, their input directly benefitted my work during my graduate studies.

Additionally, I would like to thank my research group for keeping me company during my endeavors and sharing their insight.

Table of Contents

List of Tables

List of Figures

List of Abbreviations

AM	Additive manufacturing
ASTM	American Society for Testing Materials
BUE	Built up Edge
BUL	Built up Layer
EDS	Energy Dispersive X-ray Spectroscopy
HSS	High speed steel
PM	Powder Metallurgy
SEM	Scanning electron microscope
XRD	X-ray diffraction

Chapter 1: Introduction

1.1 Background and Motivation

Titanium alloys are used mostly in the aerospace industry due to their high temperature properties, corrosion resistance, creep and oxidation resistance, low modulus of elasticity, high fracture toughness, and low density [1]. The density of steel ranges from 7.75 g/cm^3 – 8.05 g/cm^3 where as titanium's density is 4.5 g/cm^3. The strength of commercially pure titanium is equivalent to common, low grade steel alloys. Titanium has a high strength to low weight ratio compared to steel making it a desirable material. Ti-6Al-4V is most commonly used due to its mechanical properties which can be easily obtained by heat treatment processes. Titanium alloys are used in blades and discs for jet engine turbines and compressors, along with structural aircraft components and landing gear. Also, these alloys can be used in surgical implants. The issue with titanium and titanium alloys is the difficulty to machine due to its thermal and chemical properties. When machining titanium alloys, the heat generated does not dissipate into the workpiece rather the heat is absorbed by the tool tip which results in premature failure and a reduced tool life. Furthermore, the chemical property of titanium is quite reactive with the tool tip at high temperatures from 720 – 1060°C, which are easily achieved at the tool tip during drilling [2]. The chemical process that occurs during machining is diffusion between the tool tip and the workpiece. To overcome diffusion possible solutions may be to change the tool or adding a coolant which can reduce the friction and improve the tool life [3].

Powder Metallurgy (PM) is the processing of fine particles to form a solid in a near finish structure with minimal machining required. The first attempt of PM was introduced

1

by William Kroll in the early 1940s, who used a cold compaction and sintering technique

[4]. The products contained residual magnesium chloride salts which reduced the

mechanical properties. A couple decades later, more production techniques have been

formed such as hot isostatic pressing and blended elemental. The primary advantage of PM

is that production requires less processing steps, many shapes can be formed, and the need

to use metal removal processes are greatly reduced. However, the material properties of

PM titanium have not met the requirements of the aerospace industry due to the porosities.

The porosities have a huge impact on the material properties which include tensile strength,

yield strength, and fatigue. The material properties of PM titanium manufactured through

various PM methods are compared to wrought Ti-6Al-4V in Table 1 [5]. The mechanical

properties of PM titanium are not comparable to the wrought titanium. Referring to Table

1, if the density is less than 100%, the tensile strength, yield strength, and elongation of the

PM titanium is lower than that of wrought titanium.

Table 1. Mechanical properties of PM Ti-6Al-4V through various processes compared to wrought titanium [5].

	Relative density (%)	Tensile strength σ_b (MPa)	Yield strength $\sigma_{0.2}$ (MPa)	Elongation δ_s (%)	Reduced area (%)
Conventional BE	95	773	683	6	6
CIP + VS BE	95	830	740	6	10
MR-9^{TM} BE	99.2	932	849	14	29
CHIP BE	~100	960	882	17	35
P&S+HT+HIP	~100	921	1000	17	40
TIARA BE	99.6	926	809	19	31
PA	~100	992	930	15	33
Ceramic mold PA	~100	958	889	14	39
Wrought	~100	978	923	16	44

Additive manufacturing (AM) of metals is the process of building the model layer

by layer. The ASTM classification of additive manufacturing states that it can be classified

broadly into three categories powder bed systems, powder feed systems and wire feed

systems [6]. Powder bed systems rely on the principal of raking the powder onto the work

area where the electron beam melts the surface of the bed to form its desired shape. More

2

powder is raked onto the work area and the process is repeated to form a solid component. The powder feed systems are used to build the component more vertically standing than the powder bed systems. In this system, the powder flows through the nozzle onto the work area and the electron beam melts the powder forming the component. The wire feed system uses a feed stock of wire and an electron beam to form the component layer by layer. The wire feed systems tend to have the higher deposition rate. However, the product tends to require more extensive post machining than the powder bed or powder fed systems [6]. Furthermore, the mechanical properties of AM titanium manufactured through powder bed fusion are shown in Table 2 [6]. Additionally, the fatigue properties are shown in Table 3 [6]. The mechanical properties show that they are comparable to wrought titanium and the fatigue strength is superior.

Table 2. Static properties of powder bed fusion of processed Ti-6Al-4V manufactured through various methods compared to typical wrought titanium [6].

	Typical wrought	M280, HIP + solution heat treat		ARCAM, HIP	
Orientation	n/a	X-Y	Z	X-Y	Z
YS, MPa	828	887	946	848	841
UTS, MPa	897	997	1010	946	946
Elongation	15%	11.4	13.9	13.2	13.9

Table 3. Fatigue and fracture toughness properties of powder bed fusion produced Ti-6Al-4V [6].

Process	Orientation	Porosity, %	K_{IC}, MPa$\sqrt{m}$	STD, MPa$\sqrt{m}$	Fatigue strength at 10^7 cycles, MPa
As-fabricated	Z	0.19	78.1	2.3	407
As-fabricated	X-Y	0.11	96.9	0.99	441
HIP	Z	0.00	83.1	0.09	538
HIP	X-Y	0.00	99.0	1.1	607

3

1.2 Objectives of the scope

Throughout the research of the literature survey the machining of PM titanium and AM titanium have not been addressed. The objective will be to examine the machinability of PM and AM titanium alloys to determine the influence of the machining parameters, drill material, number of flutes to the machining process.

1.3 Organization of Thesis

This thesis is organized into six chapters, including chapter one which introduces the background information, the motivation for the research and the scope of the thesis. Chapter two consists of a literature survey that was studied in preparations for the experiments conducted. Chapter three outlines the details of the experimental procedure followed during the study. Chapter four discusses the experimental results throughout the study. Chapter five discusses the finding throughout the study. Chapter six concludes the study by summarizing the conclusions found as well as future recommendations.

Chapter 2. Literature Survey

2.1 Introduction to Machining

Machining is the process of transforming raw materials into parts by using machines such as lathes, drill presses and mills. Some machining process requires precise cuts to remove small amounts of materials, and some machining processes are fast to remove a lot of material. Drilling is the process of creating holes in the material.

Milling is the process of cutting away material by rotating the cutters but the process varies in the equipment. A milling machine features a moveable table where the workpiece is mounted and the table moves accordingly. Generally, the cutting tools are stationary and the tables move so that the cuts can be made. Other milling machines feature both moving tables and moving cutting tools. There are four types of milling machines which include, hand milling machines, plain milling machines, universal milling machines and omniversal milling machines. These machines feature either horizontal or vertical cutters. The omniversal milling machine features both horizontal and vertical cutters. Some operations that can be performed with a milling machine includes planing, cutting, and routing. Planing is the removal of material of the top surface to have the correct thickness as well as a smooth surface finish. Cutting consists of milling shapes out of the workpiece. Routing is used to machine the perimeter of the workpiece to create a chamfered of rounded edge [7].

Generally, there are three classifications of lathes, turret lathes, engine lathes, and special purpose lathes. Engine lathes are the most common type of lathes used generally by a machinist. The lathe performs turning operations where the material is rotated against the cutting tool and is controlled by a computer. The turning process can be performed on

5

the interior or exterior of the material. Performing the turning process on the interior is called "boring". The turning process applied on the exterior is called turning. The "boring" operation is used to create tubular components. The "facing" operation can be applied during turning where the insert moves perpendicular to the rotation motion, from end to end. Facing is typically performed at the initial and final stages of the turning process [7].

2.1.1 Drilling

In this study, the main focus of machining will be drilling. There are typically two types of drilling, short hole drilling, and deep hole drilling. Short hole drilling covers holes with a diameter up to 30 mm and a depth, not more than 5 times the diameter. Deep hole drilling consists of holes greater than 30 mm in diameter and depths greater than 2.5 times the hole diameter. The main concern with deep hole drilling is maintaining hole straightness. A solution to this is to use a hollow-core cutting to create a circular cut to ensure hole straightness. Through holes are holes which are drilled completely through the workpiece as opposed to blind holes which are drilled to a certain depth. Figure 1 shows the difference between through holes and blind holes. The drilling parameters that vary in this study include the feed rate and the cutting speed. The feed rate controls the speed at which the tool tip approaches the workpiece and the cutting speed controls the rotational speed of the tool tip.
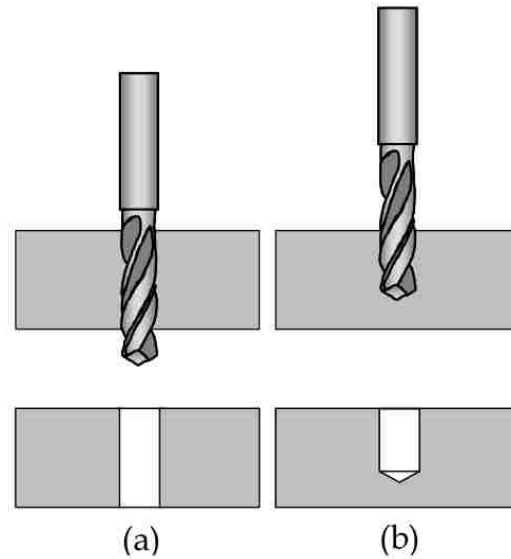
Figure 1. Type of holes when drilling, (a) through hole and (b) blind hole [8].

2.2. Machinability of Titanium Alloys

Machining titanium alloys is difficult due to work hardening, low thermal conductivity, abrasiveness, high strength level and high heat generation. Table 4 shows the physical property of Ti-6Al-4V [9]. Carbon steel has a thermal conductivity of approximately 45 W/mK. The thermal conductivity is low when compared to other materials such as steel. Heat generation is the most important factor when machining titanium alloys. Due to the low thermal conductivity and the high heat generation when machining adhesion occurs. Another factor that affects the machinability of titanium alloys is the vibration. The vibration causes a poor surface finish as well as poor cylindricity of the hole.

Abbasi [10] stated that the problem with machining titanium and its alloys will remain problematic no matter what techniques are used [10]. There have been improvements with machining titanium alloys but there are several problems which are faced during its machining which include: high thermal stresses on the cutting edge due to

7

the low thermal conductivity of the titanium workpiece, chemical reaction with most cutting materials, tool failure due to chipping, and a low modulus of elasticity and high yield stress ratio which only allows small plastic deformations. The high thermal stresses are caused due to the poor heat dissipation and low thermal conductivity when machining titanium alloys. The chemical reactivity with the tool tip and the workpiece causes rapid wear of the cutting tool. These problems are faced when machining titanium alloys, but when machining at low cutting speeds which vary from 6- 46 m/min the excessive wear of the cutting tool is reduced.

Table 4. Physical properties of Ti-6Al-4V at room temperature [9].

Tensile strength (MPa)	0.2% Proof stress (MPa)	Density (g/cm³)	Elongation 5D (%)	Reduction of area (%)	Modulus of elasticity tension (GPa)	Hardness (Hv)	Thermal conductivity (W/mK)
960–1270	885	4.42	≥8	≥25	100–130	330–370	7

2.2.1. Drilling of Titanium Alloys

The important factors in drilling titanium alloys includes, cutting force, cutting temperature, tool wear and tool life, hole quality, and chip type. A higher cutting force can indicate how difficult a material is to machine [11]. A smaller cutting force is desired since the material will be easier to machine. An increase in the cutting force can cause vibrations in the spindle which causes poor machined surfaces and can lead to premature failure and a reduction in tool life. A large torque value indicates the friction between the drill and the workpiece which causes a higher temperature at the tool-workpiece interface. During the drilling process, about 90% of the work of plastic deformation is converted into heat causing high temperatures (approximately 1060°C) between the chip, tool and workpiece interfaces [2]. The heat between the cutting tool and workpiece depends on the thermal

properties of both materials. Due to titanium's low thermal conductivity [12], a large portion (as high as 80%) of the heat generated in drilling will be absorbed by the tool [13]. In comparison, 50- 60% of the heat is absorbed by the tool tip when drilling steel [12]. Rapid tool wear is caused commonly due to the high cutting temperature. When machining titanium alloys, the tool wear progresses due to the high cutting temperature and adhesion between the workpiece and the tool. Titanium chips can easily weld to the cutting edges of the drill tip, which is known as built-up-edge (BUE) or built-up-layer (BUL). BUE can lead to chipping and premature tool failure. Wear mechanisms when machining titanium alloys include flank wear, crater wear, and chipping. Hole quality in drilling titanium alloys is evaluated through hole diameter, surface roughness, and burr. Hole quality is an important factor when machining titanium alloys since the parts require reliability, and resistance to wear. A higher surface roughness can lead to severe wear and less resistance to corrosion. The two main criteria to determine the hole quality is size and shape. Drilling titanium alloys creates burrs at the entrance and exit if through holes are generated. Burr formation requires an additional machining process. It is estimated that 30% of the machining cost of machining titanium alloys comes from deburring processes [12]. In drilling, chips can be tangled around the drill bit itself, the entangled chips make it difficult for chip ejection. There are two main shapes of chip morphology: spiral and long folded ribbon chips. The spiral chips are ejected easier so the length of the spiral cone chips can be considered as a scale to evaluate the difficulty for chip ejection [14].

The issues with drilling titanium alloys are similar to machining titanium alloys. The low thermal conductivity of the titanium alloy causes a huge issue in drilling so an alternative may be to drill different manufactured titanium alloys. Drilling PM titanium

9

and titanium may be a good alternative, although due to the porous structure, an interrupted cutting condition occurs during drilling which causes extensive tool wear. The formation of the small chip particles can get stuck in the flute of the twist drill which can cause problems with material ejection. Another problem with drilling PM titanium alloys is the use of cutting fluids during drilling. The cutting fluid will soak into the porous structure of the material and cause considerable corrosion. Czampa [15] conducts an experiment to investigate the drilling capabilities of sintered PM titanium alloys [15]. Czampa [15] uses three different types of drill bits which include, ANDRILL HSS (cheap high speed steel drill bit), HARTNER HSS (high quality high speed steel drill bit), and a Sumitomo Sumidrill (carbide drill bit). The drilling parameters used in the experiments are 15 m/min (1600 RPM) at a feed rate of 0.04 mm/ rev. Additionally, no coolant was used for the initial tests then cold air and misting was used to cool the drill bits. The initial tests with the ANDRILL HSS are shown in Figure 2 [15].
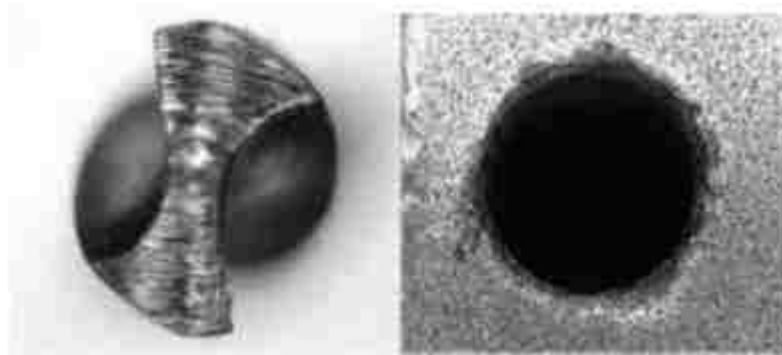
Figure 2. The top view of the drill bit of ANDRILL HSS twist drill and hole after 16 through-holes without lubrication [15].

The next test included the carbide drill bit without lubrication and it failed after 9 holes, so the appropriate step was to add lubrication. Figure 3 shows the good quality drill

bit with cold air coolant. There were moderate tool wear and reduced torque which is shown in Figure 3 [15].
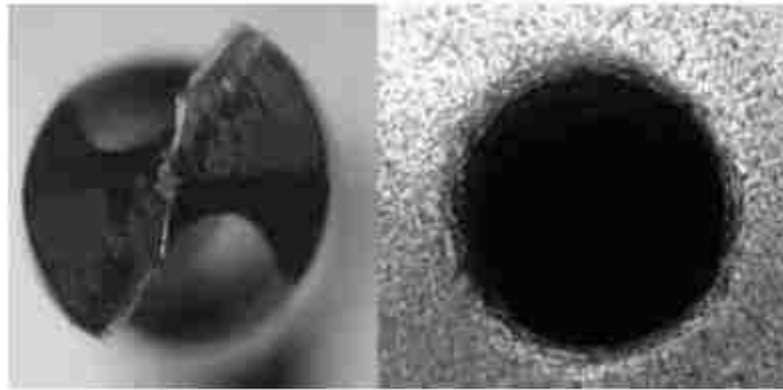
Figure 3. The top view of the drill bit of HARTNER HSS twist drill and hole after 16 through-holes with cool air coolant [15].
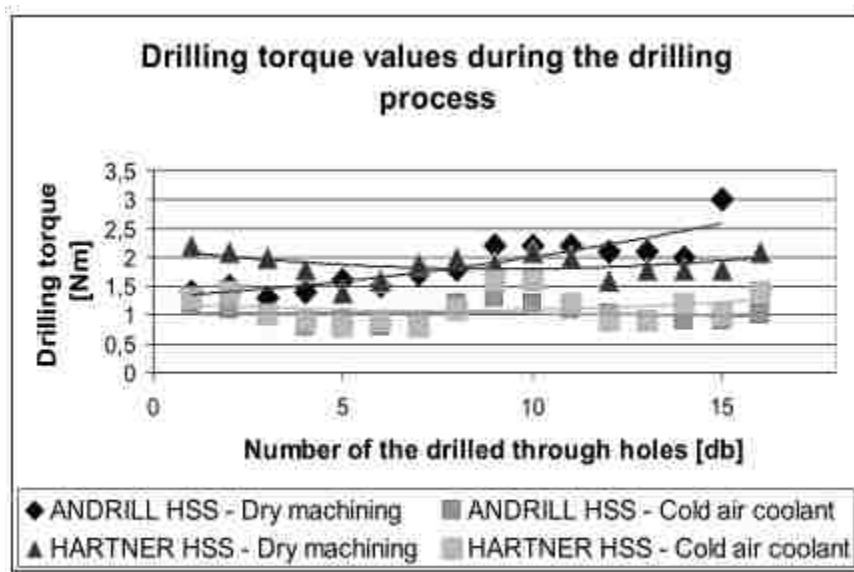
Figure 4. The top view of the drill bit of HARTNER HSS twist drill and hole after 16 through-holes with cool air coolant [15].

Figure 5 shows that the carbide tool tip with the mist lubrication drilling the most hole with the least amount of wear. Campza [15] concludes that any kind of coolant improves the drilling conditions, and improves tool life. Also, the carbide drill bits are expensive but are worth
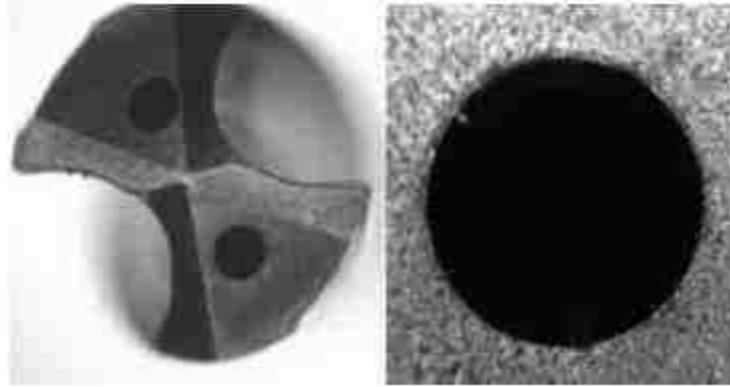
Figure 5. The top view of the drill bit of Sumitomo Sumidrill twist drill and hole after 192 through-holes with mist lubrication [15].

There are scarce amounts of research dealing with drilling additive manufactured titanium yet alone machining additive manufactured titanium. A. Bordin investigates the tool wear mechanism with turning AM titanium through the turning operation under dry and cryogenic conditions using a coated tungsten carbide insert at varying cutting speeds and feed rates [16]. The drilling parameters conducted in this experiment is shown in Table 5.

Table 5. Drilling parameters used to turn additive manufactured Ti-6Al-4V [16].

Test condition	Cutting speed [m/min]	Feed rate [mm/rev]	Depth of cut [mm]	Lubrication
1	50	0.1	0.25	Dry
2	50	0.2	0.25	Dry
3	80	0.1	0.25	Dry
4	80	0.2	0.25	Dry
5	50	0.1	0.25	Cryogenic
6	50	0.2	0.25	Cryogenic
7	80	0.1	0.25	Cryogenic
8	80	0.2	0.25	Cryogenic

The results of the experiment are shown in Figure 6. The main tool wear observed on the flank face of both dry and cryogenic conditions are abrasion, chipping and adhesion of the tool tip which is shown in Figure 6a and Figure 6b. While the rake face shown in Figure

Figure 6b, Figure 6c, and Figure 6d shows crater wear, built-up layer (BUL) and built-up edge (BUE). A. Bordin states that adhesion is the main wear mechanism observed in both dry and cryogenic turning [16]. The cryogenic turning reduced the thickness of the adhered layer on the rake face which improved the cutting time in comparison to the dry machining. Overall, cryogenic cooling improved the machining process of additive manufactured titanium.
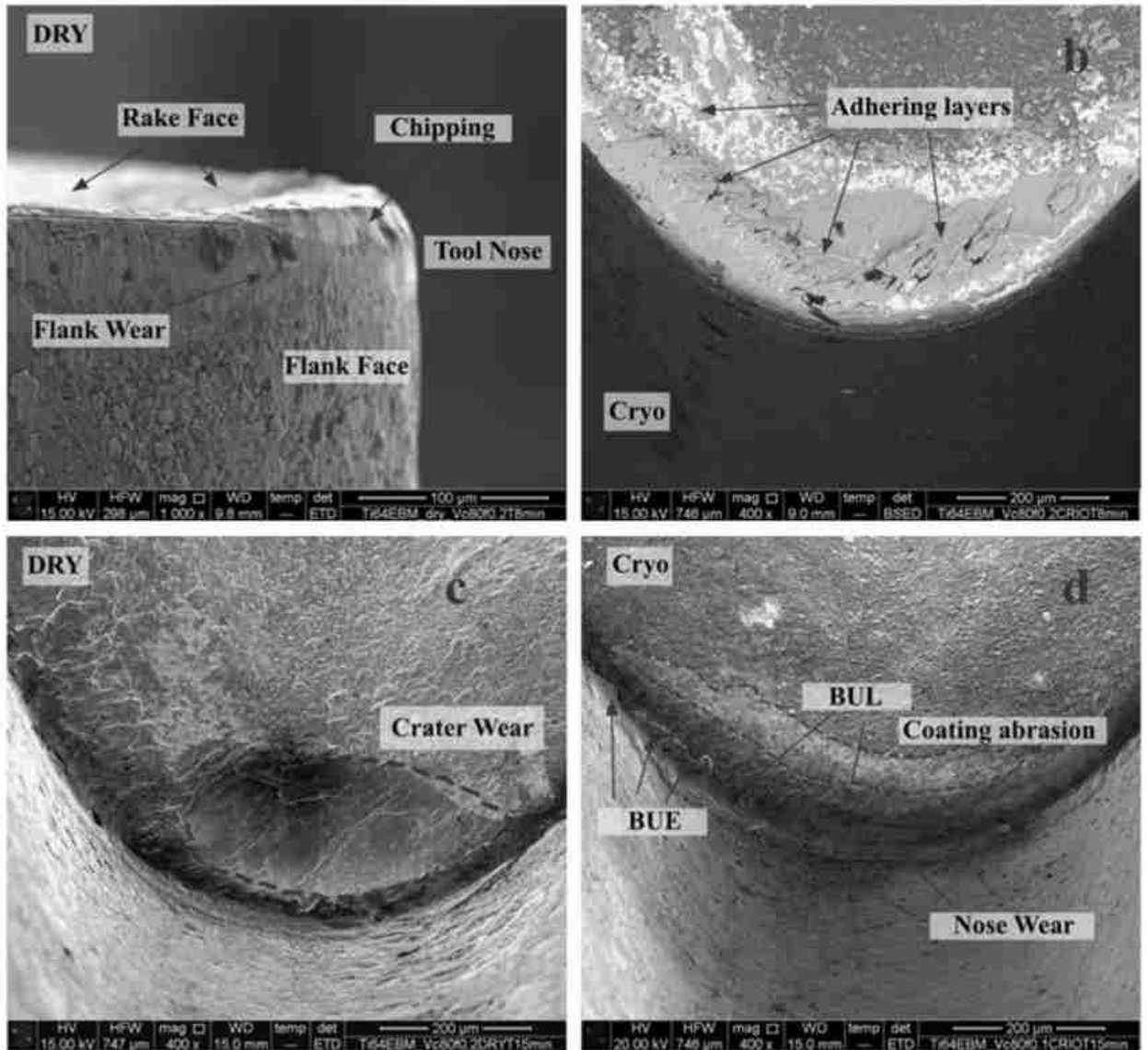
Figure 6. SEM images of tool wear on the insert after 8 min at a cutting speed of 80 m/min and a feed rate of 0.2 mm/rev under: a, c) dry conditions, b, d) cryogenic conditions [16].

2.3 Methods of Cooling

There are many methods in the machining world that require lubricant or coolant but in some scenarios that can be a bad thing. In the case of machining titanium alloys, it is a necessity to use a lubricant or coolant due to the poor thermal conductivity of the material. Although, machining PM materials with coolants or lubricants will cause

14

corrosion since the material will absorb the coolant through its porous structure. The main coolant techniques used in industry include flood cooling and minimum quantity lubrication (MQL). Flood cooling consists of a nozzle which is aimed at the workpiece and a steady flow of coolant is applied. Flood cooling uses the principle of flooding the workpiece to cool down the amount of heat generated. The coolant is either recovered or recycled back to the system as long as there is not too much contamination with the coolant. Generally, the coolant used by flood cooling is considered as toxic waste and should not be recycled because once used the coolant is used it is contaminated by bacteria. MQL uses the minimum amount of lubrication to coat the tool tip to prevent heat build up by reducing the amount of friction.

2.3.1. MQL

Minimum quantity lubrication (MQL) is the process of lubricating the drill bit during the drilling process by using the minimum amount of lubricant required. This method is cost effective, safe for the environment but does cool as much as flood cooling. Additionally, cryogenic machining uses the principal of MQL but lightly misting the drill bit but this method is costly.

Shakeel et al., [17] experimented with cryogenic cooling during drilling. Cryogenic coolant lowered the cutting zone temperatures when drilling Ti-6Al-4V. From the reduced cutting zone temperatures, the material is easily ejected from the flute. Additionally, Govindaraju et al., [18] states the use of liquid nitrogen as a coolant reduces the thrust forces and surface roughness due to less friction being present. Less serration and uniform segmentation lead to better chips and better chip morphology. Better chipping results in improved hole quality, circularity and cylindricity. Shakeel et al., [17] claims liquid

nitrogen provides better lubrication and is more effective than wet coolant. Hong et al., [19] conducted a turning experiment on Ti-6Al-4V and found that liquid nitrogen drastically reduces the cutting temperature and maintains a good tool life. Another study by Bagci et al., [20] showed that the effect of twist drill temperature increases with feed rate and decreases with cutting speed. Overall, Hong et al., [19] and Bagci et al., [20] showed that the cutting temperature reduces drastically with liquid nitrogen which results in less tool wear and improved finish. It has been consistently reported that an increase in feed rate will result in a higher thrust force and torque

Shakeel et al., [17] conducts an experiment which consists of 3 levels while looking at 2 parameters. This procedure is based on the L9 orthogonal array (3, 2). The temperature, feed rate, torque, surface roughness and hole quality have been compared between both cooling conditions. The drilling was conducted on Ti-6Al-4V using an uncoated tungsten carbide insert of grade ZCMT 06T204-KW10 with cryogenic liquid nitrogen and wet cooling conditions. Table 6 shows the experimental process parameters.

Table 6 Experimental process parameters of Ti-6Al-4V alloy [17].

S. no.	Factors	Level 1	Level 2	Level 3
1.	Cutting speed (m/min)	40	50	60
2.	Feed rate (mm/rev)	0.02	0.05	0.08

The temperature of the experiment was recorded using K-type thermocouples which range from $200^{\circ}C$ - $1250^{\circ}C$ linked with a data acquisition system. The experimental setup is shown in Figure 7 [17].

16
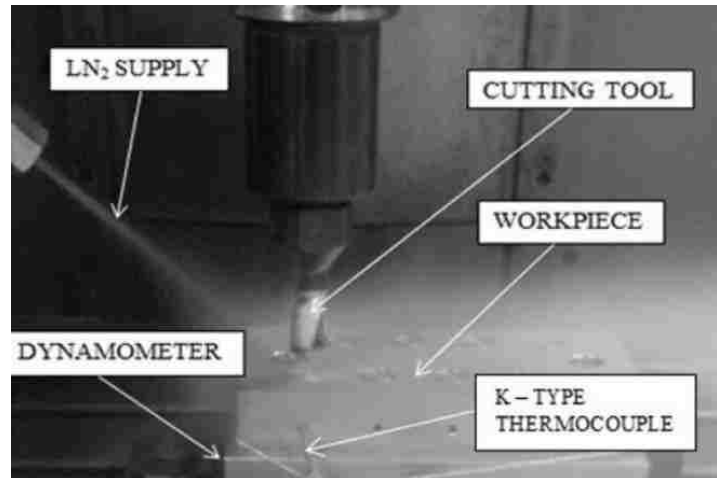
Figure 7. Liquid nitrogen delivery nozzle with respect to drill center [17].

The experimental setup consisted of supplying liquid nitrogen at a pressure of 4 bar. The liquid nitrogen was supplied through a pressurized condition with passed through the nozzle tip to the tool-work interfaces. The liquid nitrogen nozzle tip was positioned with respect to the drill center. When using the wet cooling condition, a soluble cutting fluid was obtained by mixing a 1:15 ratio of water. The temperature of the wet drilling condition vs the cryogenic cooling condition is shown in Figure 8, where the feed rate is increased from 0.02 mm/rev to 0.08mm/rev. The cutting speed is kept constant at 40 m/min. It is shown that as the feed rate increases the temperature does decrease but when comparing the coolant, the cryogenic condition reduces the temperature greater than the wet cooling condition. Additionally, Figure 8 shows the comparison of the cutting fluids when the cutting speed is increased. Overall, with an increase of cutting speed the temperature increases. When comparing the cutting fluids, the liquid nitrogen reduces the temperature more than wet cutting fluid.

17
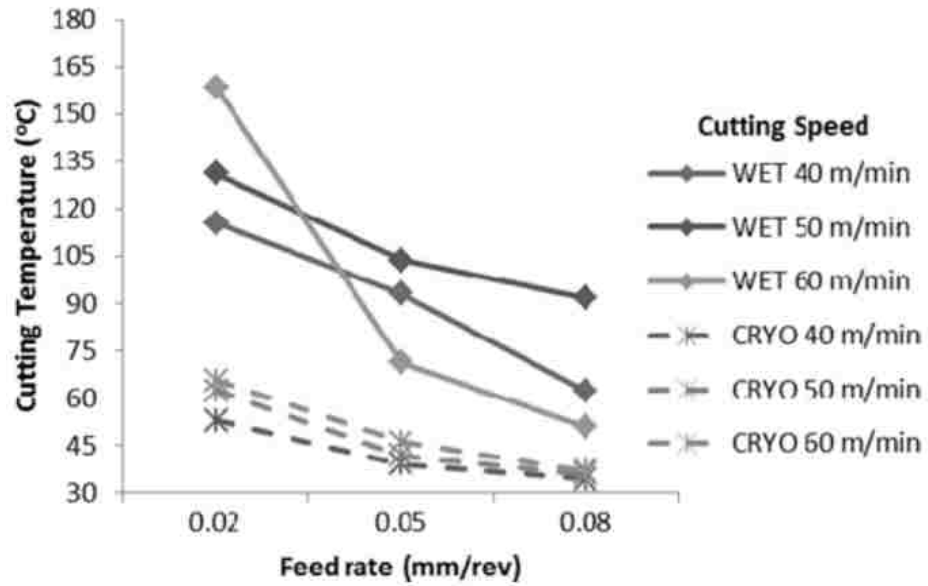
Figure 8. Cutting temperature vs. feed rate of wet coolant vs cryogenic coolant [17].

The variation of torque of the experiment with respect to feed rate and cutting speed is shown in Figure 9. Overall, the cryogenic liquid nitrogen outperformed the wet coolant in most of the tests. The only considerable condition for wet cooling is at 50 m/min with a feed rate of 0.05 mm/rev.
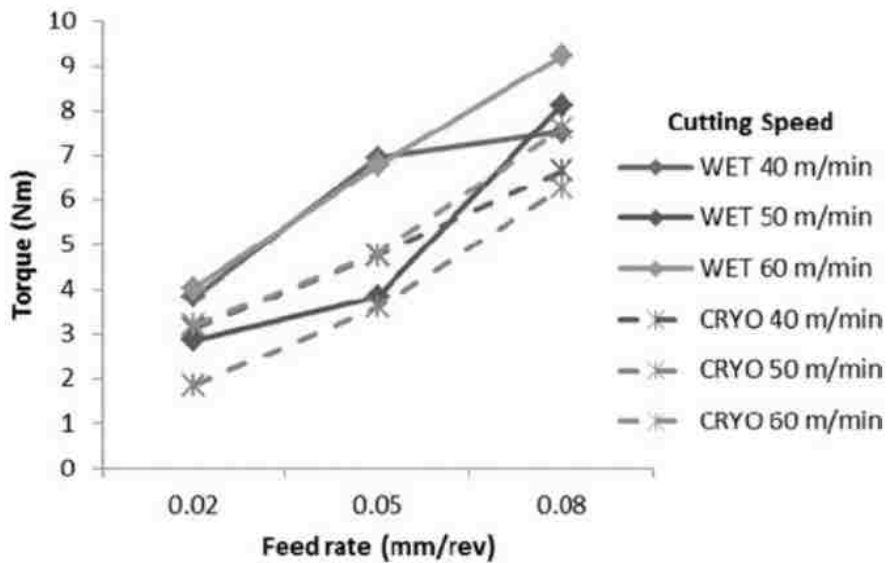
Figure 9. Torque vs. feed rate of wet coolant vs cryogenic coolant [17].

2.3.2. Flood Cooling

      Flood cooling has always been used in general machining which includes drilling. Flood cooling is the process of cooling and lubricating the drill bit, and clearing the chips. Flood cooling is an effective method for cooling but tends to have lots of waste since recycling the coolant can cause contamination in the drilling process. In a study by Rahim & Sasahara [21], they look at the thrust force and torque of drilling Ti-6Al-4V with flood cooling, MQL, and air blown. The drilling parameters used in this experiment includes a cutting speed of 60 m/min and a feed rate of 0.1 mm/rev. In Figure 10, the air blown conditions produced the highest thrust force compared to the other conditions. The minimum quantity lubrication with palm oil (MQLPO) exhibited comparable thrust force to flood coolant which had the lowest thrust force in this study. Additionally, the torque values show a similar trend to the thrust force where flood cooling showed to have the least amount of torque and MQLPO having a comparable torque value shown in Figure 11. Overall, with low torque and thrust forces, flood cooling is an effective method of cooling the drill bit.
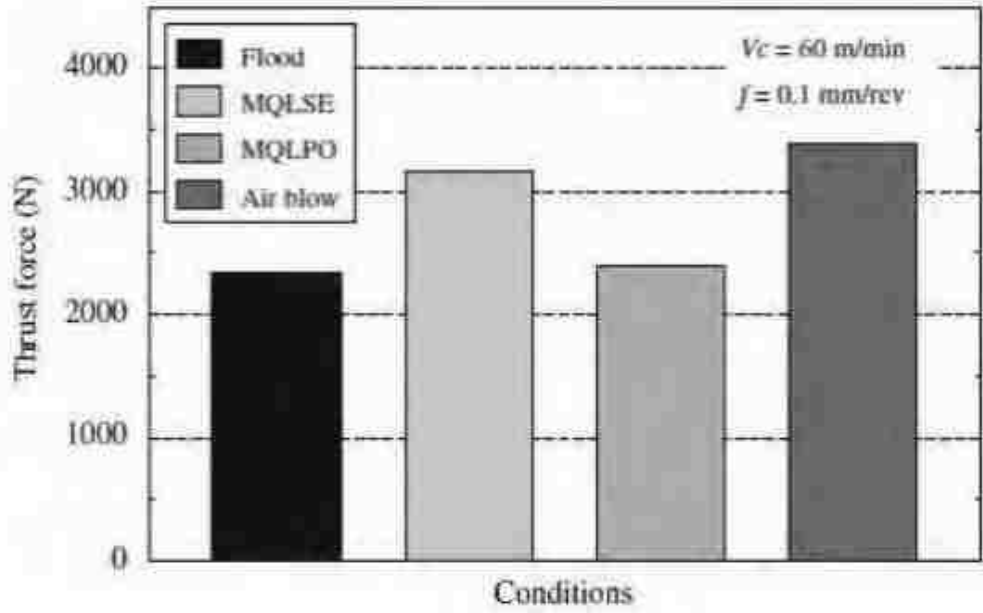
Figure 10. Thrust force when drilling Ti-6Al-4V under various coolant conditions at high speeds [21].
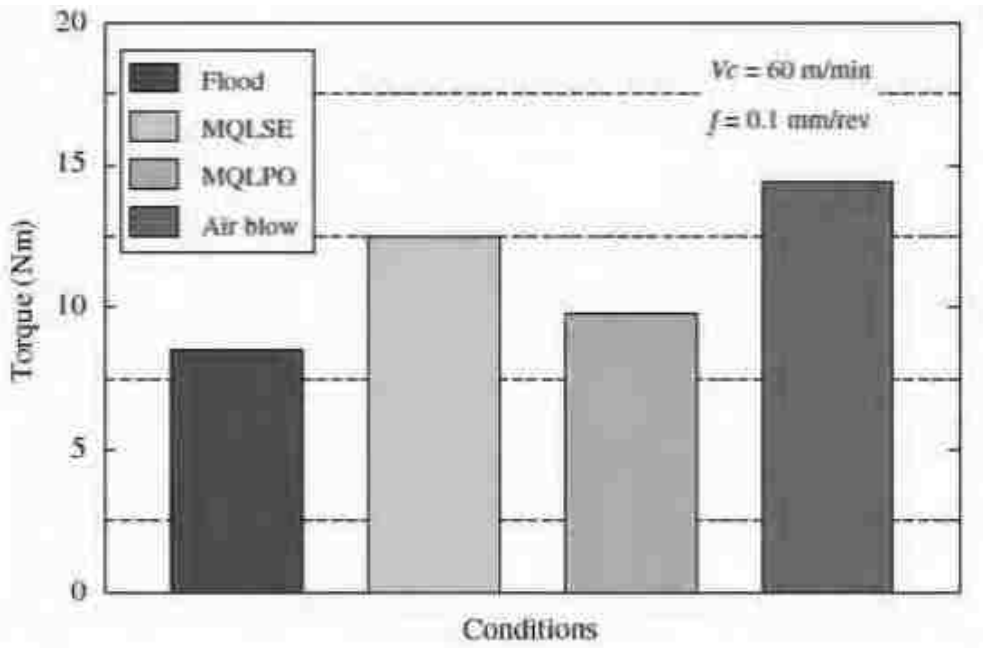
Figure 11. Torque when drilling Ti-6Al-4V under various coolant conditions at high speeds [21].

2.4 Solutions for Improving the Machinability of Ti Alloys

2.4.1. Current Solutions

There are multiple solutions to improve machining titanium alloys. One current solution is to increase the tool life by improving the coolant or the tool tip. The purpose of the coolant would be used to reduce the amount of heat generated on the tool tip, and increase lubricity to prevent adhesion. There are many tooltips used to machine titanium. The most common tooltip is the cemented carbide tip due to economic reasons. The tool tip aspect can be improved by using a tool tip with a coating which reduces the friction between the tool tip and the workpiece.

2.4.2. Tool Tips

2.4.2.1 Tool tip Geometry

The important parameters of a drill bit include the rake angle, point angle, web thickness, nominal clearance angle, drill diameter, inclination angle and chisel edge angle. The geometry of the drill bit is shown in Figure 12. The rake angle is referred to as the helix angle at the periphery. The point angle directs the flow of chips. By increasing the point angle, the orthogonal rake angle increases which decreases in the torque but increases the thrust force.
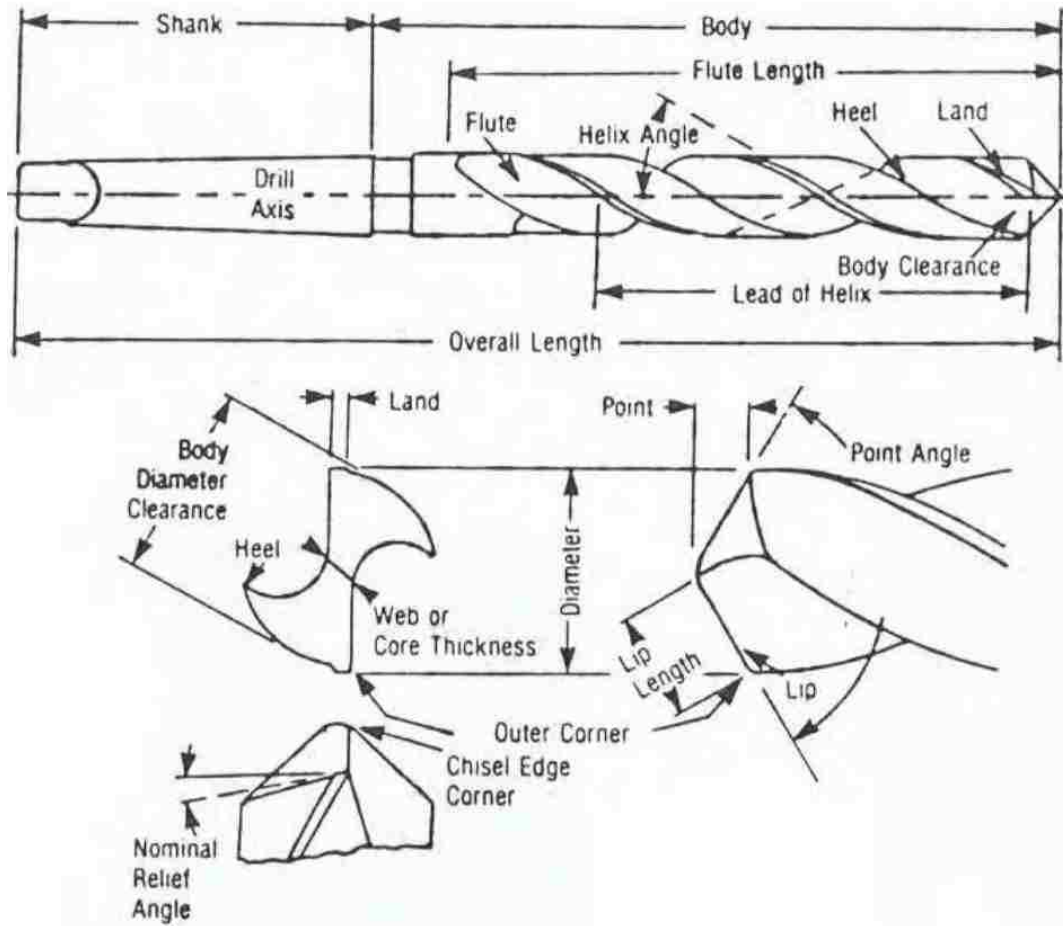
Figure 12. Various views of a twist drill bit [22].

2.4.2.2 Coated Tooltips

The durability of the tool tip can be improved by using a more expensive material such as polycrystalline diamond (PCD) or binderless cubic boron nitride (BCBN). Additionally, prolong machining causes severe chipping and fracture of the tool's cutting edge. Among the various machining processes, drilling can be considerably the most difficult process compared to milling and turning.

S. Sharif [23] investigated the effect of coated and uncoated tools when drilling Ti-6Al-4V. The tools are either coated with chemical vapor deposition (CVD) or physical vapor deposition (PVD) hard coatings. The tool tip Sharif [23] uses is the PVD-TiAlN-

coated carbide drill bit and an uncoated drill bit for comparison. TiAlN-coated carbide drills are commonly used due to their high hardness value, wear resistance, chemical stability, and better machining performance. The drilling parameters used in this experiment includes cutting speeds varying in increments of 10 m/min from 25 m/min to 55 m/min, at a constant feed rate of 0.06 mm/rev. It was observed at the lower cutting speeds (25 and 35 m/min) that the flank wear gradually increased for the coated drill and at the higher cutting speeds for the coated drill resulted in a shorter tool life as shown in Figure 13 [23]. For the uncoated drill, at all cutting speeds, it experienced rapid wear as shown in Figure 14 [23]. The wear of the coated and uncoated drill bit is shown in Figure 15 [23] and Figure 16 [23], respectively. Chipping occurred at most cutting speeds for both drills except for at 25 m/min for the coated tool tip. The coated drill at 25 m/min showed only a small amount of flank wear. It is noted that the uncoated drill failed at 55 m/min. The tool life of the coated drill lasted longer than the uncoated drill bit as shown in Figure 17 [23]. Sharif [23] concludes that the coated drill outperformed the uncoated drill by providing less wear and longer tool life at all test cutting speeds.
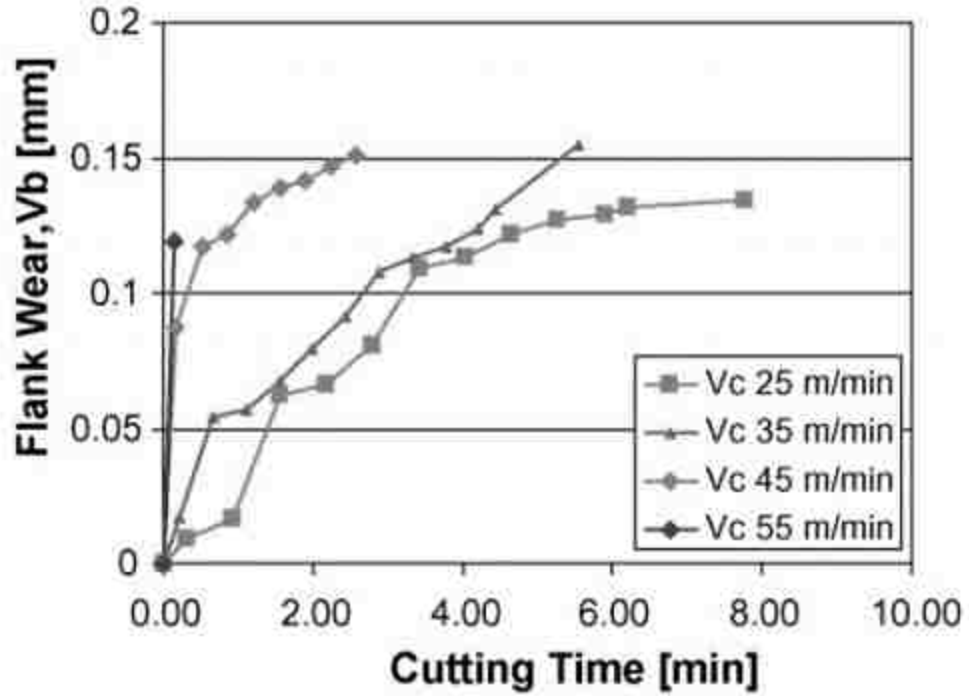
Figure 13. Flank wear vs cutting time of the Ti-AlN coated drill when drilling Ti-6Al-4V at various cutting speeds [23].
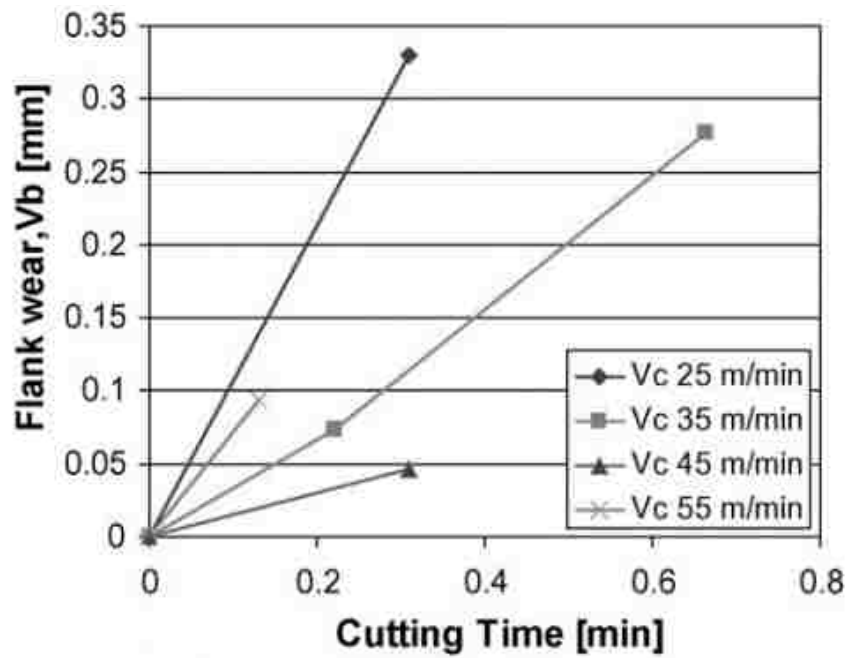
Figure 14. Flank wear vs cutting time of uncoated drill when drilling Ti-6Al-4V at various cutting speeds [23].

24
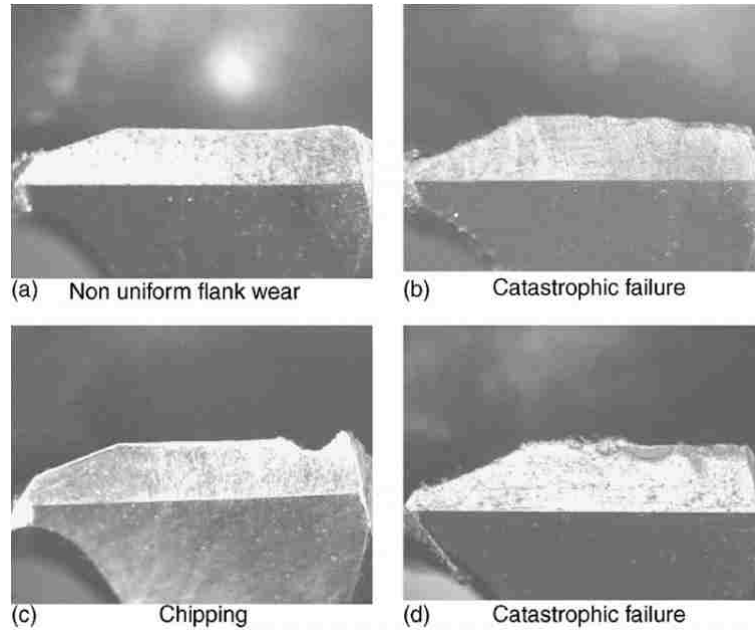
Figure 15. Wear on TiAlN coated drill when drilling Ti-6Al-4V at a feed rate of 0.06 mm/rev and a cutting speed of: (a) 25 m/min, (b) 35 m/min, (c) 45 m/min, and (d) 55 m/min [23].
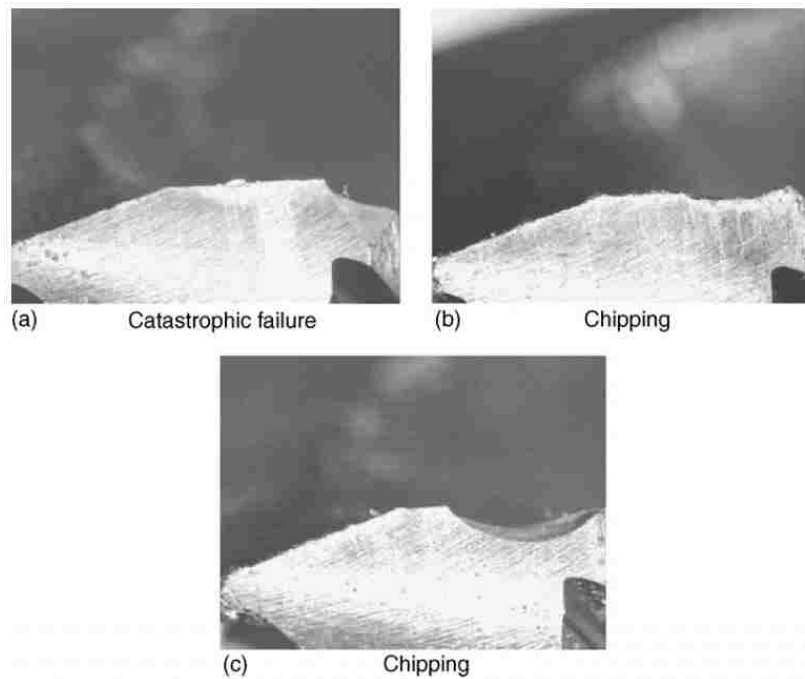
Figure 16. Wear on an uncoated carbide drill when drilling Ti-6Al-4V at a feed rate of 0.06 mm/rev and a cutting speed of: (a) 25 m/min, (b) 35 m/min and (c) 45 m/min [23].
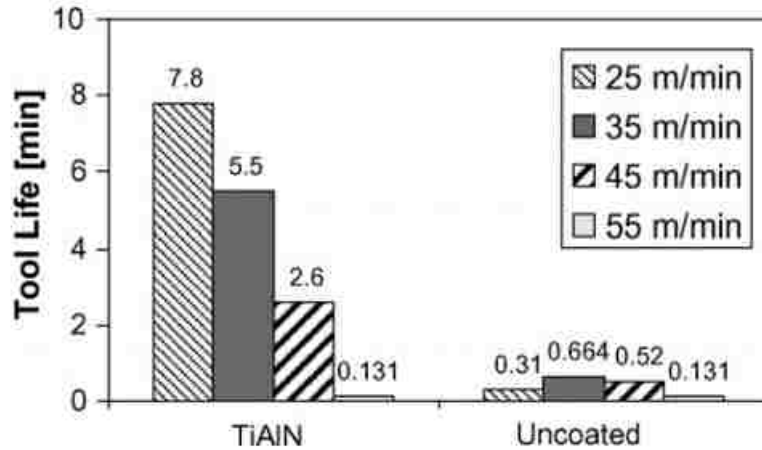
Figure 17. Tool life performance comparison between the coated TiAlN drill and the uncoated carbide tip with a feed rate of 0.06 mm/rev at various cutting speeds [23].

2.5. Analysis

There are many types of analysis which can be used in machining but the ones that will be focused on include optical microscopy, scanning electron microscopy (SEM) and x-ray diffraction (XRD). Optical microscopy will focus mostly minor inspections, whereas SEM will focus on the details at a higher magnification and XRD will confirm the elements present. The main focuses of wear on the tool tip include chipping, flank wear, and adhesion. As for the workpiece, the main concern that will be looked at is the surface finish.

2.5.1 Types of Wear

Firstly, Tool wear is comprised mainly of heat generation, pressure, friction, and stress distribution. The drill wear classification includes outer corner, flank wear, margin wear, crater wear, wear along with chisel edge and chipping at the cutting lips. Figure 18 [22] shows the various types of wear mentioned above. Wear starts at the corners of the cutting edge and the wear is distributed along the cutting edges until the chisel and drill margin. Flank wear occurs due to friction between the workpiece and the contact area of tool tip. Flank wear is a criterion to measure the performance of a drill [22]. However, the

26

outer corner wear should be used as the main criterion for tool performance due to the relative ease of measurement and the relationship between the wear and tool life [22].
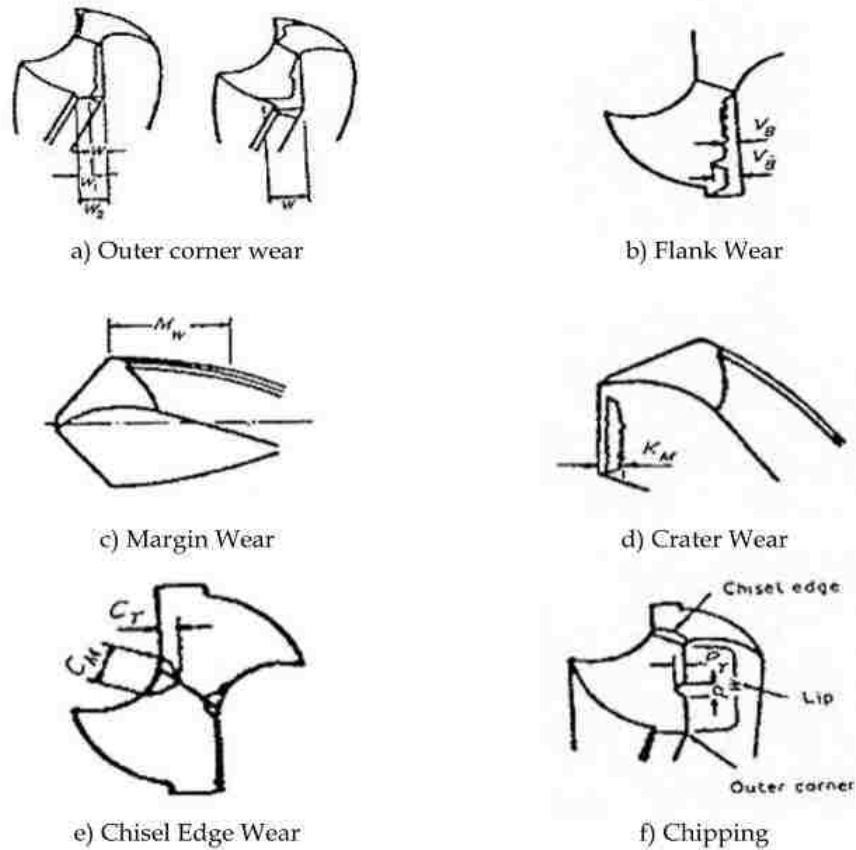
Figure 18. Various types of drill wear including a) outer corner wear, b) flank wear, c) margin wear, d) crater wear, e)chisel edge wear and f) chipping [22].

Crater wear was observed on the rake face as well as the other corner of the cutting edges. Drills which have rounded cutting edges are considered damaged as shown in Figure 19 [24]. The tool is considered unable to drill once the outer corner wear reaches 75% of the total margin width. Additionally, Sharif rejected the tooltip when the flank wear reached a maximum of 0.38 mm on the drill lips, which exhibited a squeaking noise during drilling [22].
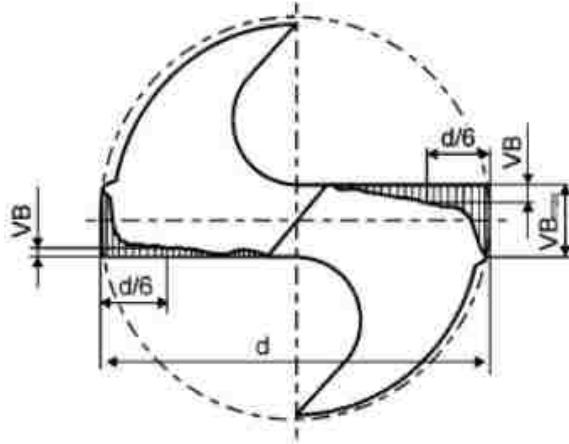
Figure 19. Location of flank wear land on the drill [22].

Tool wear occurs when there is an interaction between the tool and the workpiece, whether being physical or chemical the result is the removal of small particles of tool material from the cutting edge. Tool wear occurs in three stages as shown in Figure 20 [22]. The initial stage shows rapid wear then in the second stage shows uniform wear until it reaches the failure region. The third stage is where the tool wear is occurring rapidly and causes tool failure. Machining beyond the failure region will cause catastrophic failure on the tool and this should be avoided. The main problem with drilling titanium alloys is the rapid wear of the cutting tool. The two most dominating factors that were observed during drilling titanium alloys are flank wear and excessive chipping and micro-cracking. The wear occurs on the flank face and the cutting edge of the tool tip. An increase in cutting speed leads to an increase in flank wear and encourages adhesion which leads to build up on the edge, attrition wear and ends up in severe chipping.
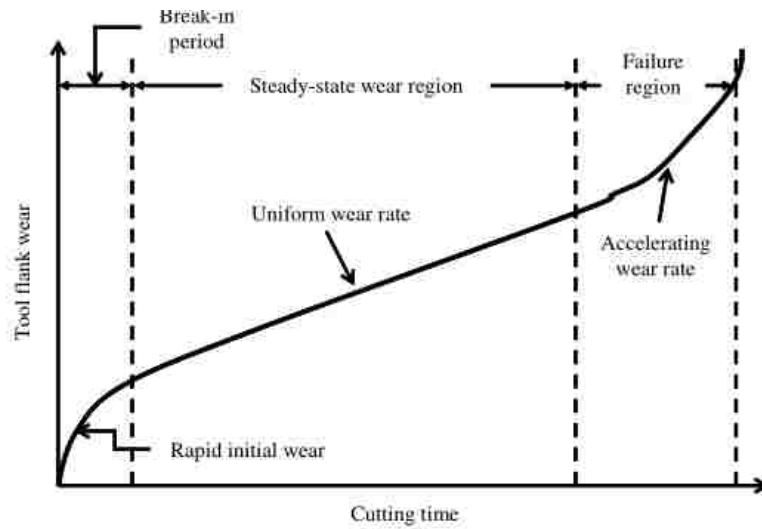
Figure 20. Typical stages of tool wear in machining including the initial rapid wear, uniform wear and the accelerating wear [22].

A study on Ti-48Al-2Mn-2Nb showed it had less adhesion than Ti-6Al-4V and concluded through SEM that adhered material was the main contribution to tool failure. At first, the adhesion may protect the cutting edge from wear as shown in Figure 21 [23] but if the machining process becomes prolonged the adhered material becomes unstable and breaks away from the tool removing both the adhesion and a small amount of the tool itself. This inevitably leads to severe chipping and cracks propagating causing fracture on the cutting edge.
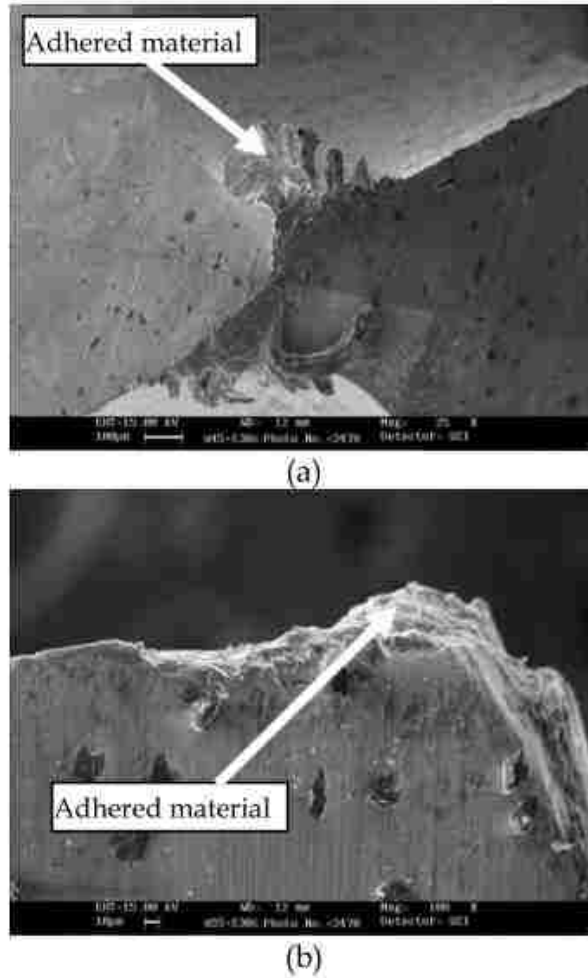
Figure 21. Adhered workpiece materials at the (a) chisel edge and (b) the cutting edge of after drilling Ti-6Al-4V [23].

Chipping is mainly generated through cyclic stresses during drilling which leads to the formation of cracks parallel on the cutting edge. These cracks propagate with prolonged machining which leads to chipping which causes failure. It is noted that chipping can occur without the presence of crack formation. Also, multiple cracks may join together and force fragments of the tool to break away. Figure 22 [23] shows a crack formation along the cutting edge.
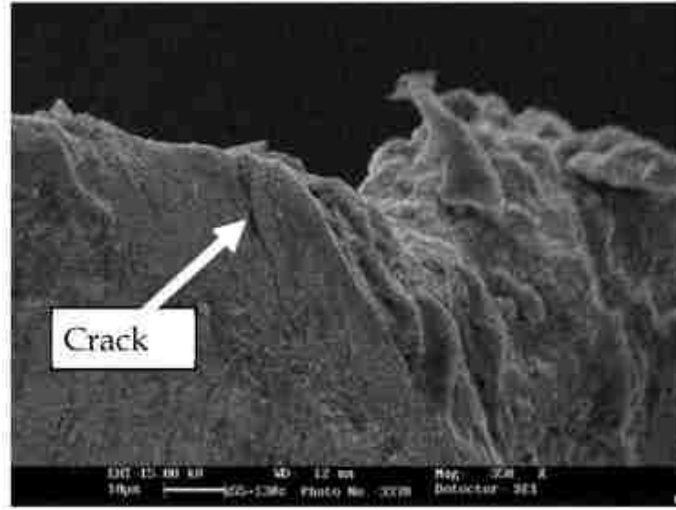
Figure 22. Crack on the flank face after drilling Ti-6Al-4V for 1 minute at 55 m/min and 0.06 mm/rev [23].

An experiment conducted by Arrazola et al. [8] using graphene oxide suspension to determine if the results are better than conventional cooling. Tungsten carbide is used as the tool tip to machine Ti-6Al-4V. The factors which are evaluated are the cutting forces, hole quality, and chip morphology. The experiment was conducted on a three-axis vertical CNC milling machine. A six-component dynamometer was used to measure the thrust force and torque. Additionally, an eight-channel charge amplifier was used to amplify the signal which was transferred to the data acquisition system. Once in the data acquisition system, the data was analyzed. Figure 23 [8] shows the scanning electron microscopy (SEM) images of the rake face of the inserts used for machining Ti-6Al-4V and Ti555.3 at 80 m/min and 50 m/min, respectively. The light grey area in Figure 23 [8] is shown as the titanium adhered to the cutting edge, and the darker area is titanium carbide. EDAX analysis was used to confirm the identity of the titanium and titanium carbide [8].

31
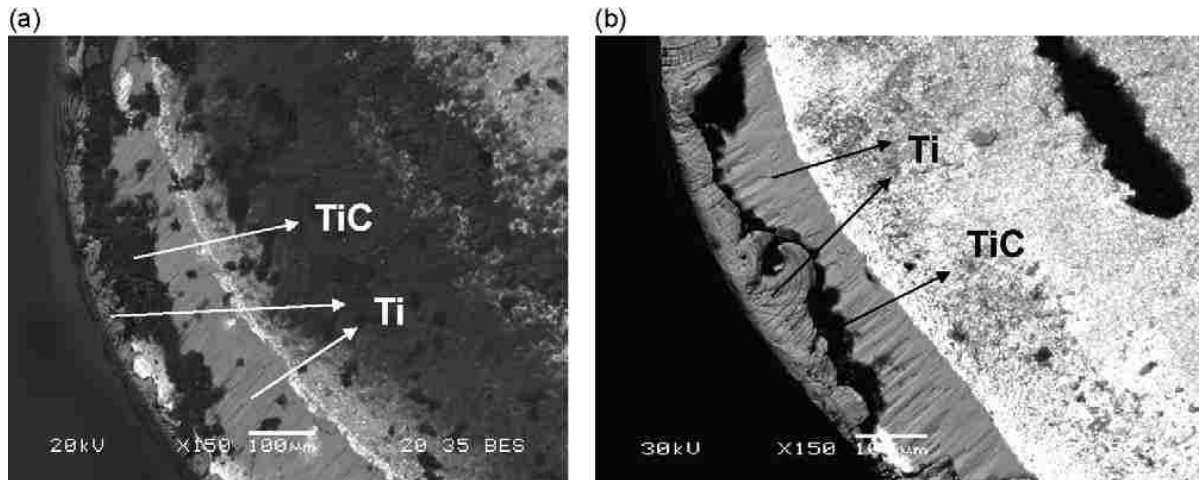
Figure 23. Adhered work material (BUE) on the tool cutting edge for (a) Ti6Al4V at 80m/min and (b) Ti555.3 at 50m/min after 15min of cutting time [8].

Arrazola et. al. [8] observed built-up edge (BUE) after machining Ti-6Al-4V at low cutting speeds which suggested that tool wear is reduced when this layer is present. This layer prevents sliding at the tool-chip interface and limits the diffusion rate of the tool. At higher cutting speeds this built-up edge (BUE) disappears which causes tool wear to occur faster. Figure 24 [8] proves that at lower cutting speeds BUE slows down tool wear but at a higher cutting speed the BUE is not present which reduces tool life.
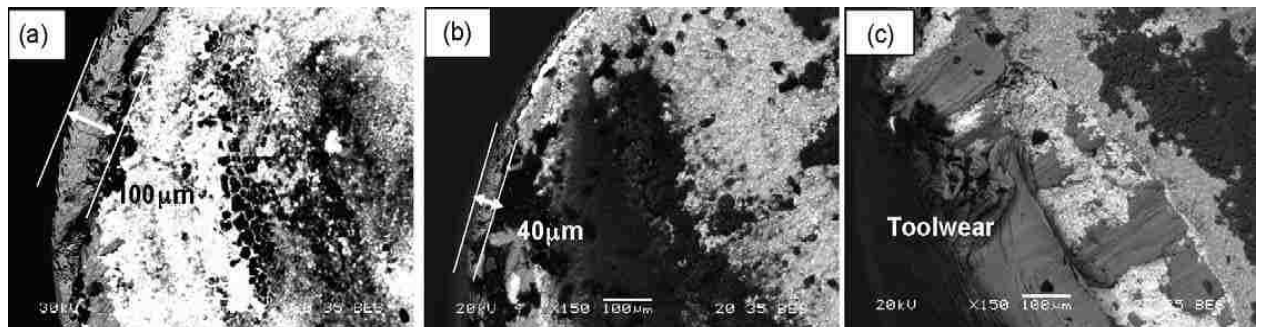
Figure 24. An evolution of the build up layer in the inserts' cutting edge at cutting speeds of (a) 50 m/min (b) 80 m/min and (c) 90 m/min for Ti6Al4V [8].

Next, the performance and mechanism of graphene oxide cutting fluid were investigated. Graphene oxide is synthesized from synthetic graphite powder, it has good

32

mechanical, electrical, thermal and optical properties. It has a similar structure to graphite but the plane of carbon atoms is surrounded by a lot of oxygen atoms. The oxygen atoms expand the interlayer distance which makes the layers hydrophilic. Graphene oxide is a good substitute for regular coolants due to its outstanding thermal conductivity. This property makes it easier for the heat to be dissipated into the graphene oxide when machining difficult to machine workpieces such as titanium alloys. Samuel et al. [25] found that the reduction in cutting temperatures could reach up to 58% compared to a commercially used lubricant. Also, the cutting forces could be reduced up to 26%. In another study Smith et al. [26] found that graphene oxide suspension resulted in a 50% reduction in cutting temperature compared to the commercially used lubricant. When compared to liquid nitrogen cryogenic cooling, the graphene oxide suspension had similar performance, if not better. Huang et al. [27] experimented with suspending graphene oxide in cutting fluid while machining titanium alloys. Lee et al. [28] concluded that the graphite nano powder increased the lubrication and reduced the friction between the tool and the workpiece. Rahim and Sashara [29] found that using minimum quantity lubrication (MQL) in combination with compressed air functions both as a coolant and lubricant. The result yielded in a reduced cutting force of 6.5%. Zeilmann and Weingaertner [30] experimented with MQL internally through the tool tip and externally. The results showed that machining with MQL with an external nozzle reduced cutting temperatures by 50%.

2.5.2 Torque and Thrust Force

Torque and thrust force are a good indication of the forces applied to the tool tip. Figure 25 [31] shows the thrust force at various cutting speeds and feed rates for both conventional coolant and graphene oxide. Thrust force decreases with the increase of

cutting speed. Thrust force generally increases with feed rate. Overall, the graphene oxide

has a lower thrust force than the conventional coolant.
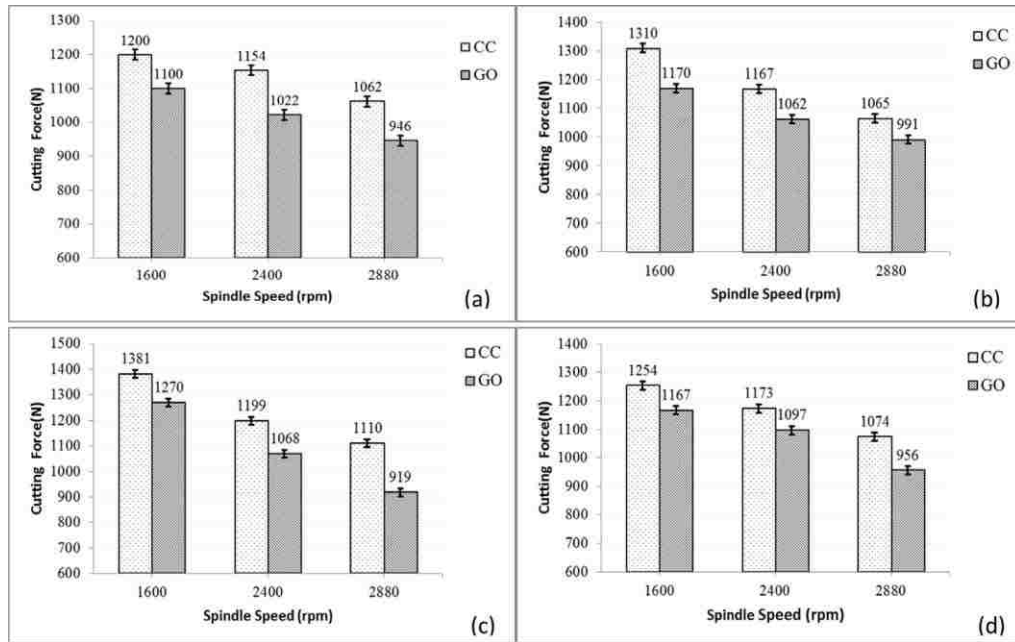
Figure 25. Thrust force with different feed rate: (a) 0.10 mm/rev (b) 0.12 mm/rev (c) 0.15 mm/rev; (d) 0.18 mm/rev [31].

In another study conducted by Zhu, Z., et al. [32][14], the experiments were designed to

investigate the effect of cutting speed, feed rate, hole accuracy, chip formation and surface

integrity. Figure 26 [14] shows the thrust force with varying feed rates and cutting speeds.

Figure 26a [14] shows thrust force as a function of feed rate and Figure 26b [14] shows the

thrust force as a function of cutting speed. Increasing the cutting speed reduces the thrust

force overall. It is seen that a feed rate of 0.05 mm/rev produces to the lowest amount of

thrust force and a feed rate of 0.2 mm/rev shows the highest thrust force. By increasing the

cutting speed raises the temperature of machining due to friction between the tooltip and

the workpiece which results in thermal softening of the material thus reducing the thrust

force.
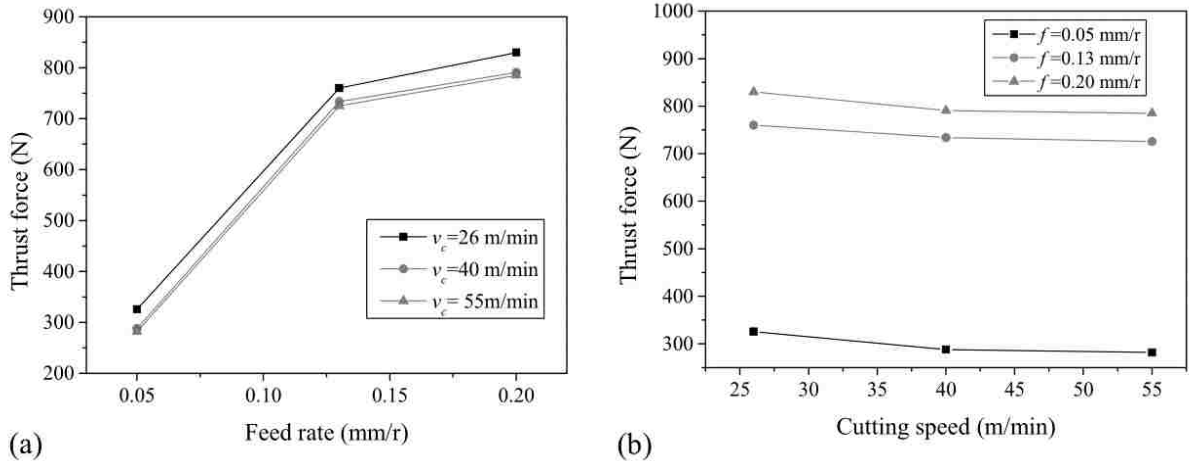
Figure 26. Evolution of the thrust force as a function of the (a) feed rate and (b) cutting speed [14].

2.5.3 Chip Morphology

There are multiple chip morphologies during machining which includes, long spiral chips, folded ribbons, and small chips. Figure 27 [14] shows the macroscopic analysis of the chips from the experimental results when varying cutting speed and feed rate without using a coolant. It was noted that the shape of the chips strongly depends on the feed rate. When increasing the feed rate from 0.05 to 0.2 mm/rev the chip length decreased from 60 to 20 mm. It was noted that drilling with a feed rate of 0.13 mm/rev, the chips are broken into small segmented chips [14]. It is also noted that the cutting speed does not play a role in chip breakability or the chip length.
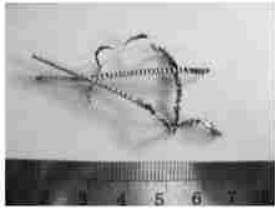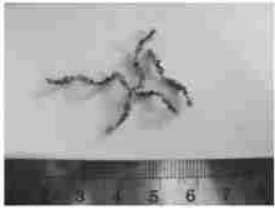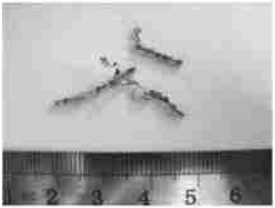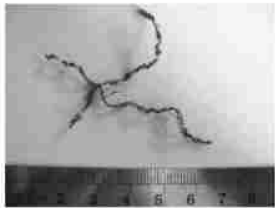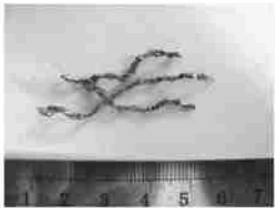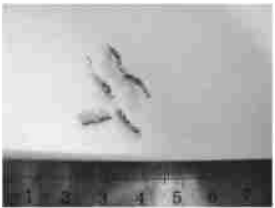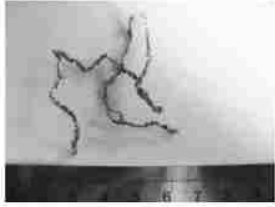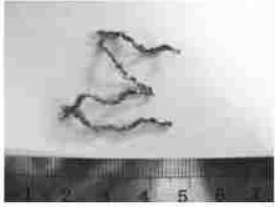
Cutting speed v_c (m/min)	Feed rate f (mm/r)		
	0.05	0.13	0.2
26			
40			
55			

Figure 27. Influence of the cutting speed and feed rate on titanium chips in dry drilling. [14]

Figure 28 [14] shows multiple stages of chip morphology which includes the initial spiral cone, steady state cone, transition between spiral and long ribbon and long ribbon. The spiral cone shown in Figure 28a [14] was generated from the initial region. After the initial region, the steady state spiral cone was generated. The next region includes the spiral transition and the folded ribbon. This is due to the increased resistance of chip ejection which causes the spiral cones to fold. This is shown in Figure 28c [14] and Figure 28d [14]. During the machining process of titanium alloys, small broken chips are desirable since the larger chips cannot move through the flute and cause the chips to wrap around the tooltip, increased cutting temperature, and increase thrust force.

36
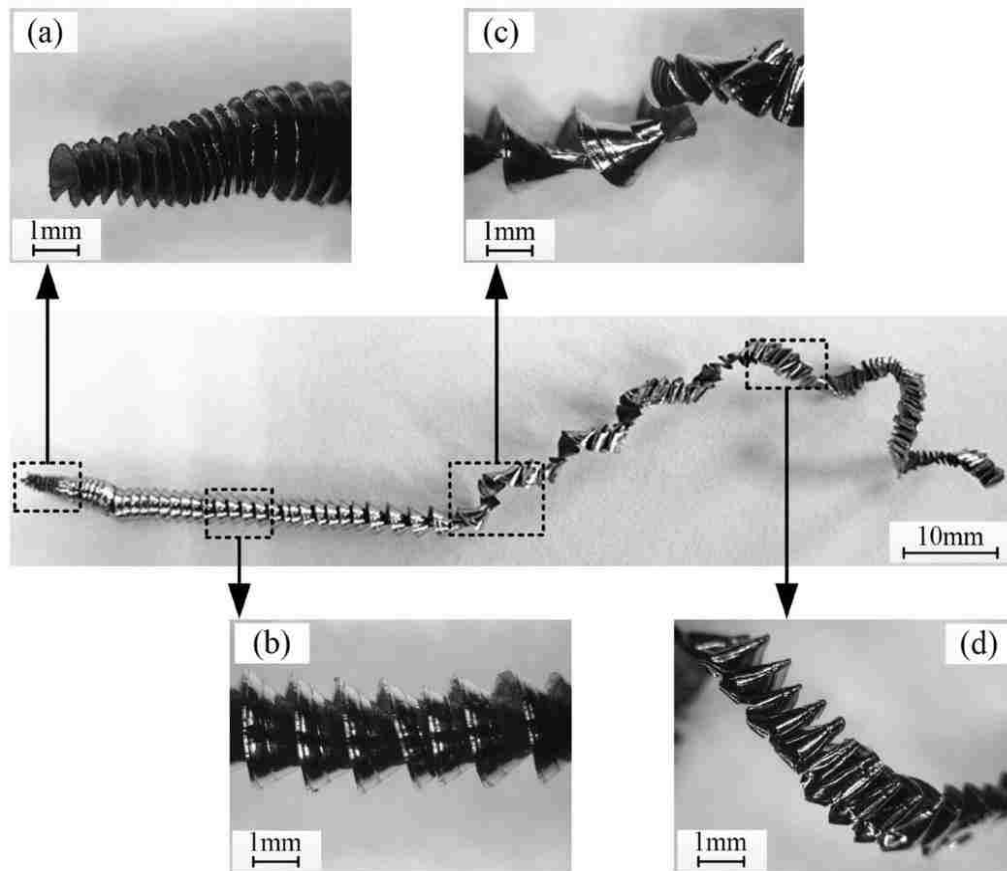
Figure 28. Chip morphology of titanium alloy Ti-6Al-4V at 26 m/min cutting speed and 0.05 mm/r in dry drilling. a. Initial spiral cone, b. Steady-state spiral cone, c. Transition between spiral cone and folded long ribbon, d. Folded long ribbon [14].

2.6 Purpose of Research

This research is conducted to determine the machinability of commercially pure PM titanium and AM titanium. Although, both these materials result in their near net finish product, some post machining may be necessary to clean up the product. Additionally, some holes are too fine to create with the manufacturing methods for AM and PM titanium. The research includes a study of wear and torque of various drill bits which include HSS, AlTiN coated carbide, and a tungsten three flute bit.

Chapter 3: Material and Experimental Methods

Chapter three outlines the materials and the experimental procedures used to characterize the wear and torque data of grade 5 titanium, powder metallurgy titanium and additive manufactured titanium.

3.1 Materials

3.1.1 Workpiece Materials

The materials used in this study include titanium alloys, various drill bits and drilling equipment. The titanium alloys include (i) wrought titanium alloy (Ti-6Al-4V), (ii) powder metallurgy commercially pure titanium, and (iii) additive manufactured commercially pure titanium. The Ti-6Al-4V was composed of 90% titanium, 6% aluminum and 4% vanadium. The powder metallurgy titanium was cold pressed and sintered. The specifics of the powder morphology, sinter temperature or the atmosphere were not provided by the manufacturer during this research project. The powder metallurgy titanium had a composition of 99.03% titanium, 0.32% silicon, 0.24% iron, 0.18% cobalt, 0.11 vanadium [33].The additive manufactured titanium was developed by plasma transferred arc solid free form fabrication where the metal powder flowed into the plasma beam where the robotic arm controlled the fabrication. The product was produced by building layer by layer through CAD and CAM software. The additive manufactured titanium used in this study had a composition of consisting of 97.3% titanium, 0.82% aluminum, 0.63% boron, 0.37% silicon, 0.2% iron.

3.1.2 Drill Bits

3.1.2.1 High Speed Steel Drill Bit

HSS is a commonly used drill bit for drilling most types of material. This is the reference drill bit since it is commonly used with many materials. The HSS drill bit used in this experiment was a Viking Drill & Tool twist drill bit with a 135° split point with a diameter of 4mm as shown in Figure 29(A). Figure 30 to Figure 32 are SEM images of the HSS drill bit chisel edge and cutting edge before drilling.

Figure 29. (A) HSS twist drill bit, (B) three flute drill bit, and (C) carbide drill bit.
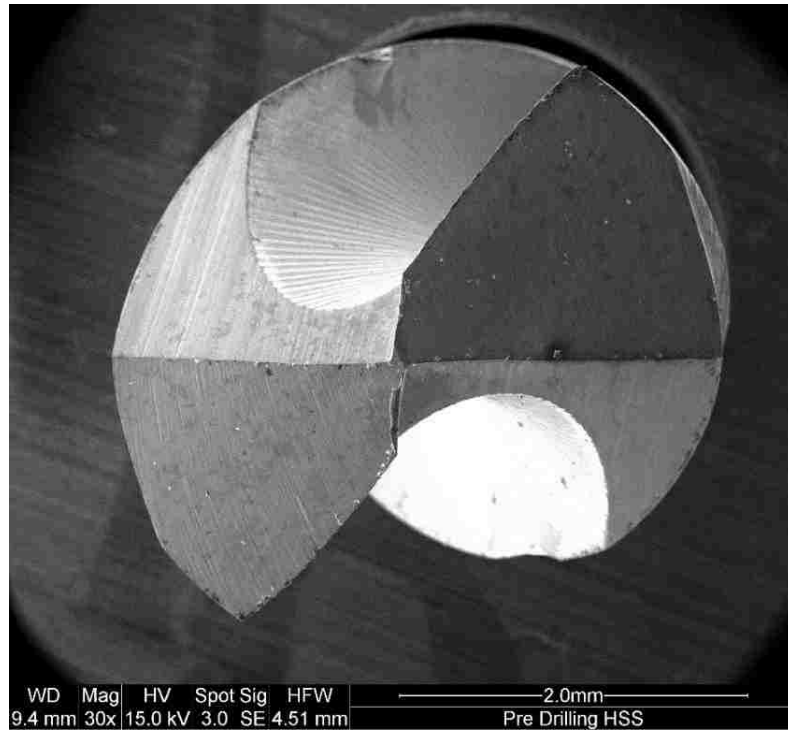
Figure 30. 30x SEM top down view of the HSS drill bit before drilling.
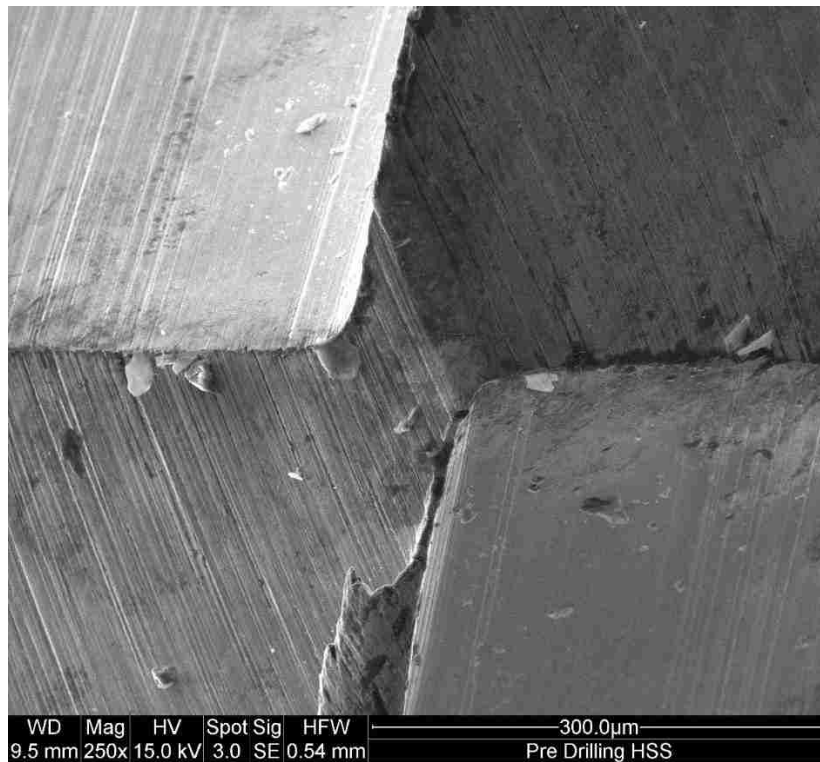
Figure 31. 250x SEM top down view of the HSS chisel edge before drilling.

40
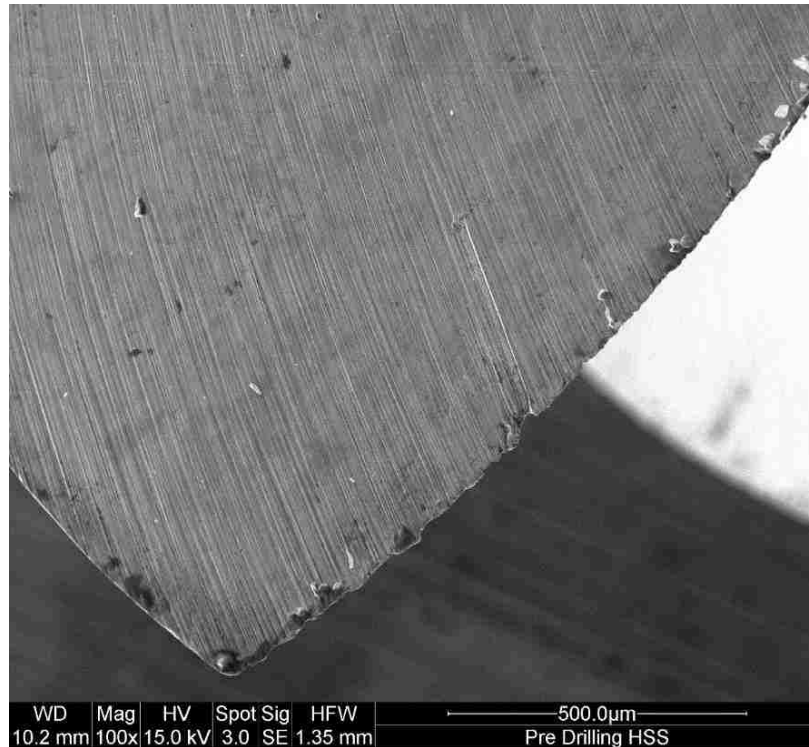
Figure 32. 100x SEM top down view of the HSS cutting edge before drilling

3.1.2.2 Three Flute Drill Bit

The three flute drill bit used in this study is the M.A. Ford 22915750 4 mm high performance 3-flute carbide drill bit which features a point angle of 150°. The point angle of the drill bit is flatter compared to the 135° point angle drill which means the cutting edge engage with the workpiece material sooner. The side view of the drill bit is shown in Figure

29 (B). Figure 33 to Figure 35 shows the SEM images of the chisel edge and cutting edge before drilling.
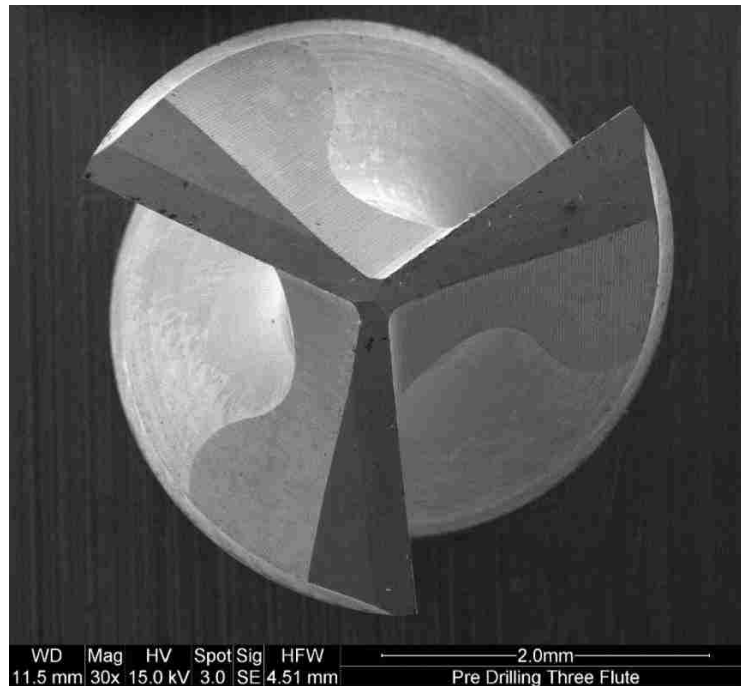
Figure 33. 30x SEM top down view of the HSS drill bit before drilling.
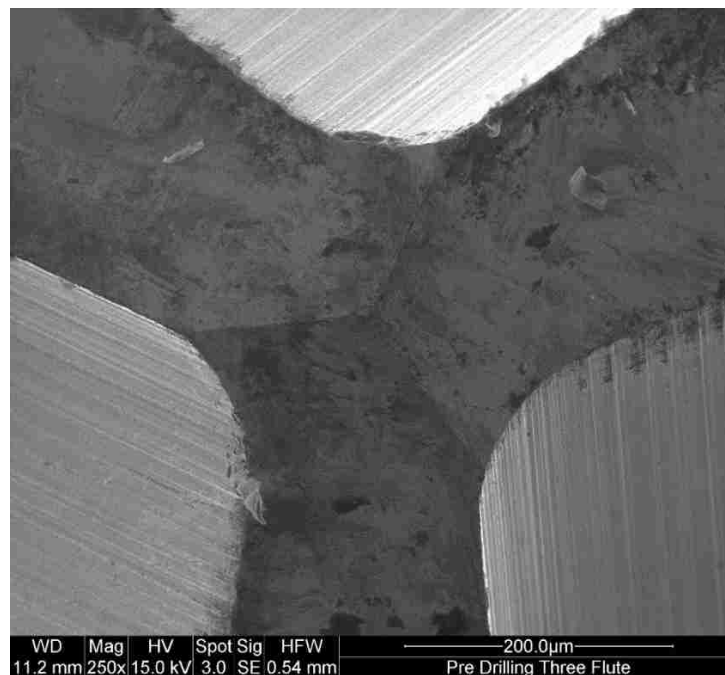
Figure 34. 250x SEM top down view of the three flute chisel edge before drilling.
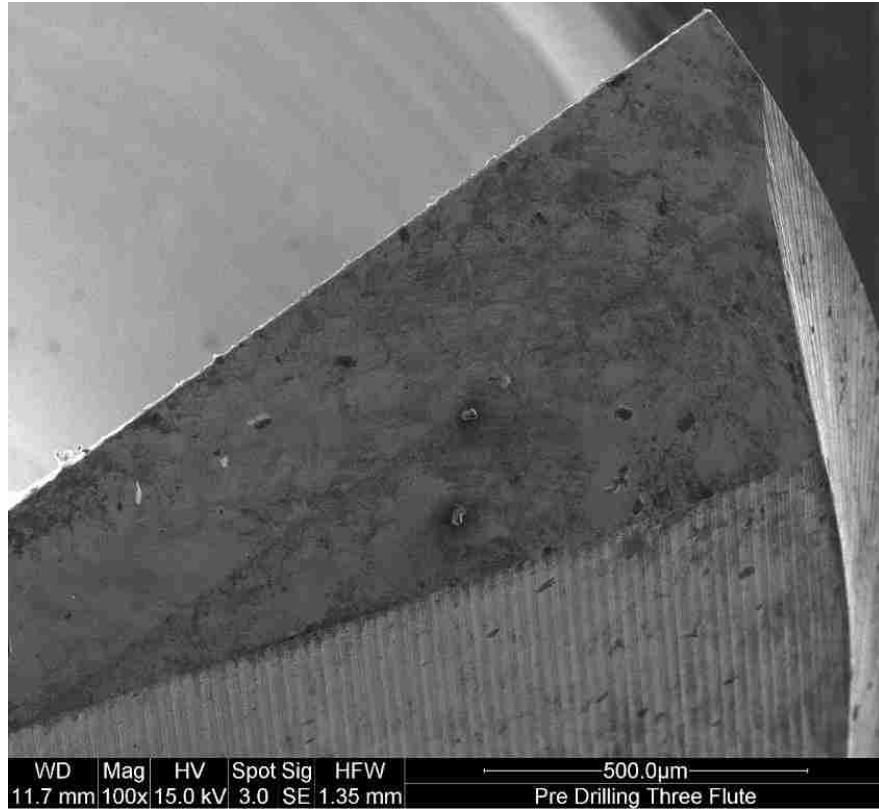
Figure 35. 100x SEM top down view of the three flute cutting edge before drilling.

3.1.2.2 Carbide Drill Bit

The carbide drill bit used in this study is the M.A. Ford 2XDSS1575A 4 mm coated carbide drill bit which features a point angle of 140°. The coating used on the carbide drill is AlTiN. The side view of the drill bit is shown in Figure 29 (C). Figure 36 to Figure 38 show the chisel edge and cutting edge before drilling under the SEM.
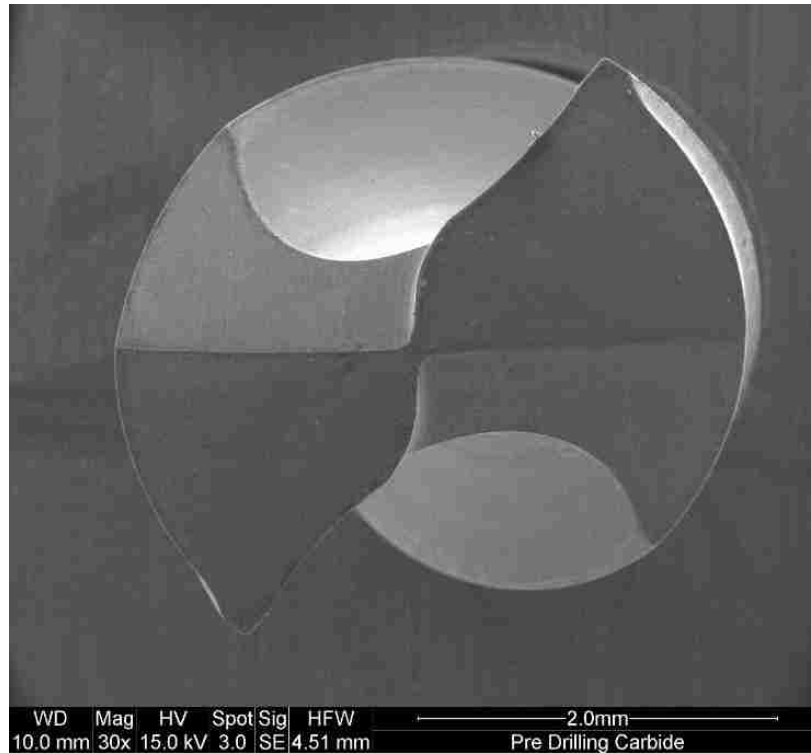
Figure 36. 30x SEM top down view of the HSS drill bit before drilling.
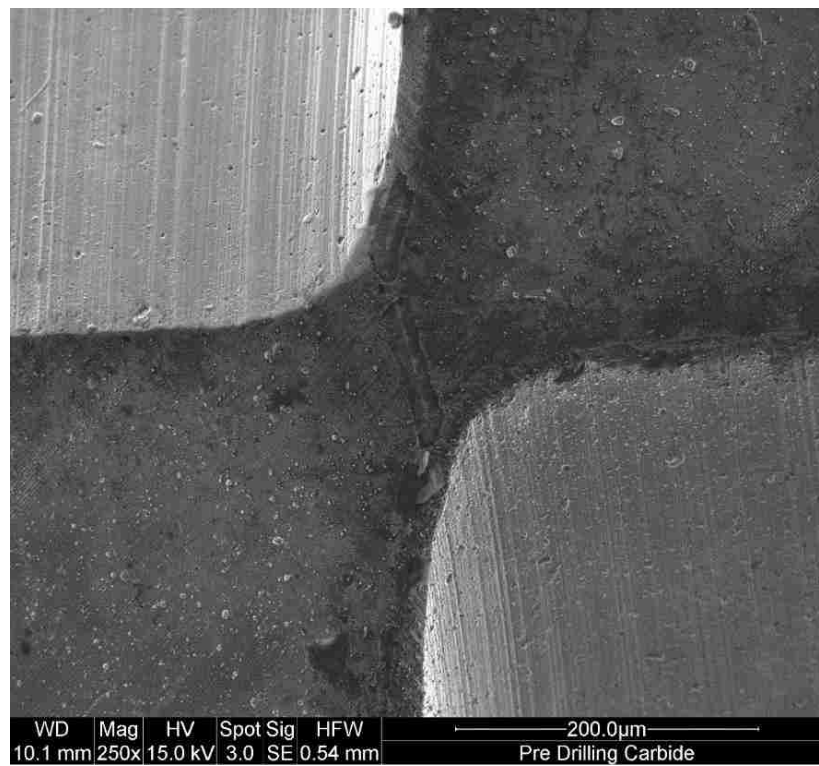
Figure 37. 250x SEM top down view of the carbide chisel edge before drilling.

44
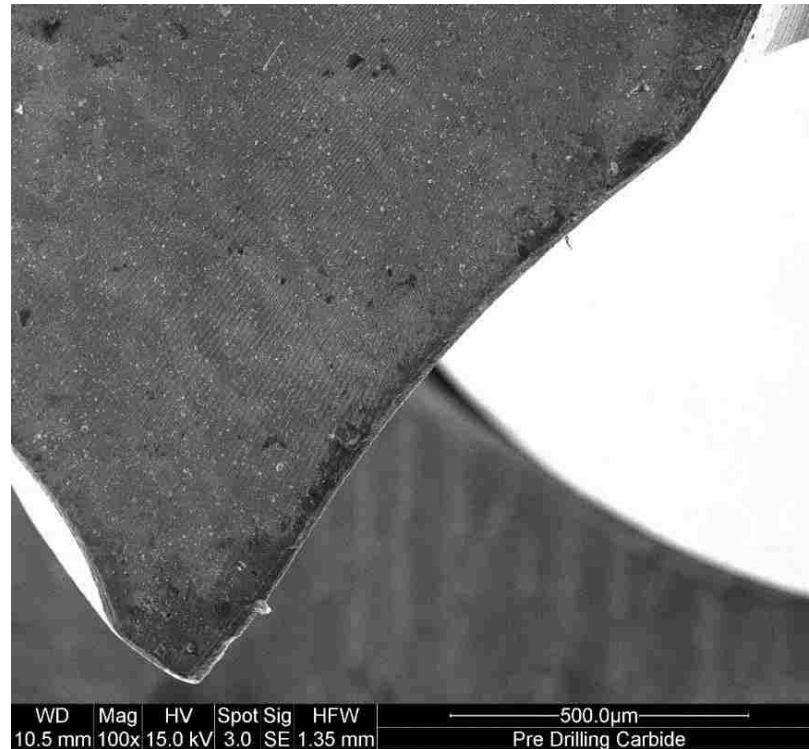
Figure 38. 100x SEM top down view of the carbide chisel edge before drilling.

3.2 Drilling Procedure

3.2.1 Experimental Setup

The experimental setup included a drill press modified so that it may be automated by a computer. The drill press has four motors including the spindle motor. The other three motors were used to control the x, y and z plane of the drill press. The drill press was comprised of the spindle motor, the drill bit, the vice and the chuck. The spindle motor controlled the rotation of the drill bit. The chuck was the component in the drill press which held the shank of the drill bit in place during the experiments. The drill bit is the tool tip that cuts the material. It possessed a diameter of the 4 mm. The vice was bolted down to the infrastructure of the drill bit and held the workpiece material in place during the experiments. The setup is shown in Figure 39. Additionally, the drill press is equipped with

45

a lubrication system and a data acquisition system. The lubrication system consisted of the nozzle, a three-way valve, a small motor, and the reservoir. The nozzle was where the coolant sprays the drill bit in action and when the drill bit is above the workpiece material, the nozzle is shut off by the three-way valve. Additionally, when the drill bit was above the workpiece material, the motor was continually pumping the coolant but the three-way valve switches valves automatically so the coolant was being recycled back into the reservoir rather than cooling the drill bit. The software used in the experiments were Mach3 and instruNet. Mach3 is a CAM software used to CNC holes by programming in G-code to the three planes and the lubricant. InstuNet was used to collect the torque data.

Figure 39. Drilling setup showing the CNC drill press and computer.

3.2.2 Drilling Parameters

The drilling parameters used in this study reflect the industry drilling parameters employed during the drilling of titanium alloys. Drilling parameters include cutting speed, feed rate and coolant spray rate. The cutting speed is the rotational speed of the drill. If the drill bit is too slow or too fast in conjunction with the feed rate, the results can yield excess

wear on the drill bit and premature failure. The feed rate is the rate at which the drill bit approaches the workpiece material. The coolant method can be flood cooling or MQL. Flood cooling is the process of flooding the drill bit and workpiece material so the temperature of the drill bit can be reduced to improve tool life. MQL is the process of using the minimum amount of lubrication to lubricate and prevent heat build up. The feed rate used in this study is 0.05 mm/ rev, the cutting speed used is 500 RPM or 12.56 m/min, and the coolant spray rate used was flooding with a spray rate of 19.8 mL/min.

3.2.3 Drilling Methodology

Firstly, the images of the drill bits are examined under optical microscopy and SEM to get a clear image of the cutting edge and chisel edge. The experiments were conducted by drilling the grade 5 titanium alloy with the HSS drill bit for 60 holes, 20 holes, 15 holes, 10 holes, 5 holes and 1 hole. The 60 holes was to determine the wear over a prolonged period of drilling. The holes from 20 holes to 1 hole were to see the progression of wear. The experiment was then repeated two more times to ensure repeatability and consistent results. Once completed, the procedure was repeated again but with the coated carbide drill bit and then the three-flute drill bit. After that, the material was changed to the powder metallurgy titanium and the procedure was repeated once again. Lastly, the additive manufactured titanium was tested with the same procedure. The data acquisition system was turned on before each experiment as it records the torque of each hole drilled.

3.2.4 Torque Data

The data acquired was then analyzed for each hole and the average torque for each hole was reported in Chapter 4. The analyzing of the torque data consisted of an

examination of the peaks on the graphs plotted from the torque data which were used to interpret the difficulty or ease of chip ejection.

3.3 Imaging

3.3.1 Microscopy

Optical microscopy was used to identify wear on the cutting edges and chisel edge of the drill bit. Further investigation of wear was conducted with the scanning electron microscopy (SEM). SEM uses a focused beam of electrons to scan the surface of the drill bit and the electrons interact with the atoms on the drill bit to produce signals to determine the surface topography and composition. The SEM examinations were used to show key wear features on the drill bit.

3.3.2 Energy Dispersive X-Ray Spectroscopy

EDS is conducted by exciting a sample by shooting it with a focused electron beam which causes the sample to emit x-rays which is then detected by an x-ray detector. The detector measures the difference in energy between the two shells of the atomic structure. The results are compared to a charted spectrum. The drill bits were observed and scanned by the cutting edge where the adhesion was expected. Additionally, the flute view of the drill bit was observed in EDS to confirmed adhesion and wear. After EDS, an imaging software was used to determine the area covered with adhesion on the cutting edge of the drill bit.

3.4 Analysis Methodology

3.4.1 Wear Analysis

Flank wear is determined by measuring the amount of material lost after drilling. The measurements of the flank wear are measured by using an INSIZE digital microscope and the included software. Furthermore, after measuring the flank wear, the samples are observed with SEM and EDS to further examine the adhesion and wear on the cutting edge and chisel edge. EDS is used to confirm the adhesion on the samples. An image analysis software was used to calculate the percentage of titanium adhesion on the cutting edge. The area that was used to calculate the adhesion was a 1000 µm by 200 µm fixed box.

3.4.2. Chip Analysis

The chip morphology of the different titanium alloys were collected and analyzed after drilling them with the HSS drill bit, three flute drill bit and the carbide drill bit. This was used for an improved understanding of the machinability of the alloys and tool wear. Chips were examined after the 1st, 5th, 10th, 15th, 20th and the last hole drilled.

Chapter 4: Experimental Results

This chapter outlines the results obtained through experiments following the procedure in chapter 3. The test results are split into two categories, wear, and torque. The wear section consists of flank wear, chisel wear and adhesion.

4.1 Wear of High Speed Steel Twist Drill Bit

4.1.1 Ti-6Al-4V

After drilling 1 hole, 5 holes, 10 holes, 15 holes, 20 holes, and 60 holes in the grade 5 titanium the flank wear of the drill bit was measured and summed into a table shown in Table 7. The progression from hole 1 to hole 60 shows an increase of flank wear on the cutting edge.

Table 7. Grade 5 Titanium Alloy (Ti-6Al-4V) Flank Wear on the cutting edge after drilling various number of holes.

	HSS-60 holes	HSS-20 holes	HSS-15 holes	HSS-10 holes	HSS-5 holes	HSS-1 hole
Average Wear (mm)	0.045	0.044	0.040	0.039	0.037	0.032
Std. Dev. (mm)	0.012	0.011	0.010	0.010	0.019	0.017

Figure 40. 30x SEM top down view of the HSS drill bit after drilling 60 holes in grade 5 titanium (Ti-6Al-4V).

Figure 40 to Figure 46 shows the SEM images taken after drilling 60 holes in grade 5 titanium (Ti-6Al-4V). The SEM images highlight the flank wear and adhesion (circled) on the cutting edge at various magnifications from 50x to 500x from the top view and the flute view. Additionally, the chisel edge is shown to further emphasize the adhesion during drilling titanium alloys.

Figure 41. 250x SEM view of the HSS drill bit chisel edge after drilling 60 holes in grade 5 titanium (Ti-6Al-4V).
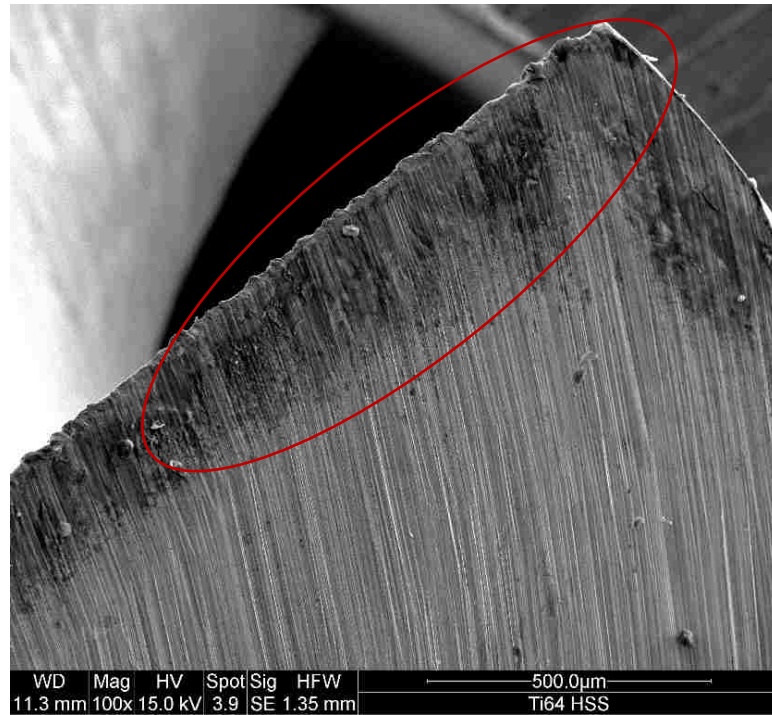
Figure 42. 100x SEM view of the HSS drill bit cutting edge after drilling 60 holes in grade 5 titanium (Ti-6Al-4V).
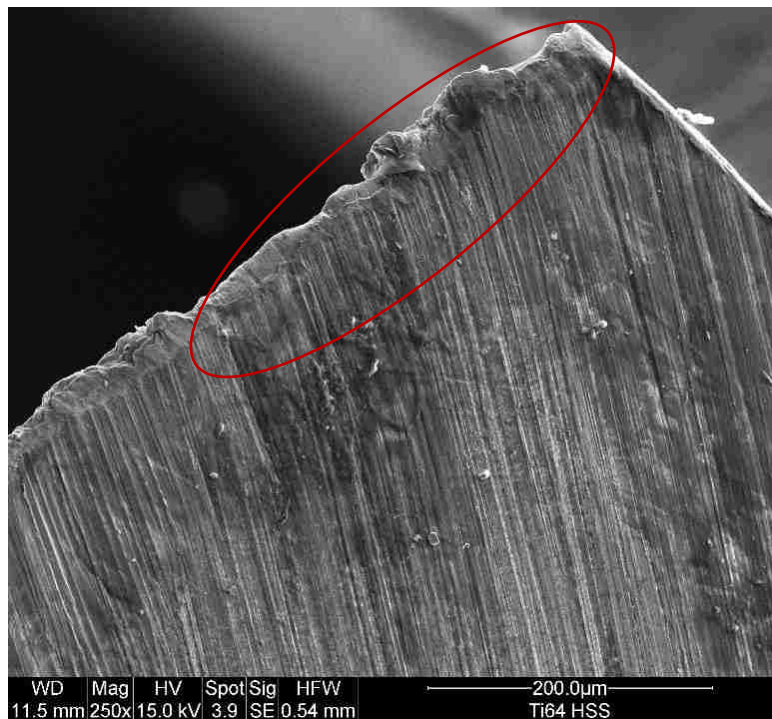
Figure 43. 250x SEM view of the HSS drill bit cutting edge after drilling 60 holes in grade 5 titanium (Ti-6Al-4V).

52
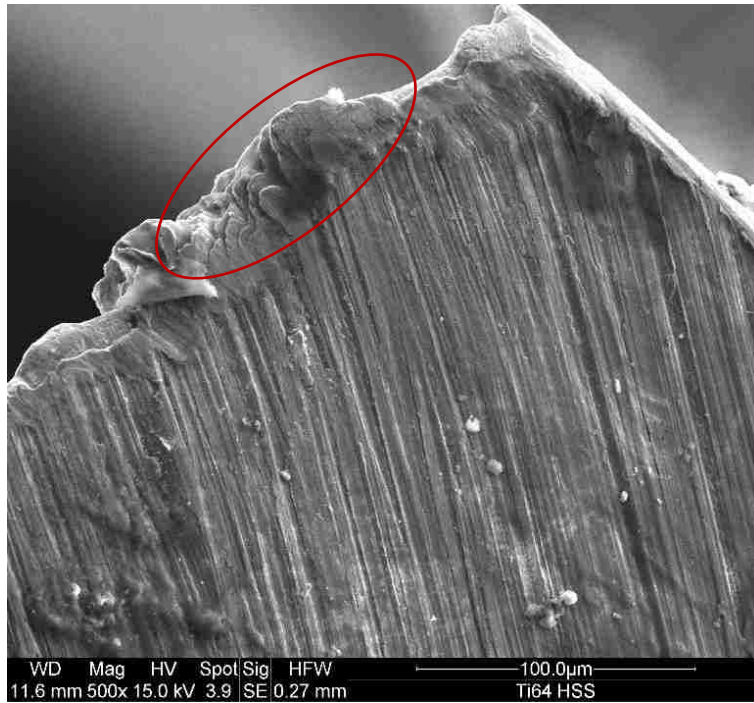
Figure 44. 500x SEM view of the HSS drill bit cutting edge after drilling 60 holes in grade 5 titanium (Ti-6Al-4V).
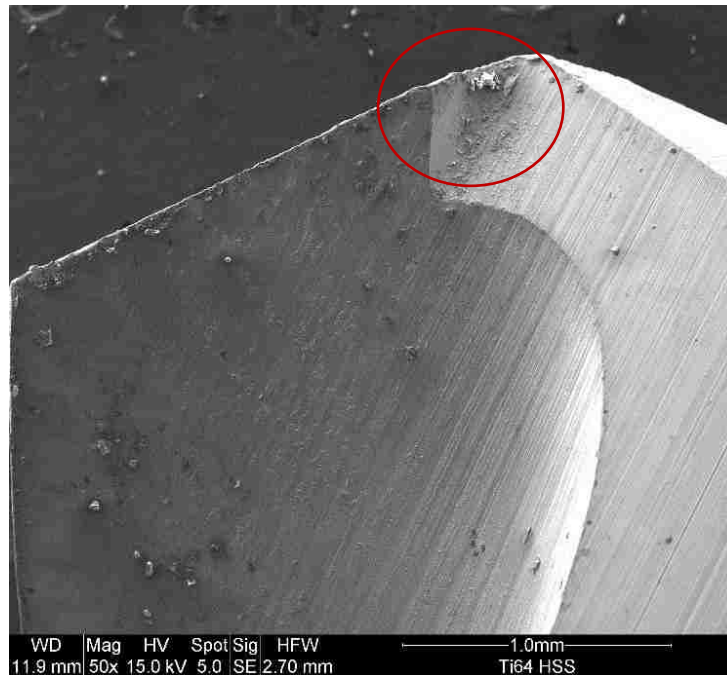
Figure 45. 50x SEM flute view of the HSS drill bit cutting edge after drilling 60 holes in grade 5 titanium (Ti-6Al-4V).

53
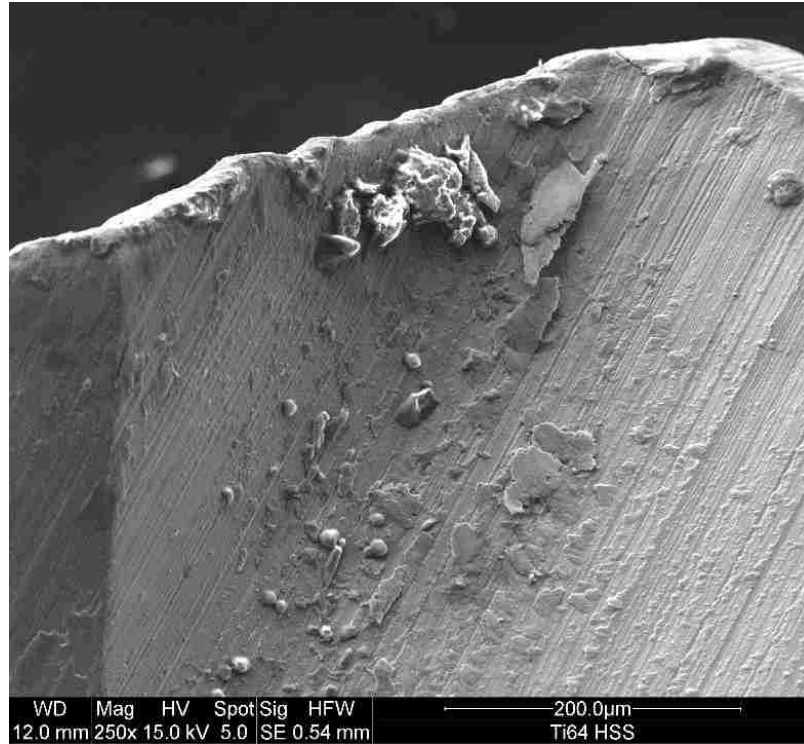
Figure 46. 250x SEM view of the HSS drill bit cutting edge after drilling 60 holes in grade 5 titanium (Ti-6Al-4V).
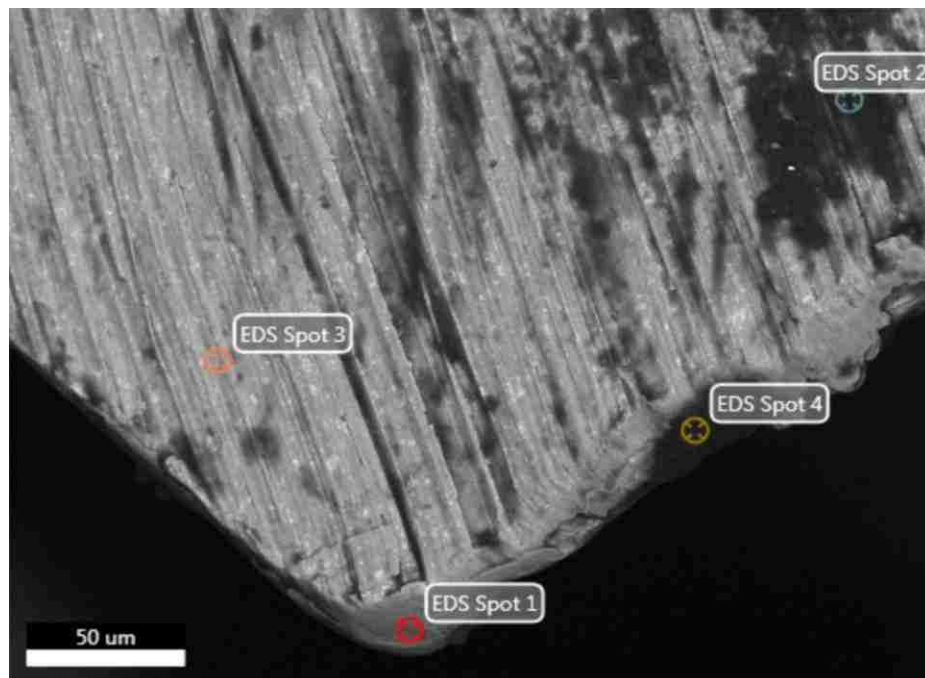
Figure 47. EDS spot analysis of the HSS drill bit cutting edge after drilling 60 holes in grade 5 titanium (Ti-6Al-4V).

54

Figure 47 and Figure 48 show the EDS spot analysis of the drill bit. Referring to Figure 48 (A), spot 1 confirms the adhesion on the cutting edge, while spot 3 in Figure 48 (C) shows the material of the drill bit composing of iron. Figure 49 shows the overlay of titanium and iron. This EDS map shows where the adhesion occurred on the drill bit from the flute view.
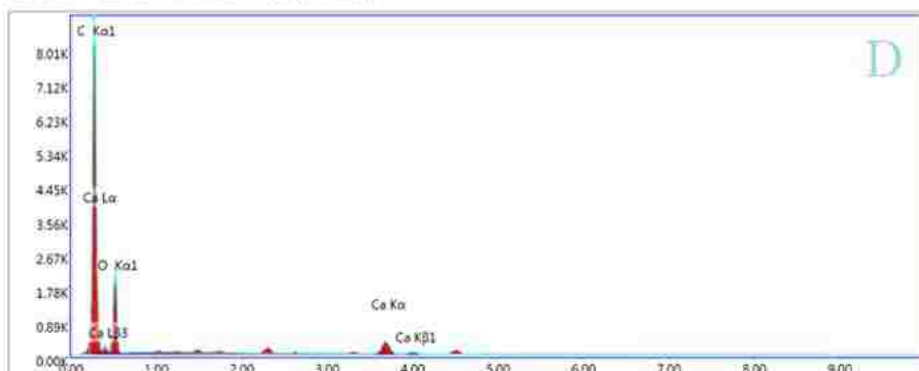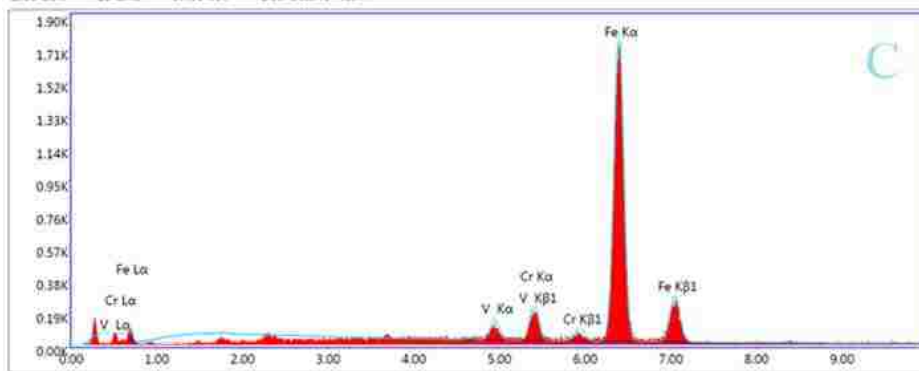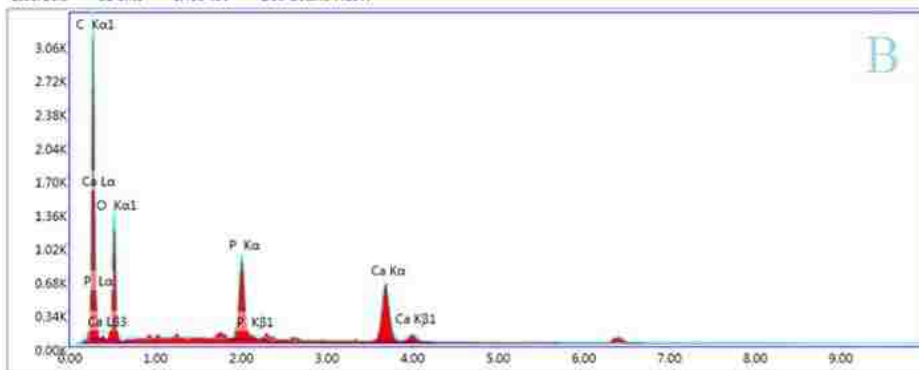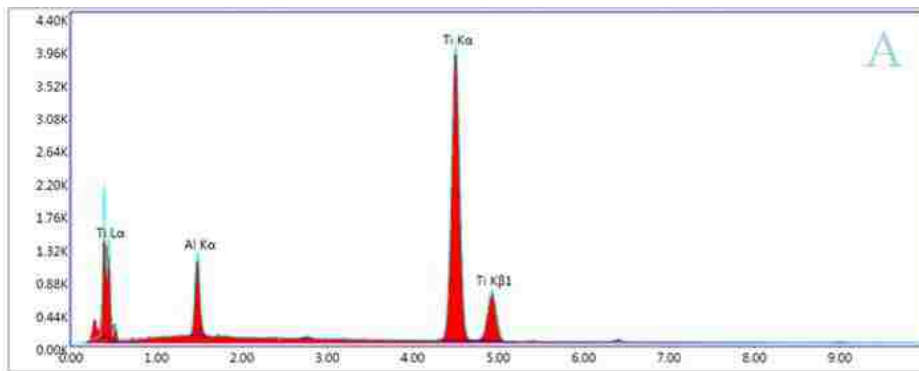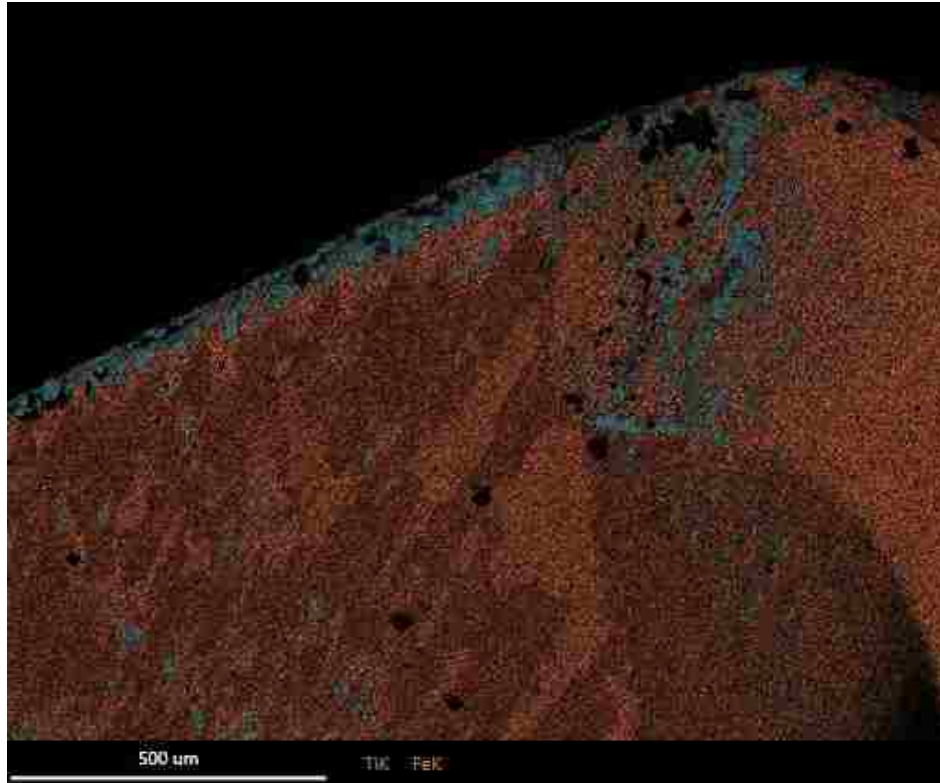
Figure 49. EDS mapping of the HSS drill bit cutting edge after drilling 60 holes in grade 5 titanium (Ti-6Al-4V).

4.1.2 Powder Metallurgy Titanium

After drilling 1 hole, 5 holes, 10 holes, 15 holes, 20 holes, and 60 holes in the grade 5 titanium the flank wear of the drill bit was measured and summed into a table shown in Table 8. The progression of the flank wear on the cutting edge increased as the number of holes increased for the HSS drill bit.

Table 8. PM Titanium Flank Wear on the cutting edge after drilling various number of holes.

	HSS-60 holes	HSS-20 holes	HSS-15 holes	HSS-10 holes	HSS-5 holes	HSS-1 hole
Average Wear (mm)	0.072	0.070	0.059	0.059	0.056	0.052
Std. Dev. (mm)	0.012	0.022	0.013	0.019	0.013	0.020
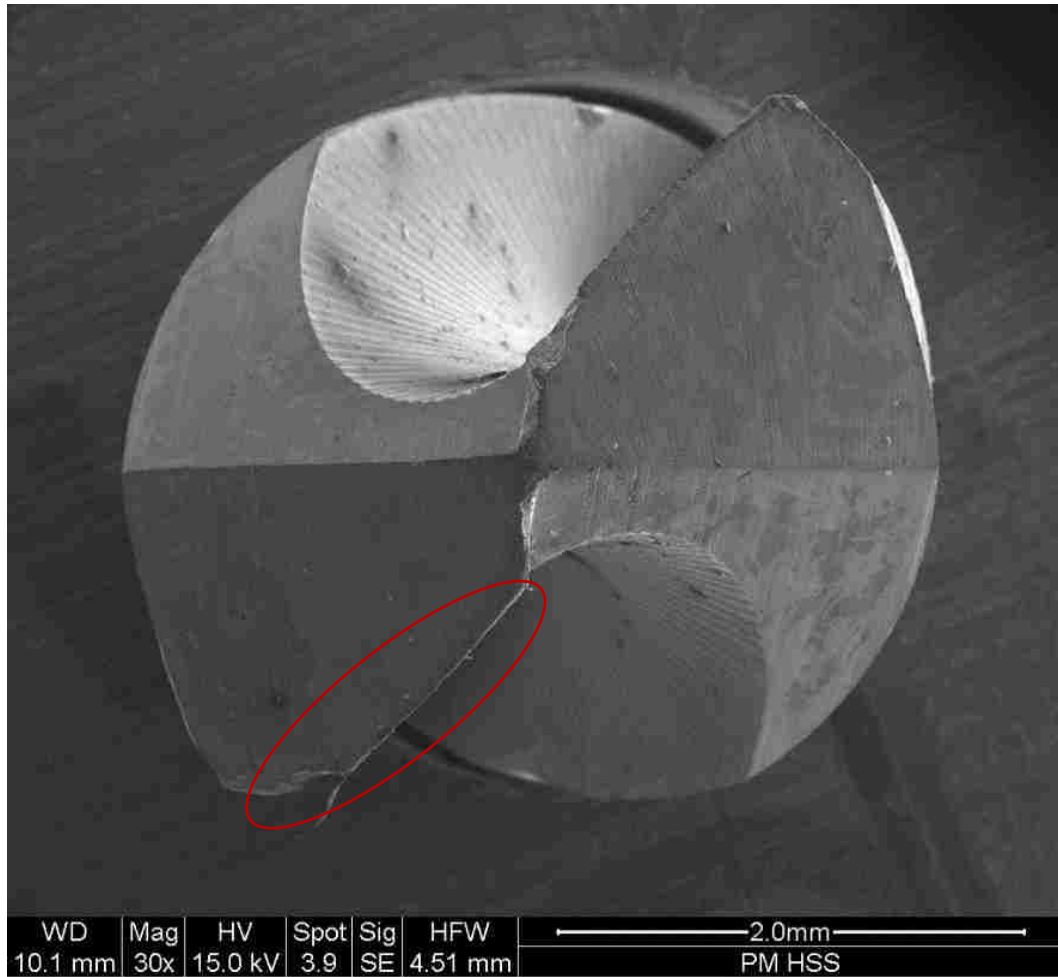
Figure 50. 30x SEM top down view of the HSS drill bit after drilling 60 holes in PM titanium.

Figure 50 to Figure 56 shows the SEM images taken after drilling 60 holes in PM titanium. The SEM highlights the flank wear and adhesion (circled) on the cutting edge at various magnifications from 50x to 500x from the top view and the flute view. Additionally, the chisel edge is shown in Figure 51 to further emphasize the adhesion during drilling titanium alloys. Figure 52 showed chipping and adhesion on the cutting edge while Figure 55 showed chipping on the cutting edge near the chisel edge of the HSS drill bit.

58
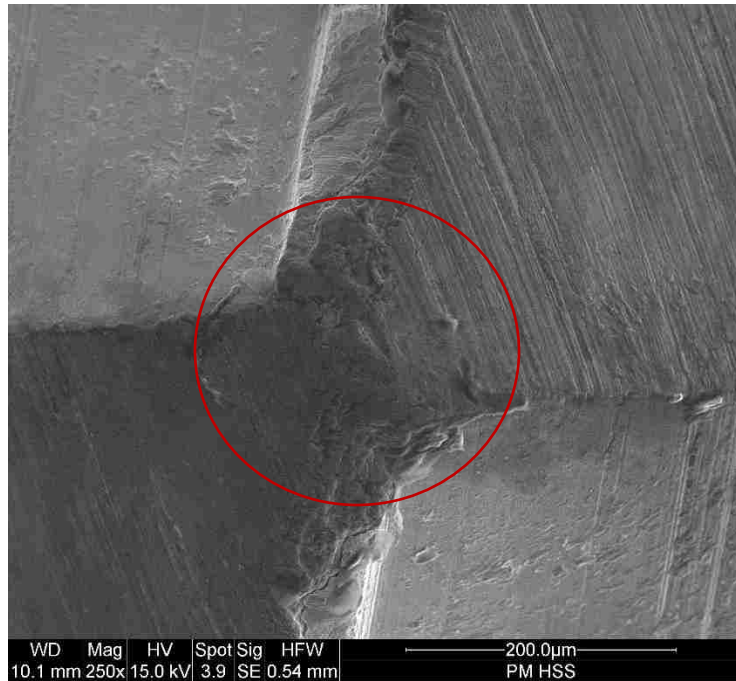
Figure 51. 250x SEM top down view of the chisel edge of the HSS drill bit after drilling 60 holes in PM titanium.
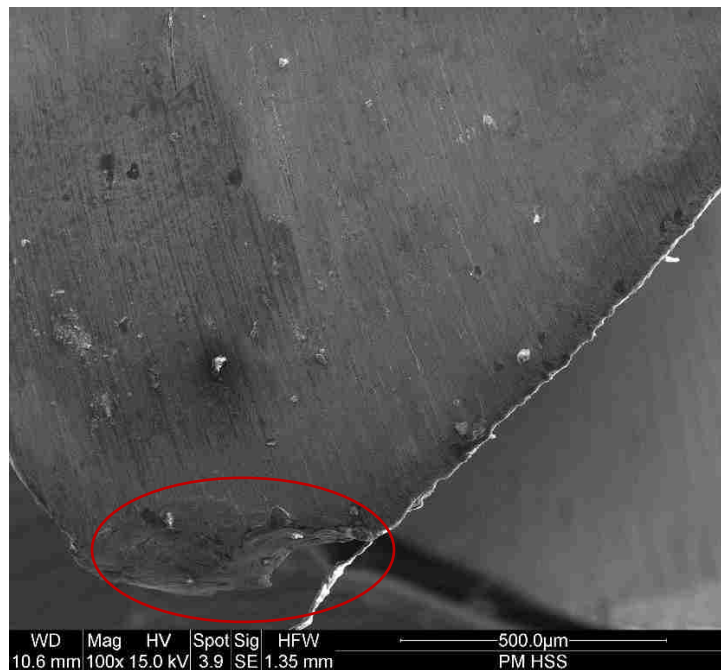
Figure 52. 100x SEM top down view of cutting edge HSS drill bit after drilling 60 holes in PM titanium.
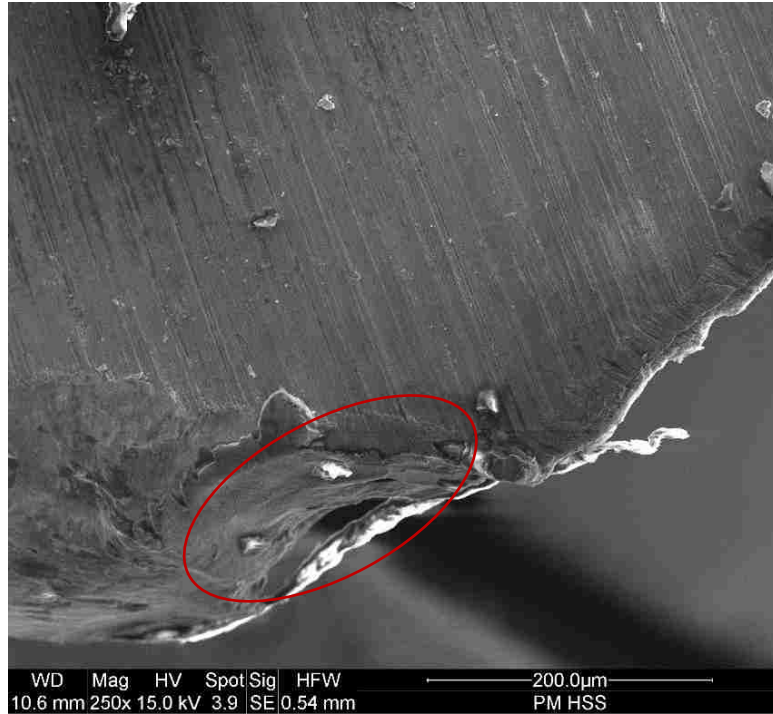
Figure 53. 250x SEM top down view of cutting edge HSS drill bit after drilling 60 holes in PM titanium.
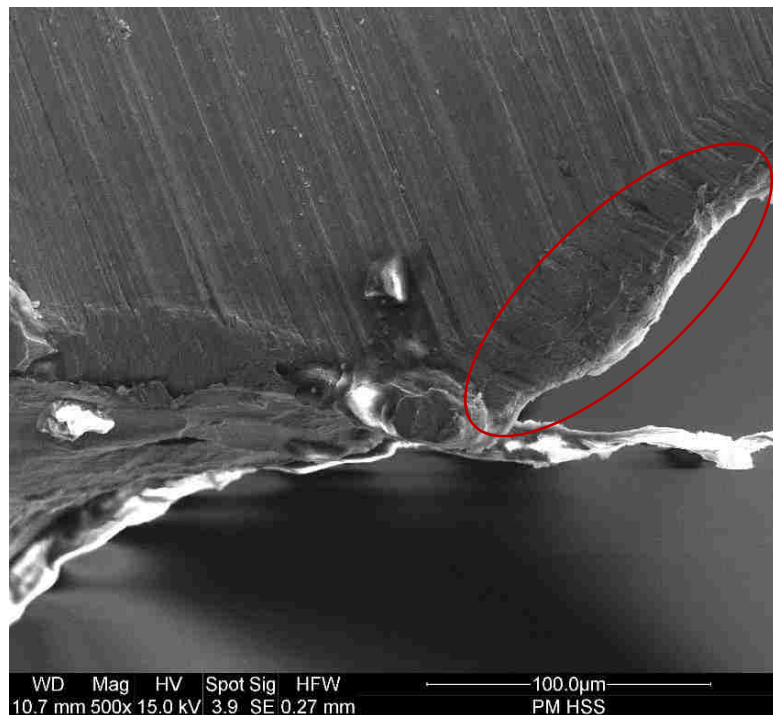
Figure 54. 500x SEM top down view of cutting edge HSS drill bit after drilling 60 holes in PM titanium.
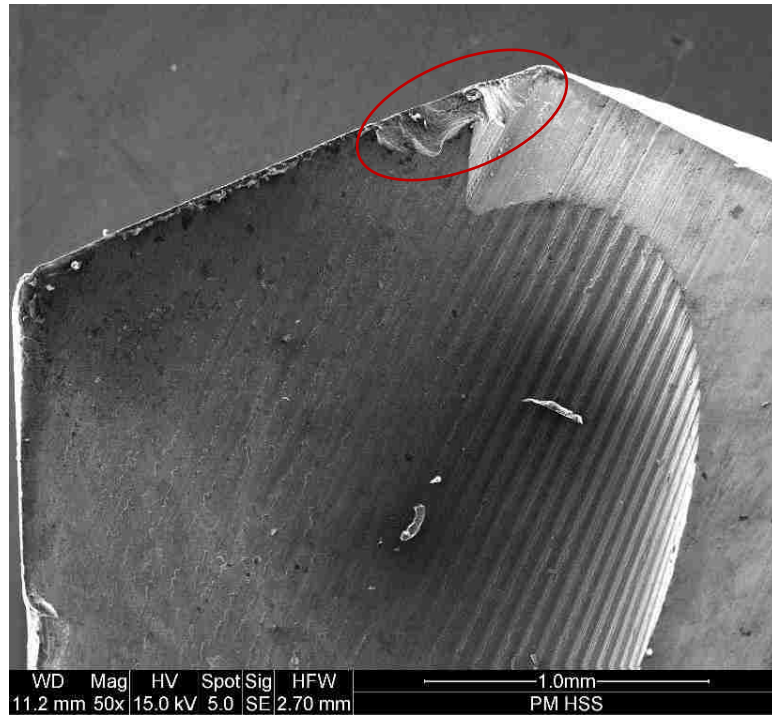
Figure 55. 50x SEM flute view of cutting edge HSS drill bit after drilling 60 holes in PM titanium.
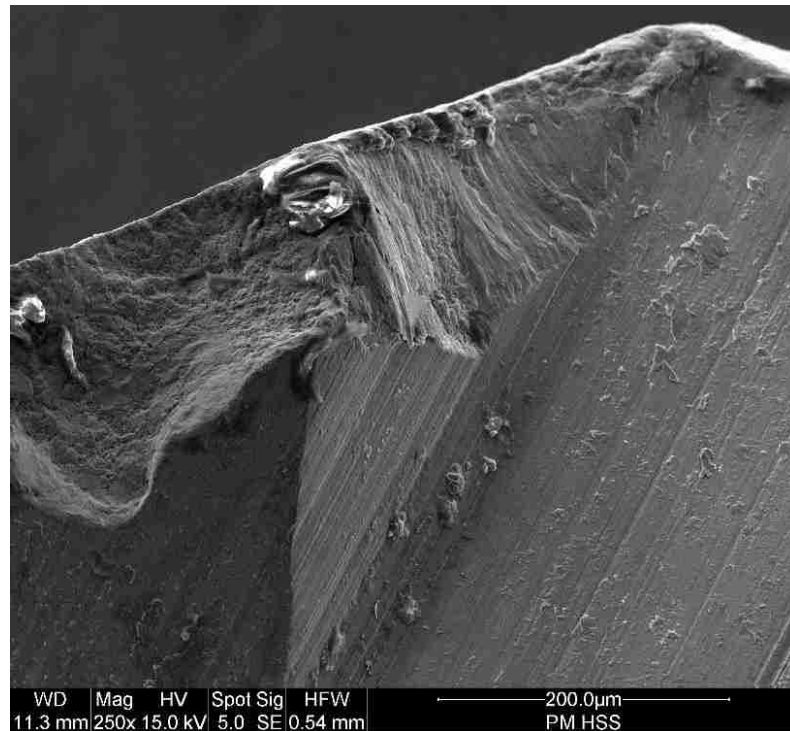
Figure 56. 250x SEM flute view of cutting edge HSS drill bit after drilling 60 holes in PM titanium.
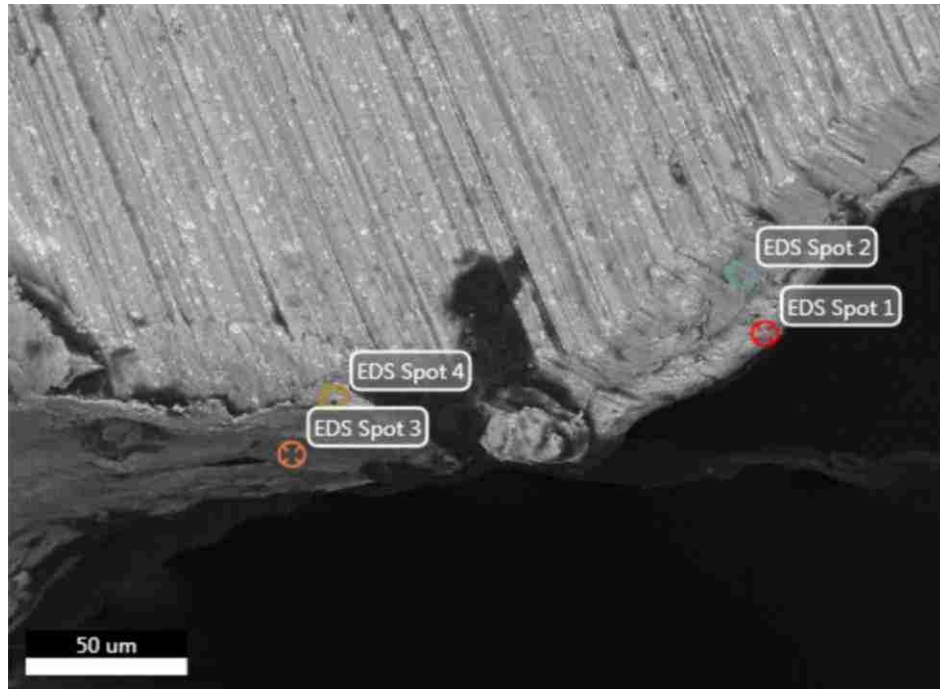
Figure 57. EDS spot analysis of the HSS drill bit cutting edge after drilling 60 holes in PM titanium.

Figure 57 and Figure 58 show the EDS spot analysis of the HSS drill bit. Referring to Figure 57 (B), spot 2 confirms the adhesion on the cutting edge, while spot 1 in Figure 57 (A) shows the material of the drill bit. Figure 59 shows the overlay of titanium and iron. Figure 59 shows the flute view of the HSS drill bit where the titanium is shown as cyan, iron is shown as brown and oxygen is shown as green. This EDS map shows where the adhesion occurred on the drill bit from the flute view.
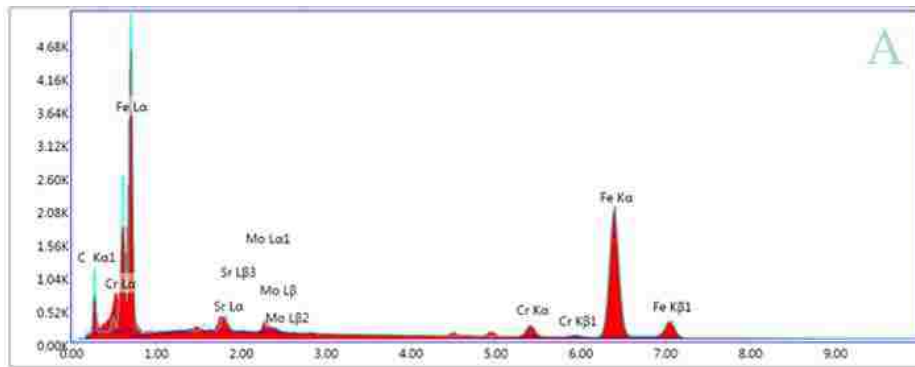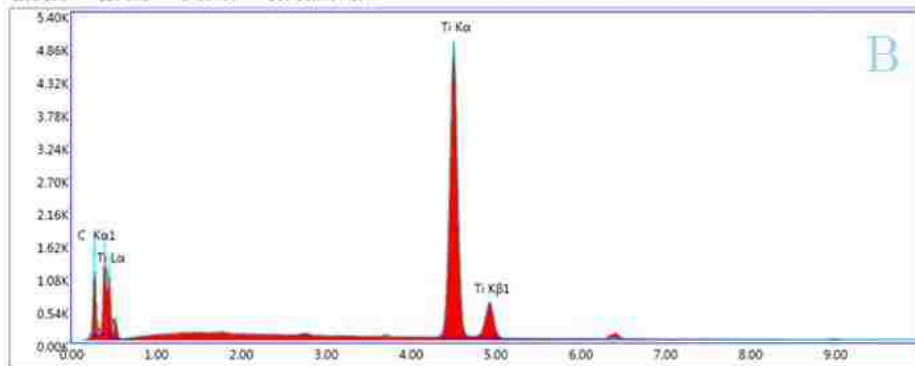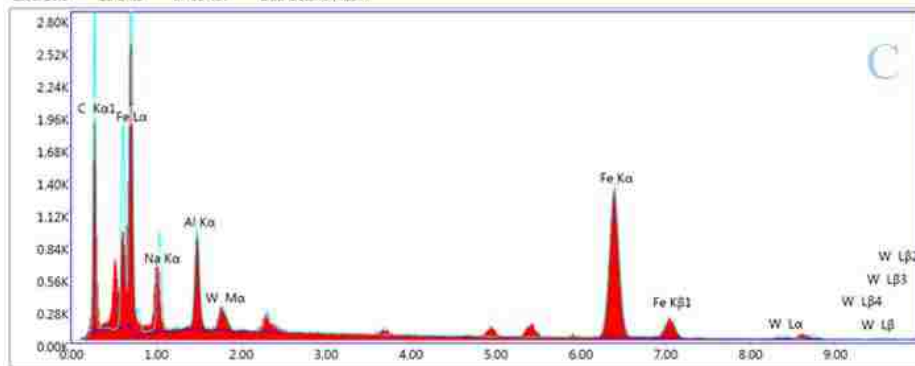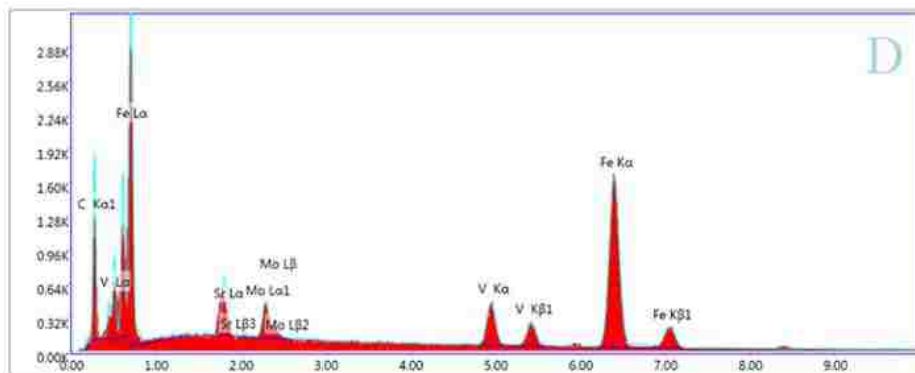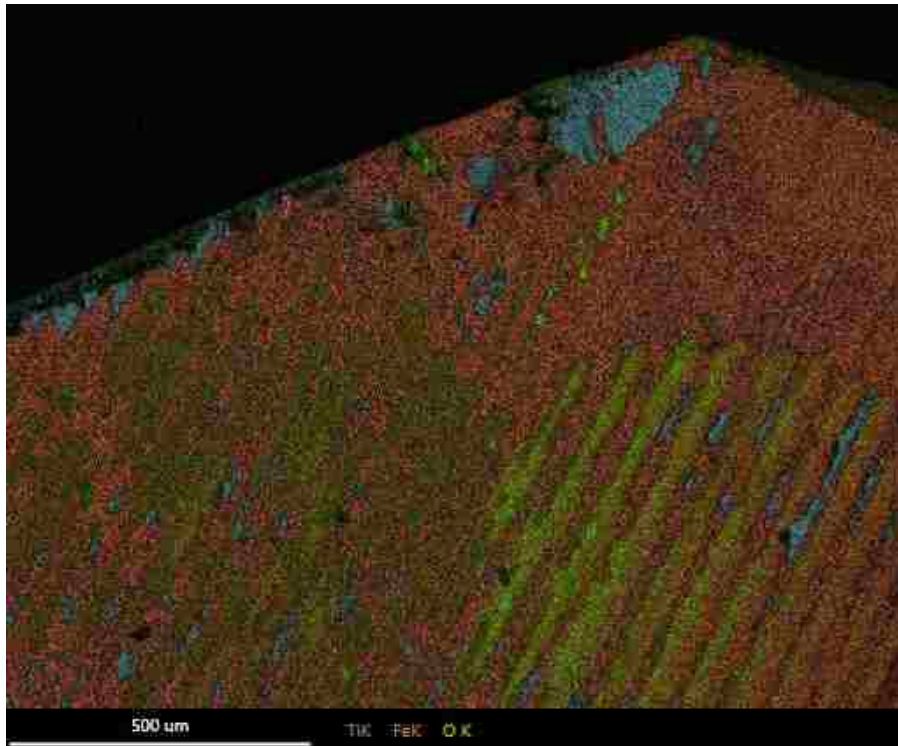
Figure 59. EDS mapping of the HSS drill bit cutting edge after drilling 60 holes in PM titanium.

4.1.3 Additive Manufactured Titanium

Attempting to drill for 60 holes, the drill failed twice at eight holes and once at three holes afterward. After failing at eight holes in the AM titanium the flank wear of the drill bit is shown in Figure 60. The wear for the HSS drill bit when drilling additive manufactured titanium resulted with an average wear of 0.372 mm.
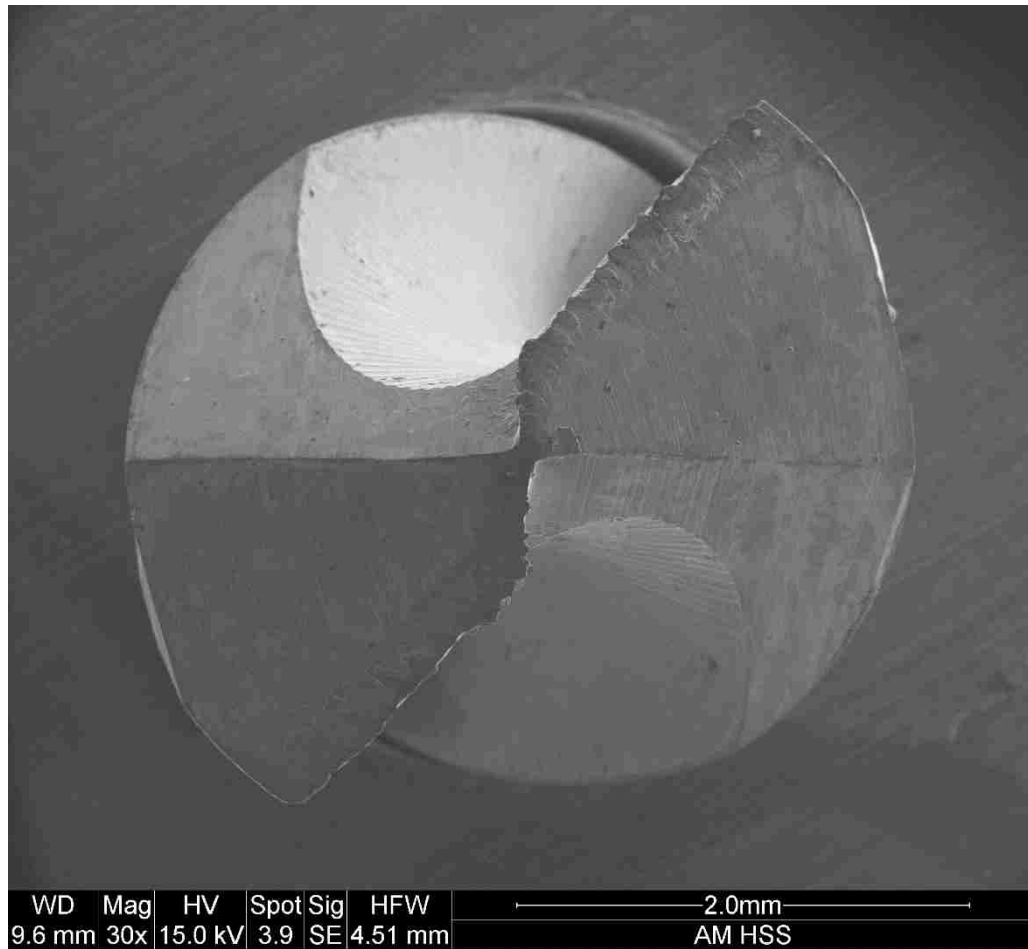
Figure 60. 30x SEM top down view of the HSS drill bit after failing at hole 8 when drilling AM titanium.

Figure 60 to Figure 66 shows the SEM images of the HSS drill bit after failing at eight holes when drilling AM titanium. The SEM highlights the flank wear and adhesion on the cutting edge at various magnifications from 50x to 500x from the top view and the flute view. Additionally, the chisel edge is shown to further emphasize the adhesion during drilling titanium alloys.
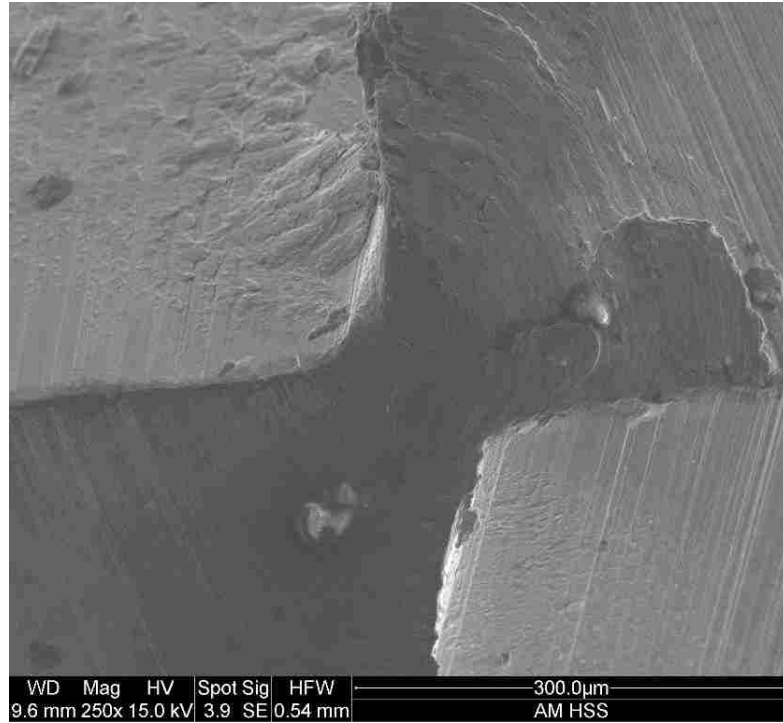
Figure 61. 250x SEM top down view of the HSS drill bit chisel edge after failing at hole 8 when drilling AM titanium.
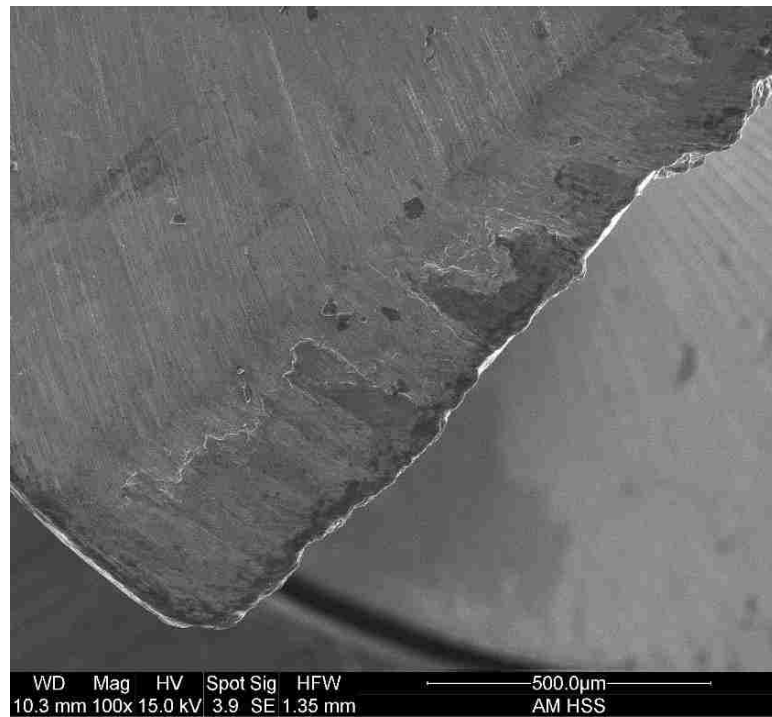
Figure 62. 100x SEM top down view of the HSS drill bit cutting edge after failing at hole 8 when drilling AM titanium.

66

Figure 63. 250x SEM top down view of the HSS drill bit cutting edge after failing at hole 8 when drilling AM titanium.
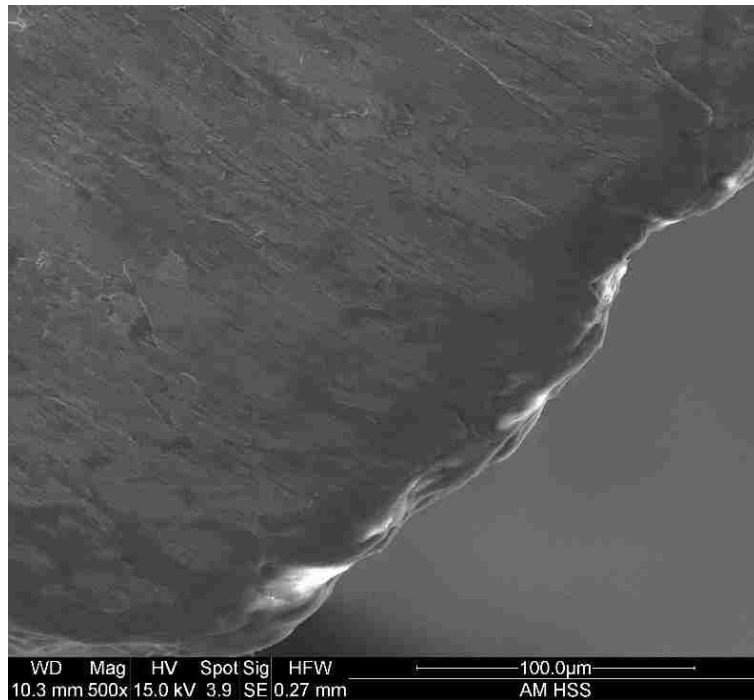
Figure 64. 500x SEM top down view of the HSS drill bit cutting edge after failing at hole 8 when drilling AM titanium.

67
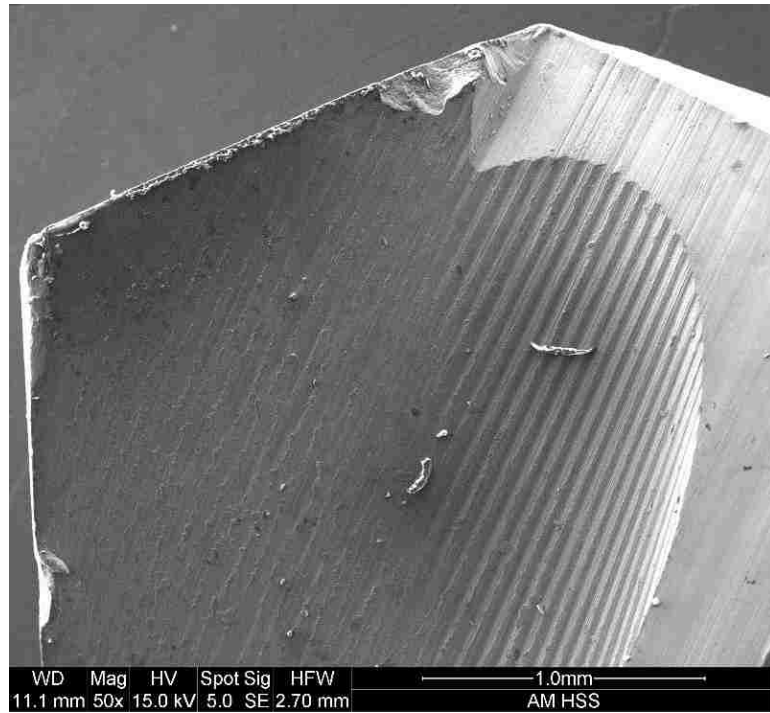
Figure 65. 50x SEM flute view of cutting edge HSS drill bit after drilling 60 holes in AM titanium.
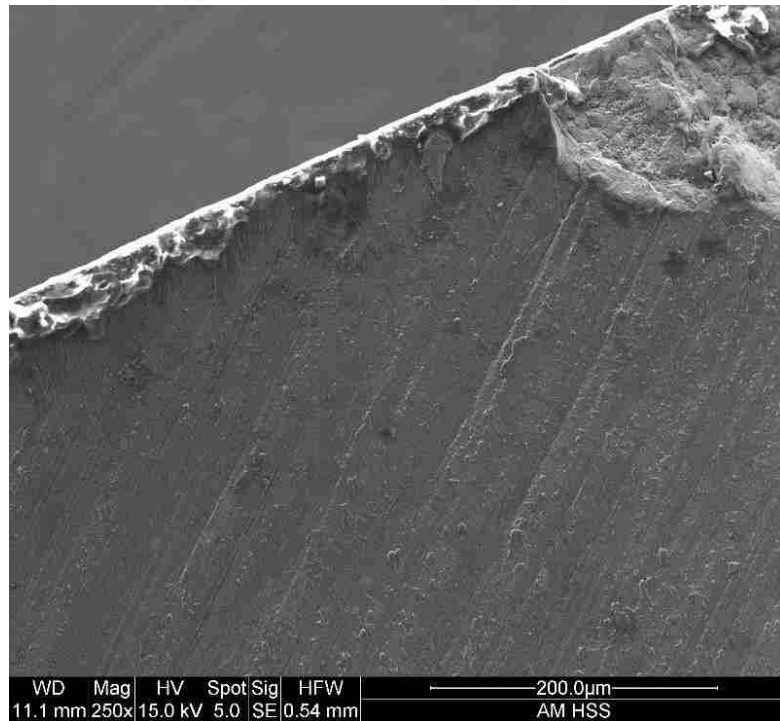
Figure 66. 250x SEM flute view of cutting edge HSS drill bit after drilling 60 holes in AM titanium.
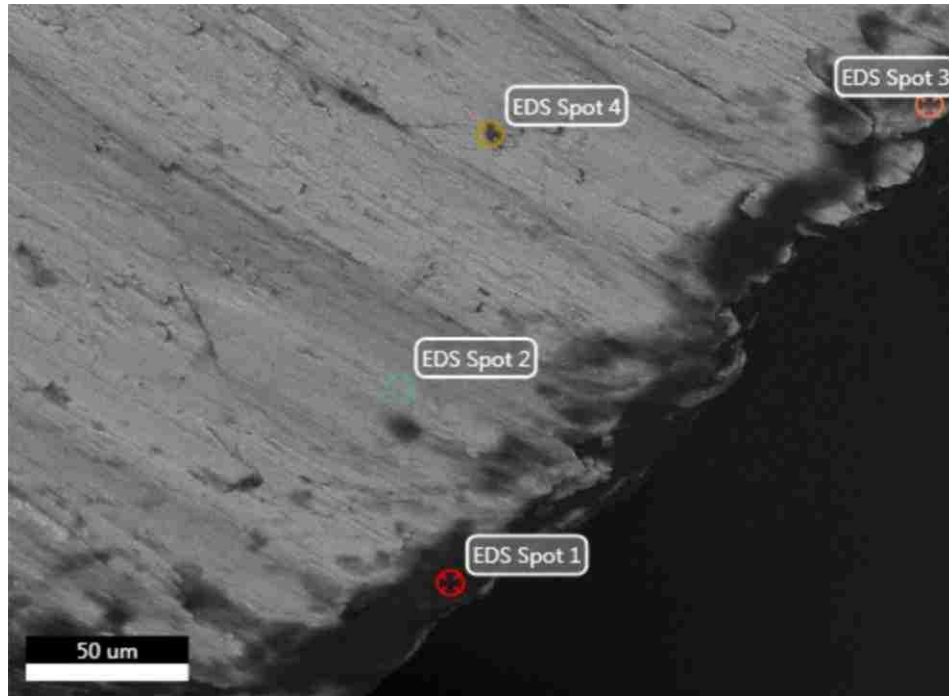
Figure 67. EDS spot analysis of the HSS drill bit cutting edge after failing at hole 5 when drilling AM titanium.

Figure 67 and Figure 68 show the EDS spot analysis of the drill bit. Referring to Figure 68 (B), spot 2 confirms the adhesion on the cutting edge, while Figure 68 (C), (D), respectively known as spot 3 and spot 4 attempt to show the material of the drill bit but is covered with titanium adhesion. Figure 69 shows the overlay of titanium and iron. The titanium is shown for the adhesion on the drill bit while the iron is shown for the main component of the drill bit. This EDS map shows where the adhesion occurred on the drill bit from the flute view.
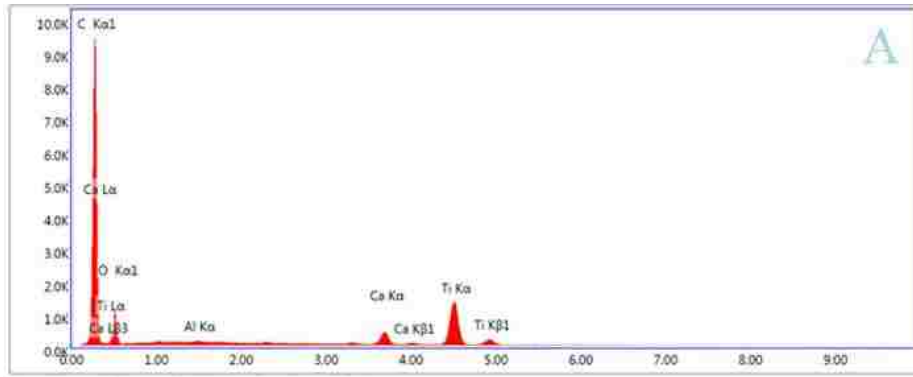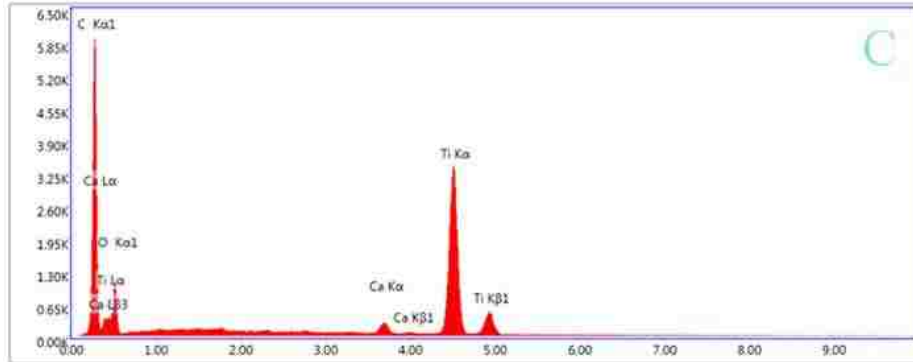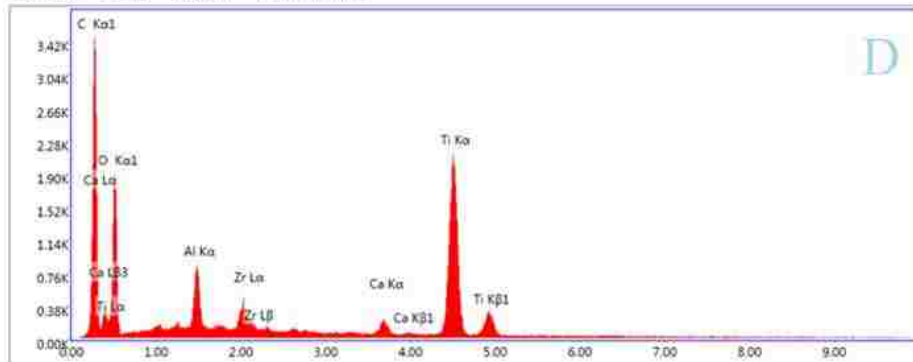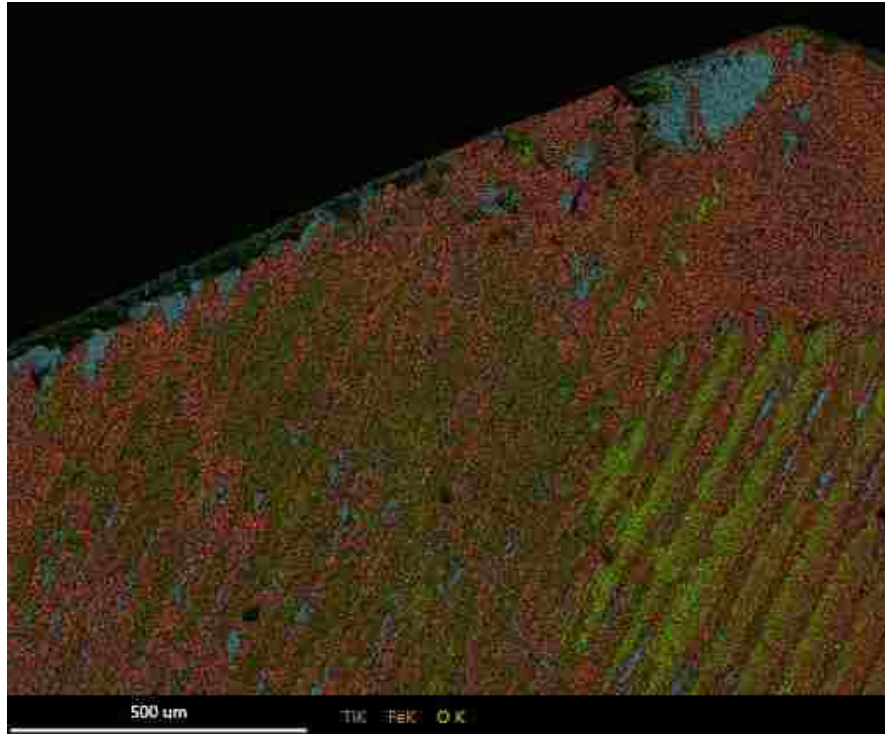
Figure 69. EDS mapping of the HSS drill bit cutting edge after failing at hole 8 when drilling AM titanium.

4.2 Wear of Three Flute Drill Bit

Depending on the titanium alloy, the drilling methodology for the carbide drill bit varied pertaining the number of holes drills due to the failure of the drill.

4.2.1 Ti-6Al-4V

After drilling 60 holes in the grade 5 titanium the flank wear of the drill bit is measured to be an average of 0.168 ± 0.053 mm.
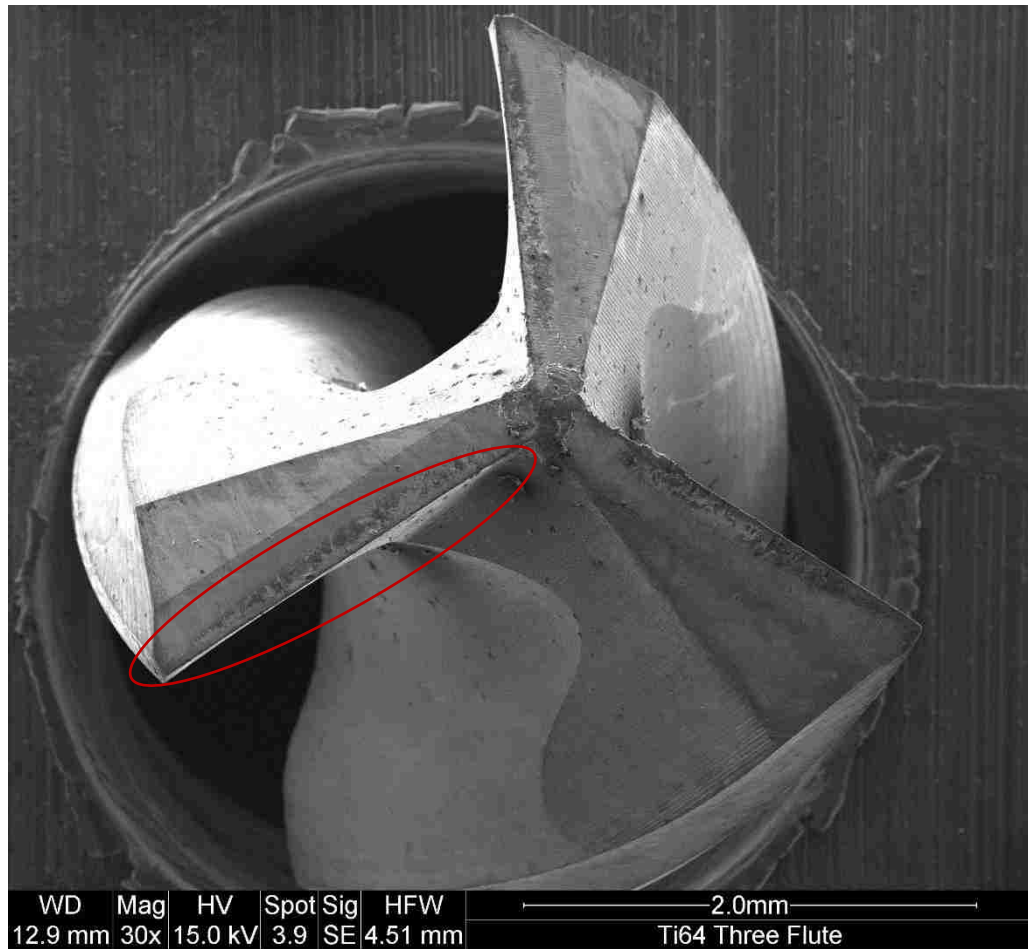
Figure 70. 30x SEM top down view of the three flute drill bit after drilling 60 holes in grade 5 titanium (Ti-6Al-4V).

Figure 70 to Figure 76 shows the SEM images taken after drilling 60 holes in grade 5 titanium (Ti-6Al-4V). The SEM highlights the flank wear and adhesion on the cutting edge at various magnifications from 50x to 500x from the top view and the flute view. Additionally, the chisel edge is shown to further emphasize the adhesion during drilling titanium alloys in Figure 71.
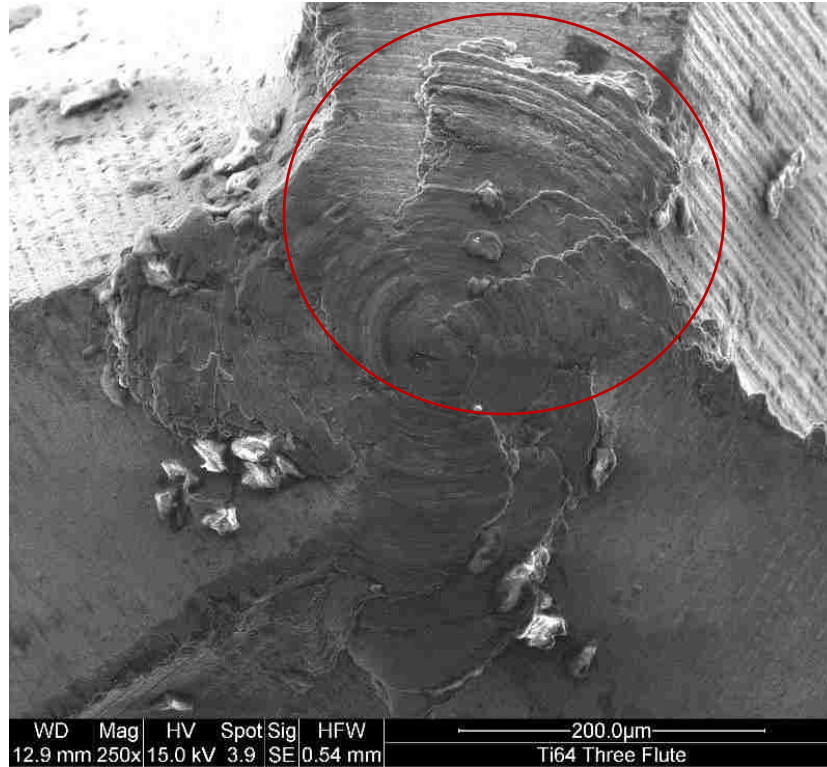
Figure 71. 250x SEM top down view of the three flute drill bit chisel edge after drilling 60 holes in grade 5 titanium (Ti-6Al-4V).

Figure 77 and Figure 78 show the EDS spot analysis of the drill bit. Referring to Figure 78 (B), spot 2 confirms the adhesion on the cutting edge, while spot 3 from Figure 78 (C), shows the material of the drill bit composing of tungsten. Referring to Figure 79, the EDS overlay map is shown where titanium is the cyan and tungsten is the brown. The EDS overlay map shows the titanium is adhered onto the drill bit which is made of tungsten.
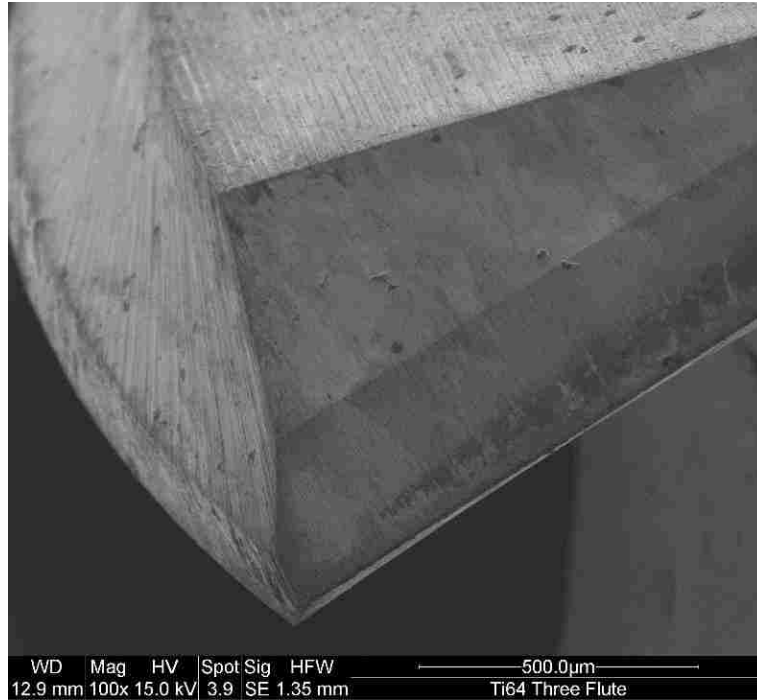
Figure 72. 100x SEM top down view of the three flute drill bit cutting edge after drilling 60 holes in grade 5 titanium (Ti-6Al-4V).
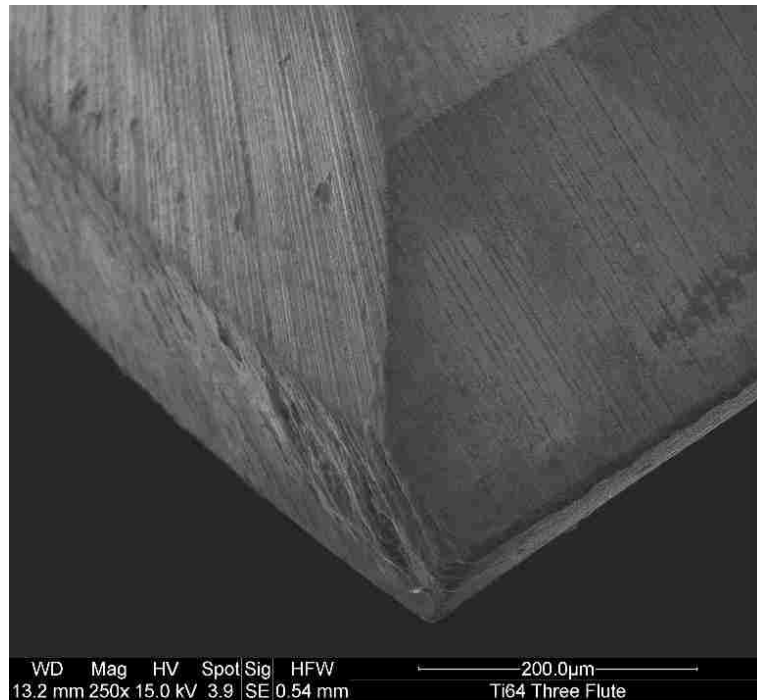
Figure 73. 250x SEM top down view of the three flute drill bit cutting edge after drilling 60 holes in grade 5 titanium (Ti-6Al-4V).

74

Figure 74. 500x SEM top down view of the three flute drill bit cutting edge after drilling 60 holes in grade 5 titanium (Ti-6Al-4V).

Figure 75. 50x SEM flute view of the three flute drill bit cutting edge after drilling 60 holes in grade 5 titanium (Ti-6Al-4V).

Figure 76. 250x SEM flute view of the three flute drill bit cutting edge after drilling 60 holes in grade 5 titanium (Ti-6Al-4V).

Figure 77. EDS spot analysis of the three flute drill bit cutting edge after drilling 60 holes in grade 5 titanium (Ti-6Al-4V).
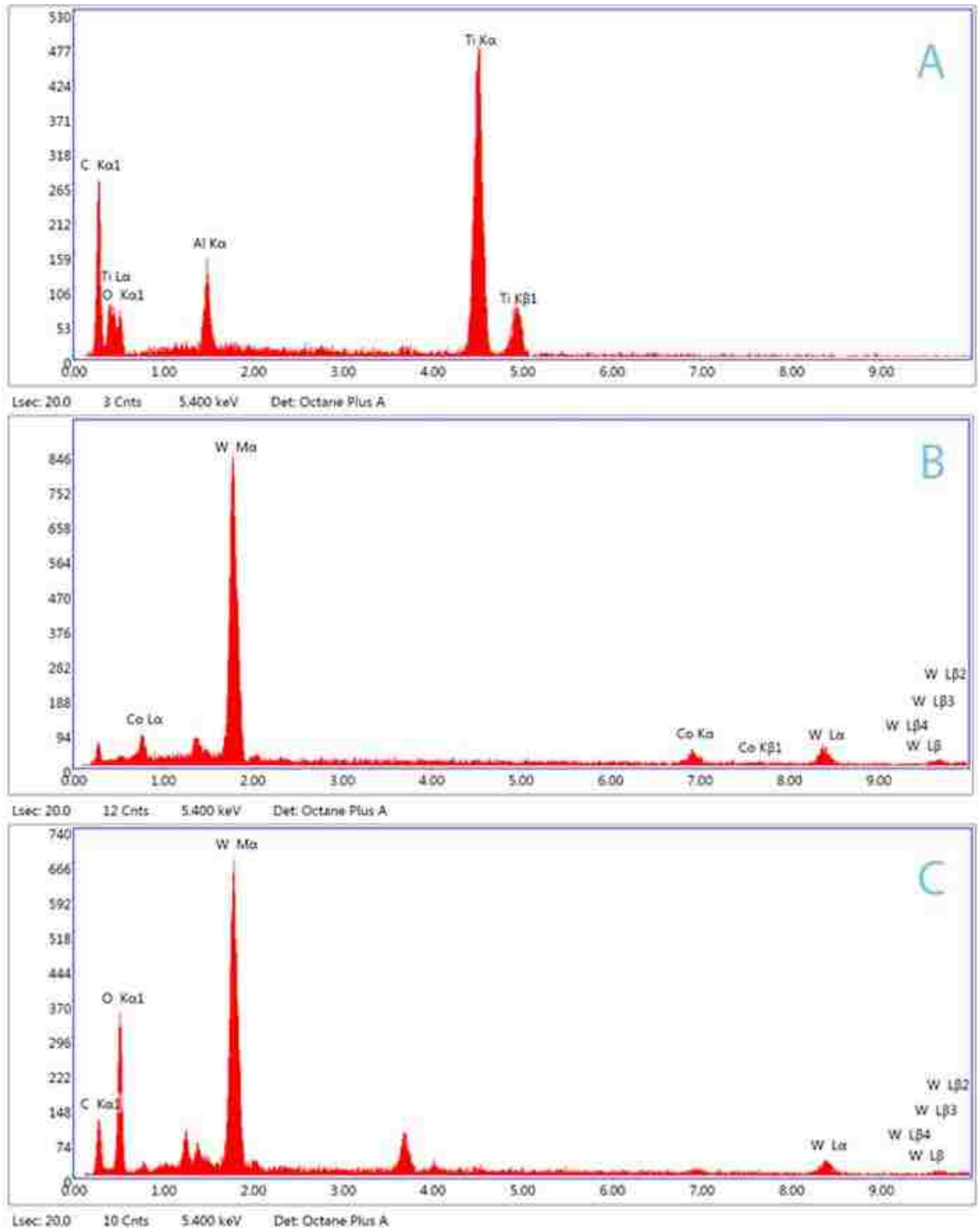
Figure 78. EDS spot analysis of the three flute drill bit after drilling 60 holes in grade 5 titanium (Ti-6Al-4V) where, (A) is Spot 1, (B) is Spot 2, (C) is Spot 3, (D) is Spot 4.
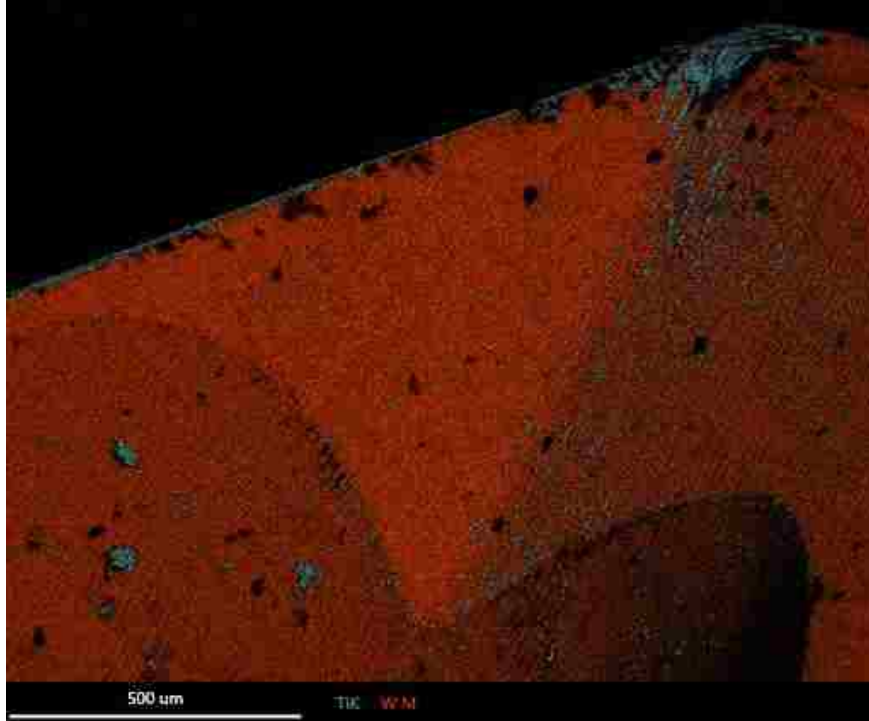
*Figure 79. EDS mapping of the three flute drill bit cutting edge after drilling 60 holes in grade 5 titanium (Ti-6Al-4V).*

4.2.2 Powder Metallurgy Titanium

After drilling 60 holes in the PM titanium workpiece, the flank wear of the drill bit measured to be an average of 0.075 ± 0.053 mm. Figure 80 to Figure 86 shows the SEM images taken after drilling 60 holes in PM titanium. The SEM highlights the flank wear and adhesion on the cutting edge at various magnifications from 50x to 500x from the top view and the flute view. Additionally, the chisel edge is shown to further emphasize the adhesion during drilling titanium alloys.
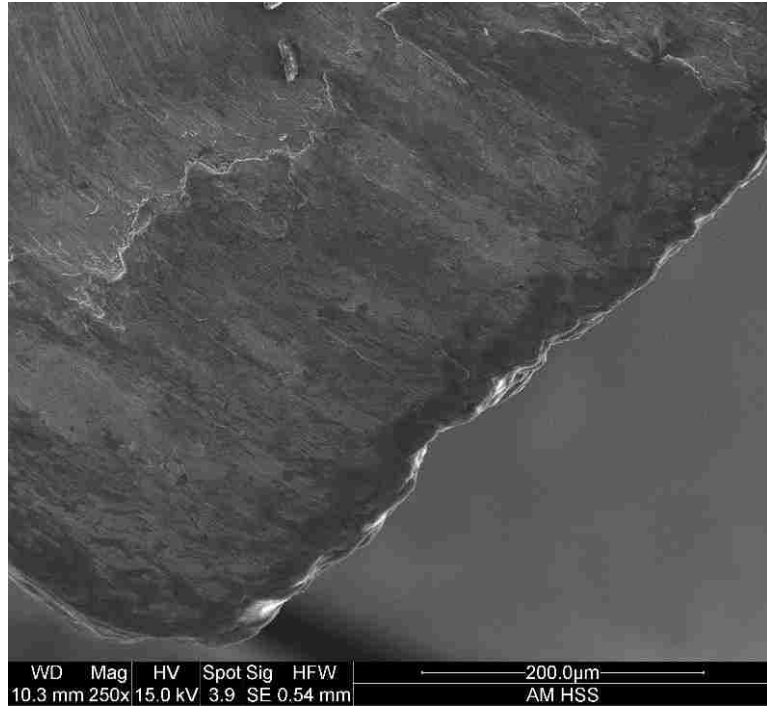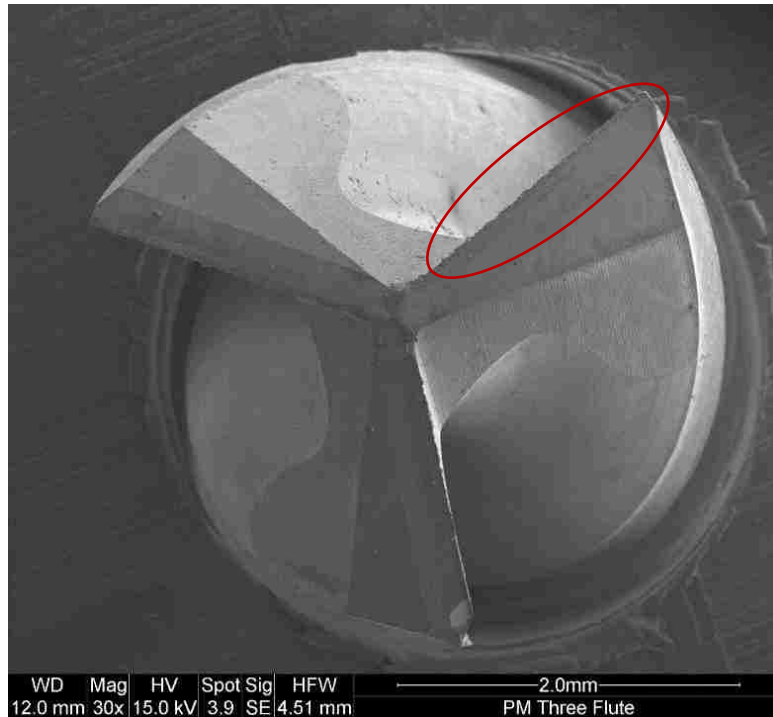
Figure 80. 30x SEM top down view of the three flute drill bit after drilling 60 holes in PM titanium.
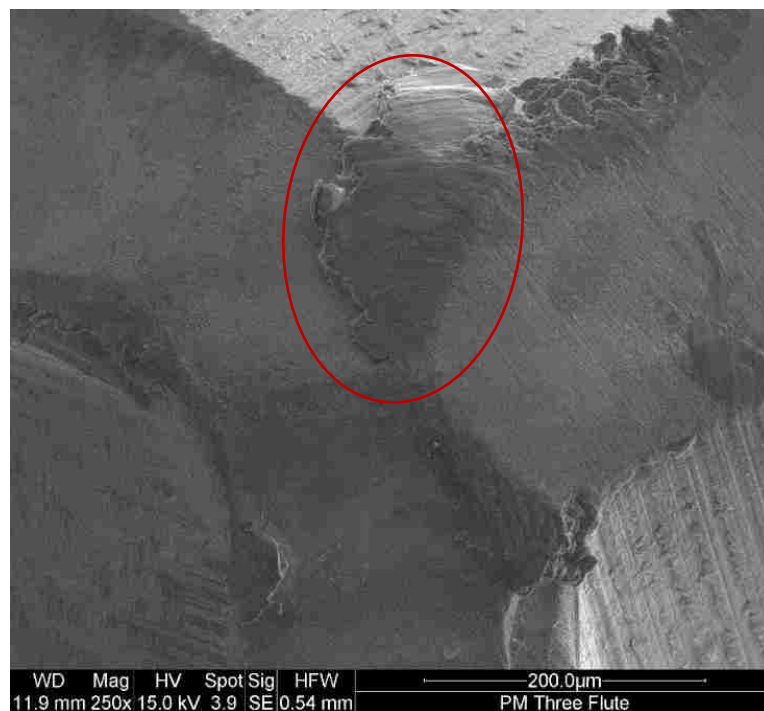
Figure 81. 250x SEM top down view of the three flute drill bit chisel edge after drilling 60 holes in PM titanium.

79
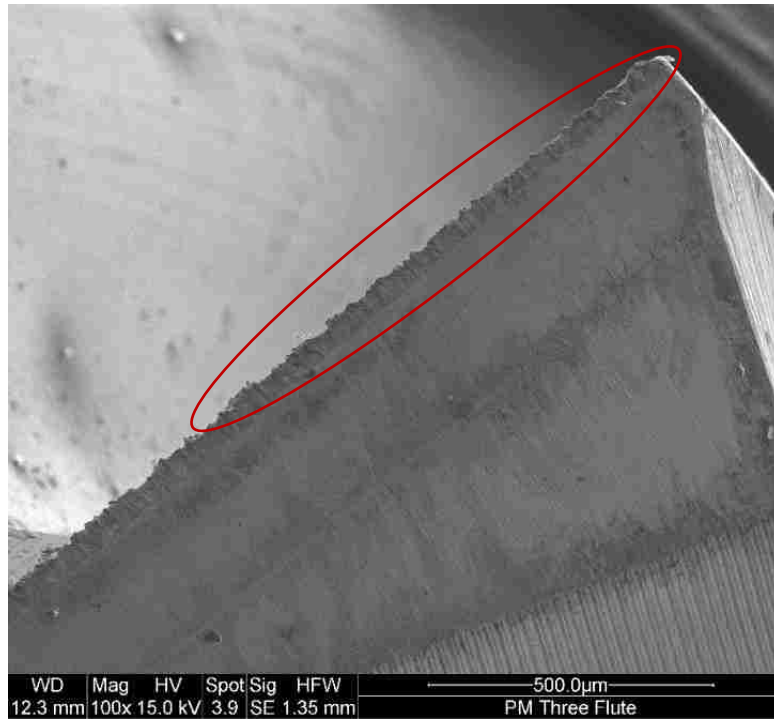
Figure 82. 100x SEM top down view of the three flute drill bit cutting edge after drilling 60 holes in PM titanium.
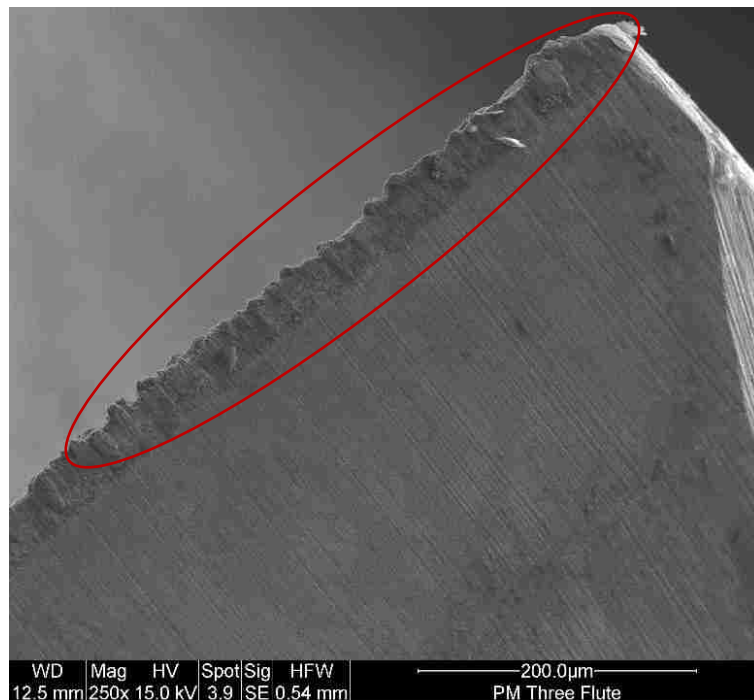
Figure 83. 250x SEM top down view of the three flute drill bit cutting edge after drilling 60 holes in PM titanium.

80
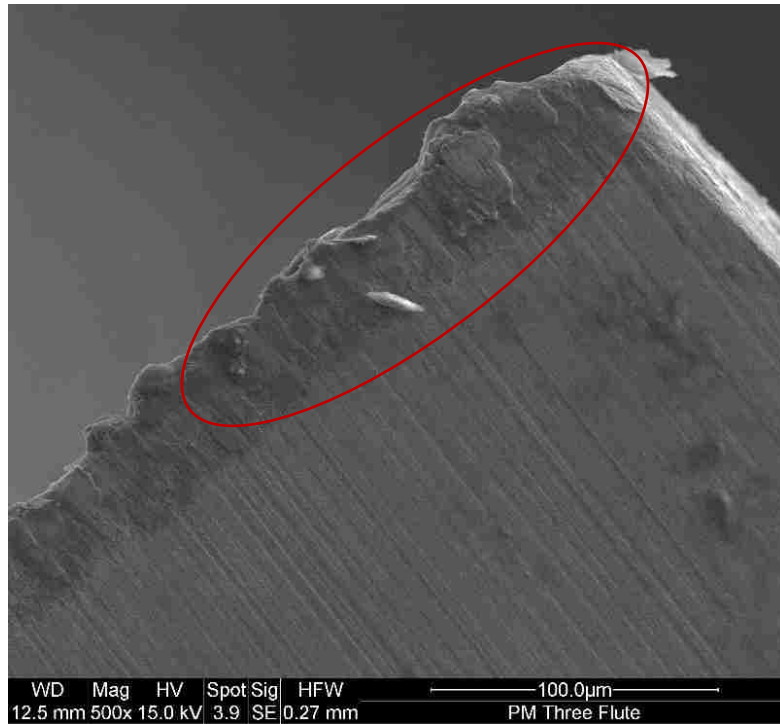
Figure 84. 500x SEM top down view of the three flute drill bit cutting edge after drilling 60 holes in PM titanium.
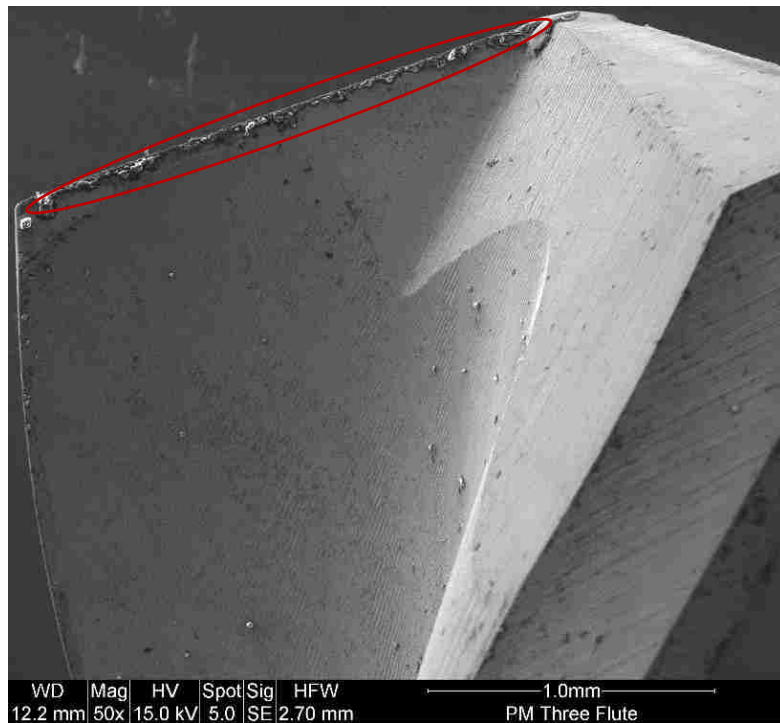
Figure 85. 50x SEM flute view of the three flute drill bit cutting edge after drilling 60 holes in PM titanium.
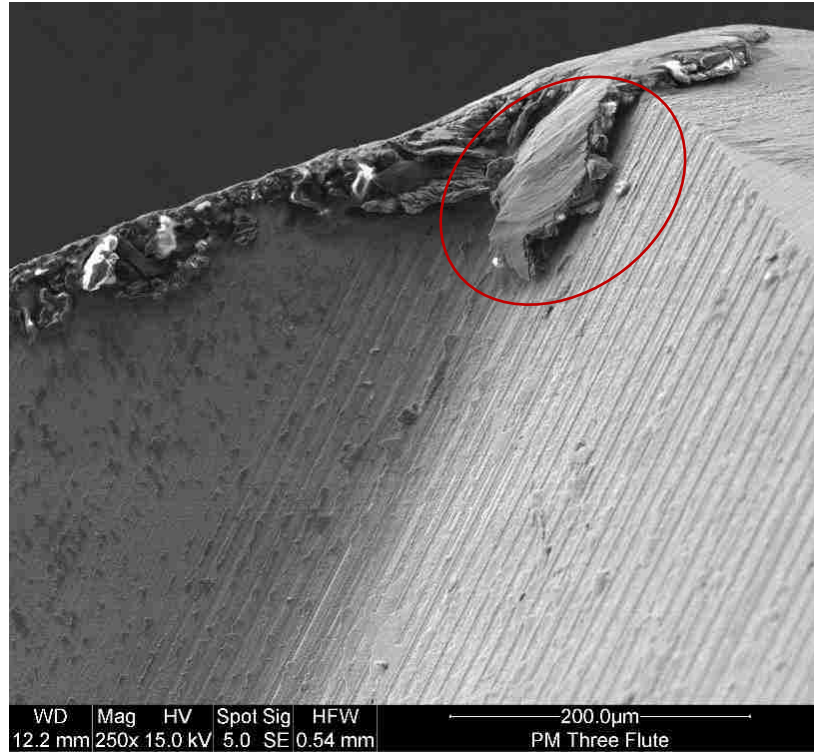
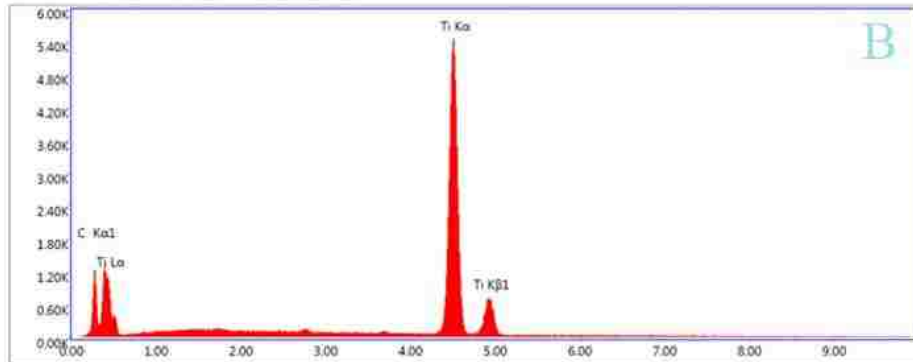*Figure 86. 250x SEM flute view of the three flute drill bit cutting edge after drilling 60 holes in PM titanium.*
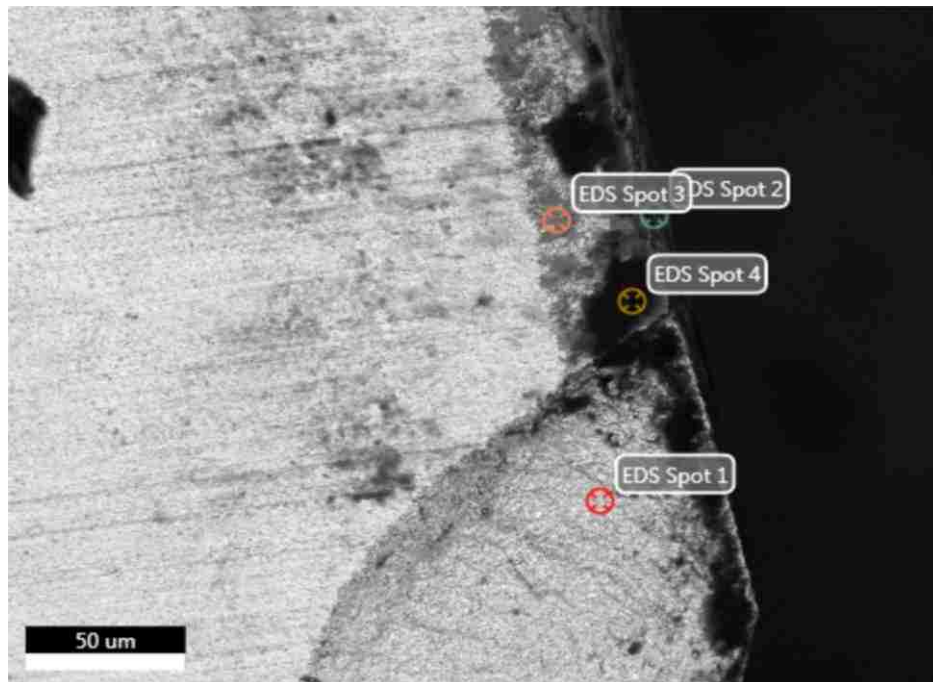
Figure 87. EDS spot analysis of the three flute drill bit cutting edge after drilling 60 holes in PM titanium.

Figure 87 and Figure 89 show the EDS spot analysis of the drill bit. Referring to Figure 89 (B), spot 2 confirms the adhesion on the cutting edge, while Figure 89 (A) spot 1 shows the material of the drill bit composing of tungsten. Figure 88 shows the overlay of titanium and tungsten. The EDS overlay map shows the titanium is adhered onto the drill bit which is made of tungsten.
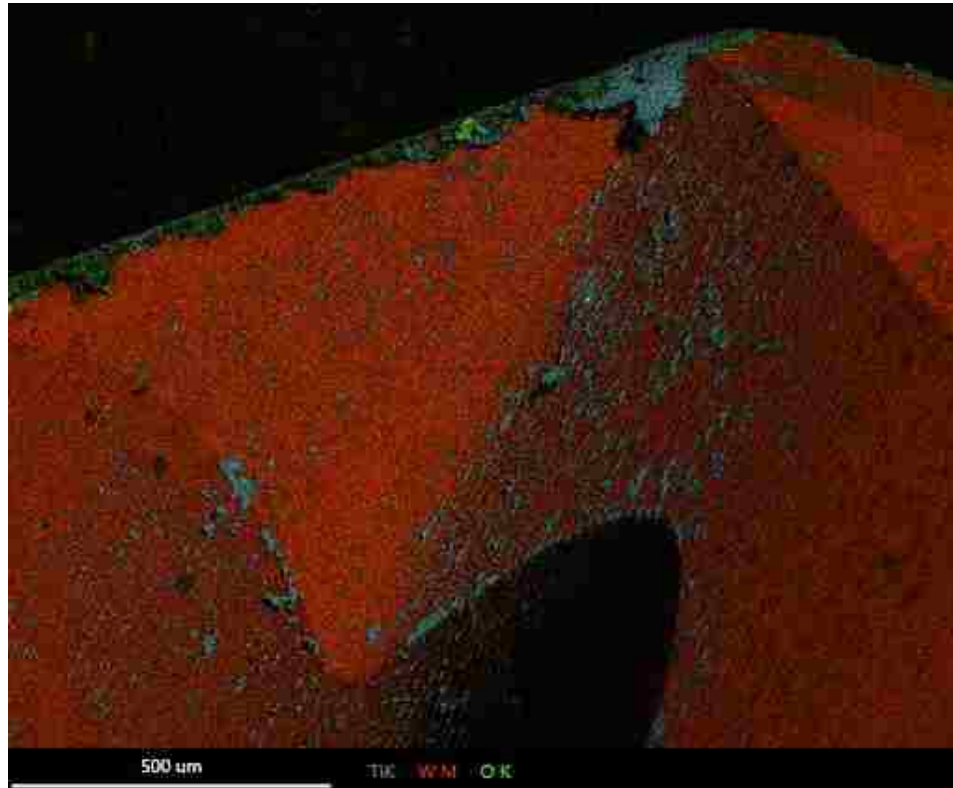
Figure 88. EDS mapping of the three flute drill bit cutting edge after drilling 60 holes in PM titanium.
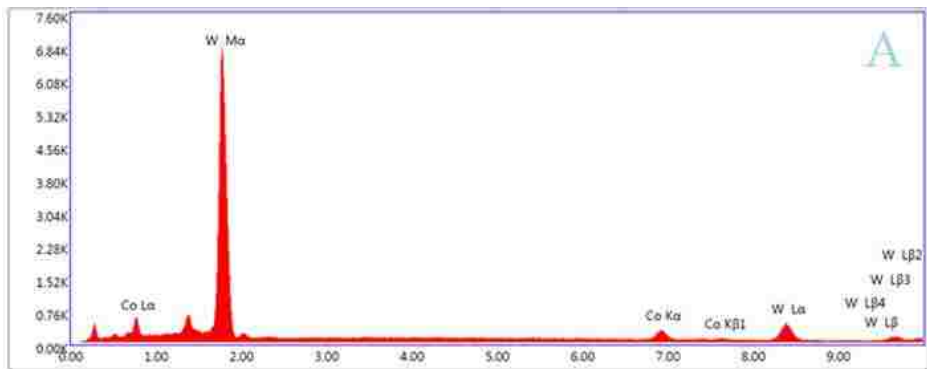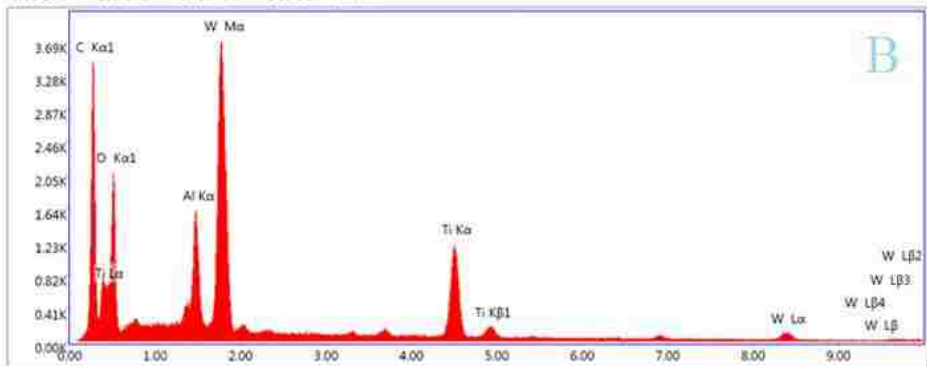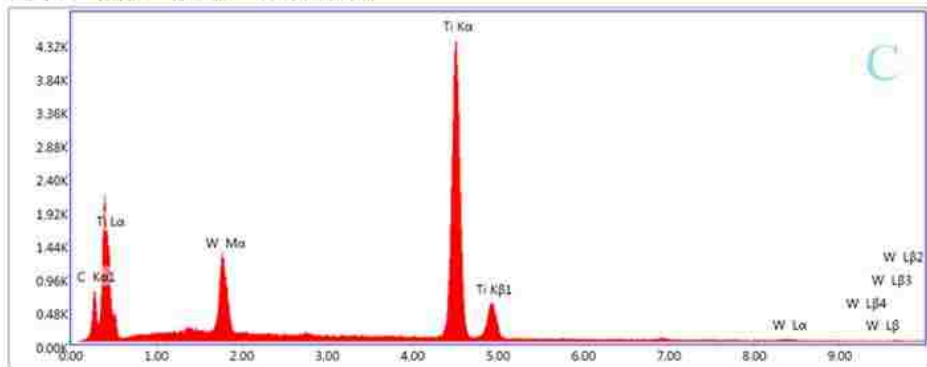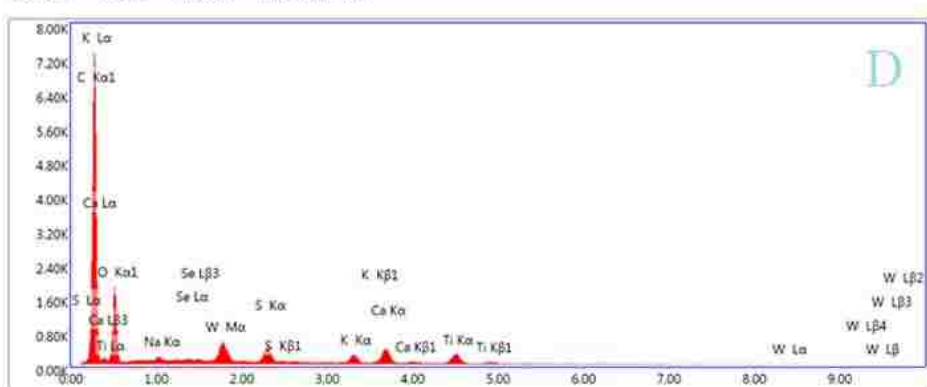
4.2.3 Additive Manufactured Titanium

After failing at hole 23 when drilling AM titanium workpiece, the flank wear was measured to be 0.213 ± 0.036 mm.
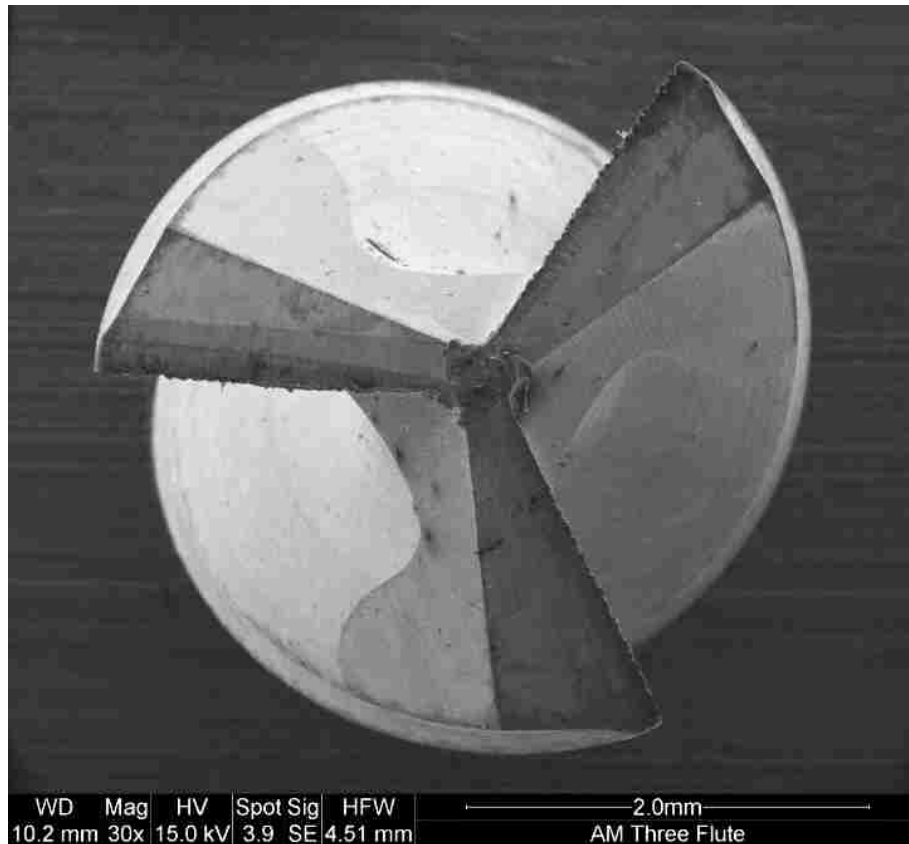
Figure 90. 30x SEM top down view of the three flute drill bit after failing at hole 23 when drilling AM titanium.

Figure 90 to Figure 96 shows the SEM images taken after failing at 23 holes when drilling AM titanium. The SEM highlights the flank wear and adhesion on the cutting edge at various magnifications from 50x to 500x from the top view and the flute view. Additionally, the chisel edge is shown to further emphasize the adhesion during drilling titanium alloys.
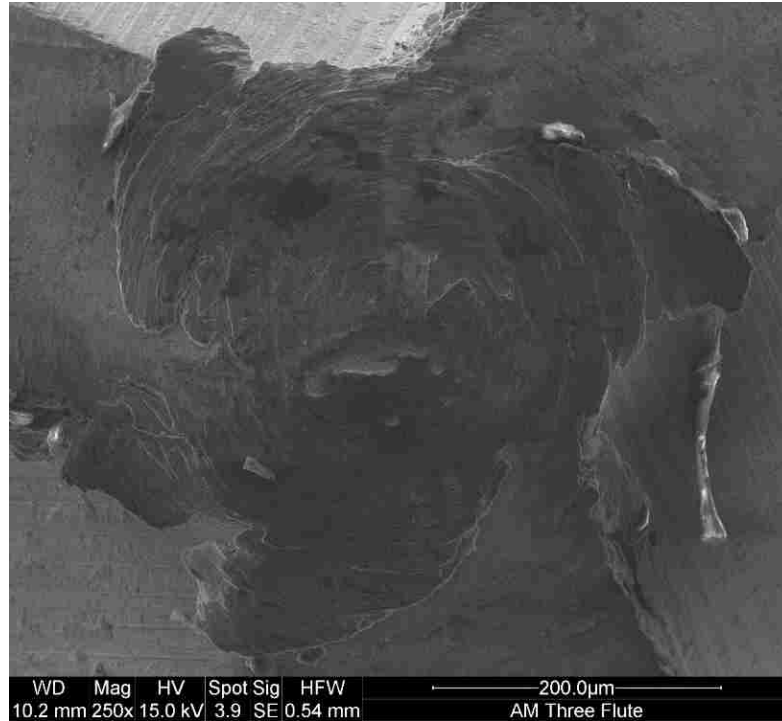
Figure 91. 250x SEM top down view of the three flute drill bit chisel edge after failing at hole 23 when drilling AM titanium.
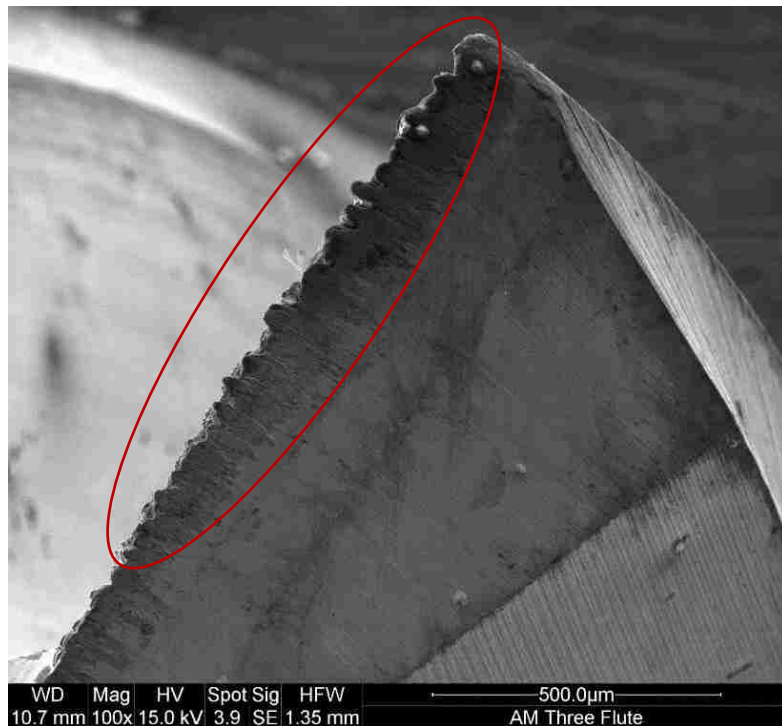
Figure 92. 100x SEM top down view of the three flute drill bit cutting edge after failing at hole 23 when drilling AM titanium.

86
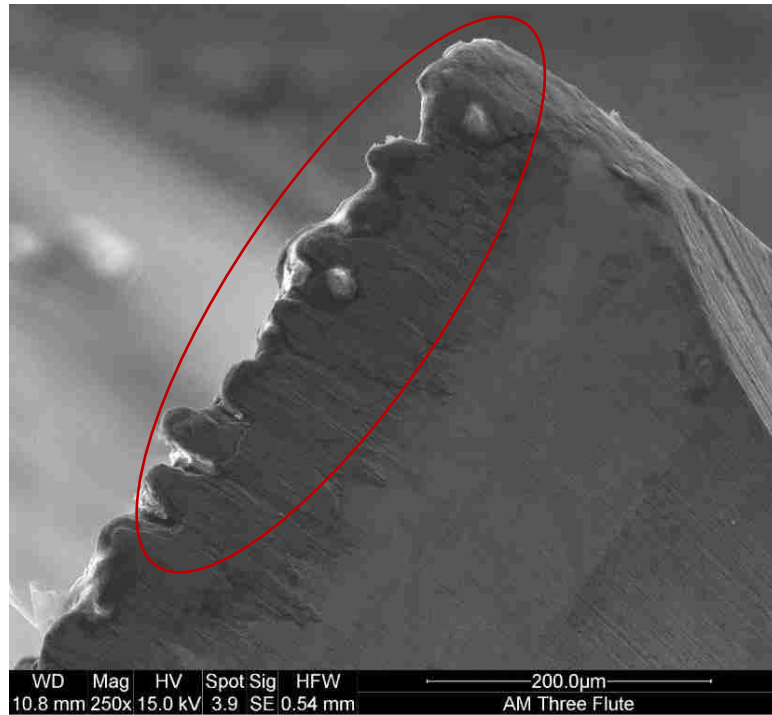
Figure 93. 250x SEM top down view of the three flute drill bit cutting edge after failing at hole 23 when drilling AM titanium.
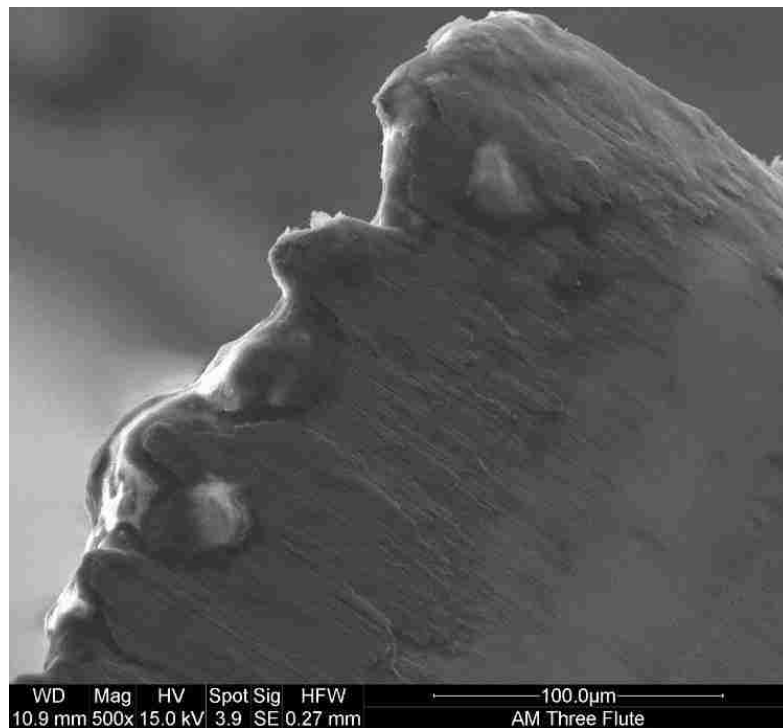
Figure 94. 500x SEM top down view of the three flute drill bit cutting edge after failing at hole 23 when drilling AM titanium.

87
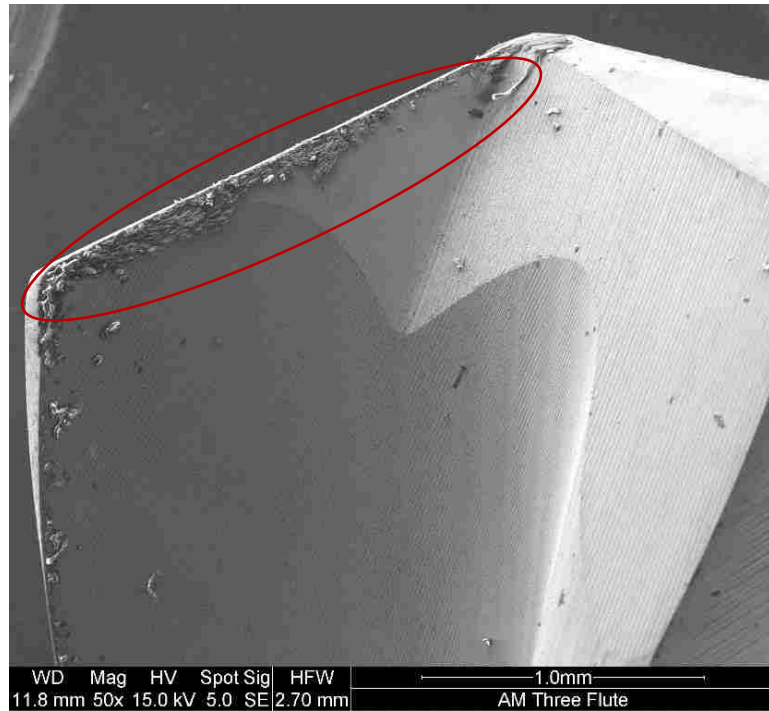
Figure 95. 50x SEM flute view of the three flute drill bit cutting edge after failing at hole 23 when drilling AM titanium.
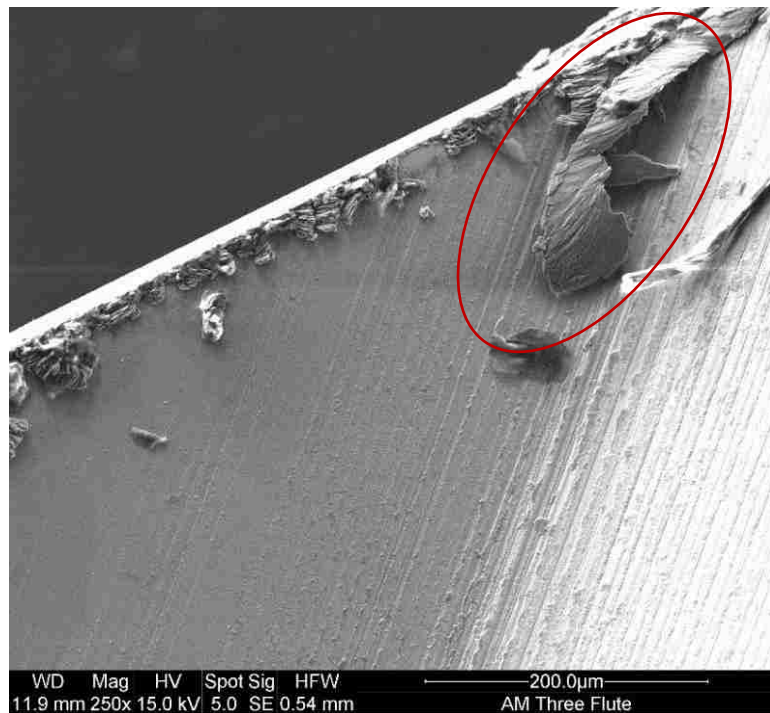
Figure 96. 250x SEM flute view of the three flute drill bit cutting edge after failing at hole 23 when drilling AM titanium.
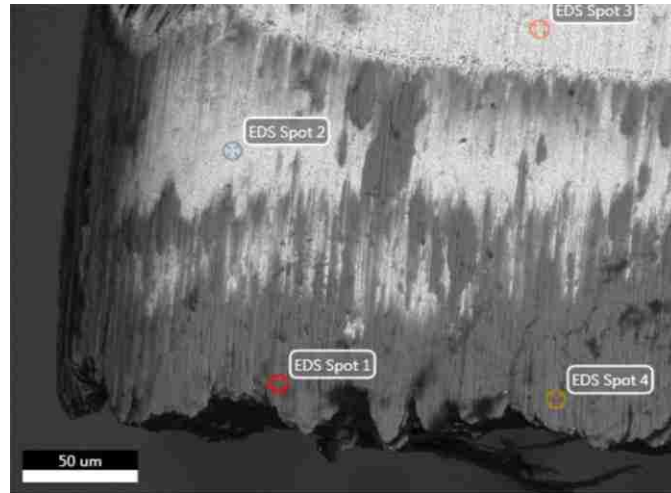
Figure 97. EDS spot analysis of the three flute drill bit cutting edge after failing at hole 23 when drilling AM titanium.

Figure 97 and Figure 99 show the EDS spot analysis of the drill bit. Referring to Figure 99 (B), spot 2 confirms the adhesion on the cutting edge, while spot 1 from Figure 99 (A) shows the material of the drill bit composing of tungsten. Figure 98 shows the overlay of titanium and tungsten. The EDS overlay map shows the titanium is adhered onto the drill bit which is made of tungsten.
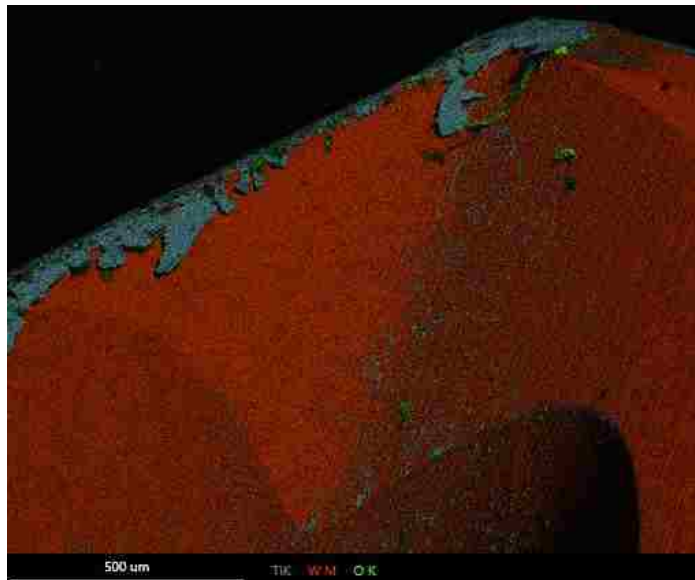
Figure 98. EDS mapping of the three flute drill bit cutting edge after failing at hole 23 when drilling AM titanium.

Figure 99. EDS spot analysis of the three flute drill bit after failing at 23 holes in AM titanium where, (A) is Spot 1, (B) is Spot 2, (C) is Spot 3, (D) is Spot 4.

90

4.3 Wear of Carbide Drill Bit

Depending on the titanium alloy, the drilling methodology for the carbide drill bit varied pertaining the number of holes drills due to the failure of the drill.

4.3.1 Ti-6Al-4V

After drilling 60 holes in the grade 5 titanium the flank wear of the drill bit was measured and the average was 0.080 ± 0.018 mm. Figure 100 to Figure 106 shows the SEM images taken after drilling 60 holes in grade 5 titanium (Ti-6Al-4V). Figure 105 shows a crack on the inside of the flute near the cutting edge. The SEM highlights the flank wear and adhesion on the cutting edge at various magnifications from 50x to 500x from the top view and the flute view. Additionally, the chisel edge is shown to further emphasize the adhesion during drilling titanium alloys.
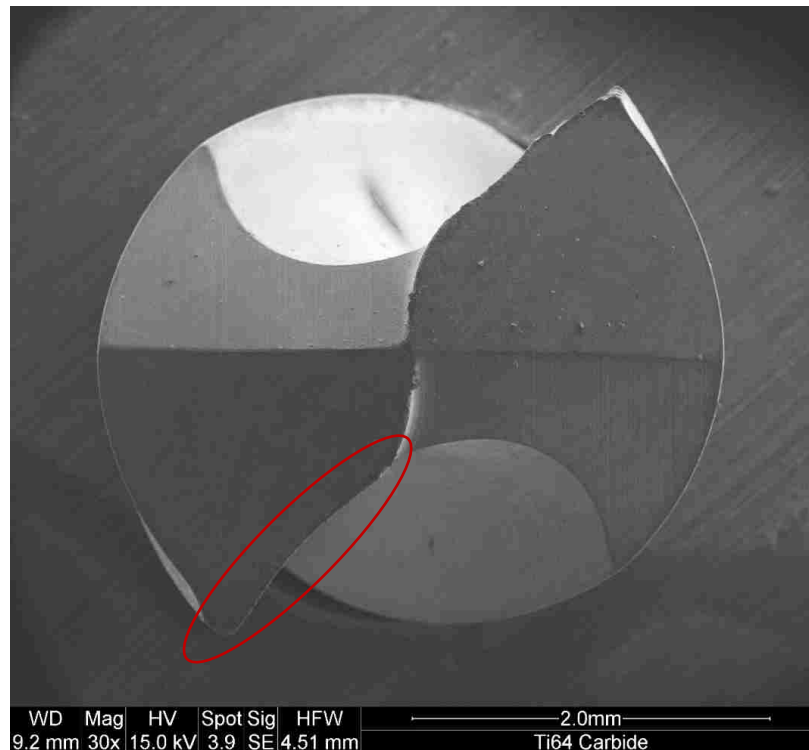
Figure 100. 30x SEM top down view of the carbide drill bit after drilling 60 holes in grade 5 titanium (Ti-6Al-4V).
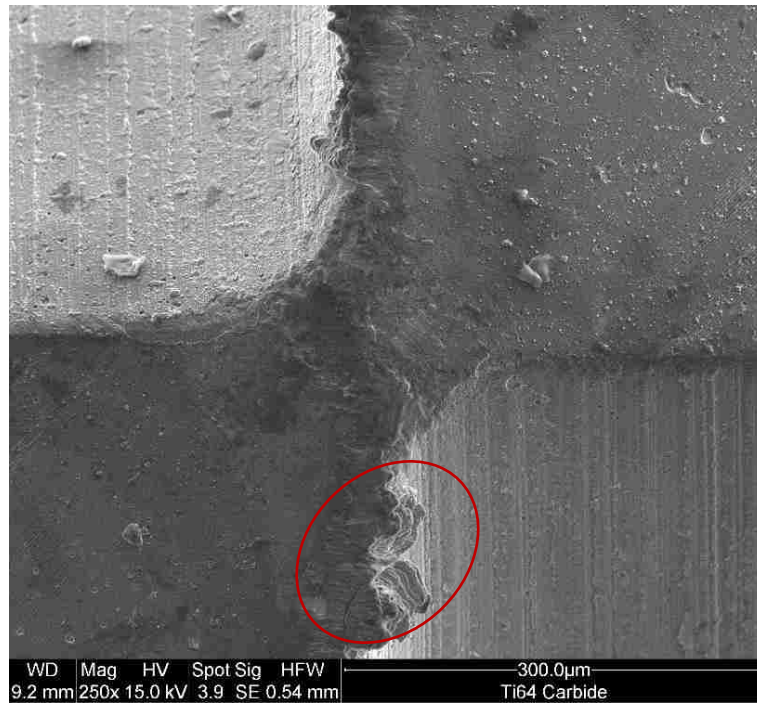
Figure 101. 250x SEM top down view of the carbide drill bit chisel edge after drilling 60 holes in grade 5 titanium (Ti-6Al-4V).
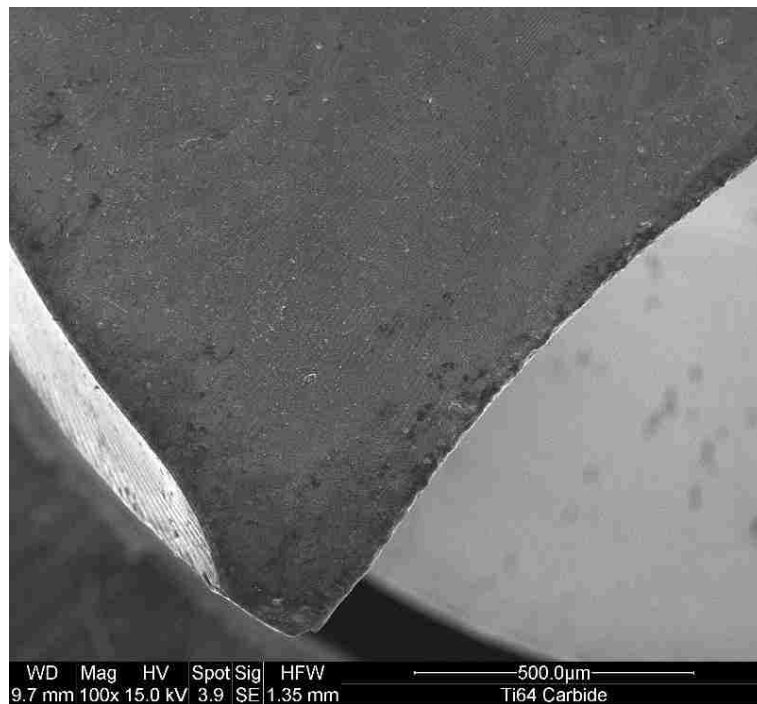
Figure 102. 100x SEM top down view of the carbide drill bit cutting edge after drilling 60 holes in grade 5 titanium (Ti-6Al-4V).
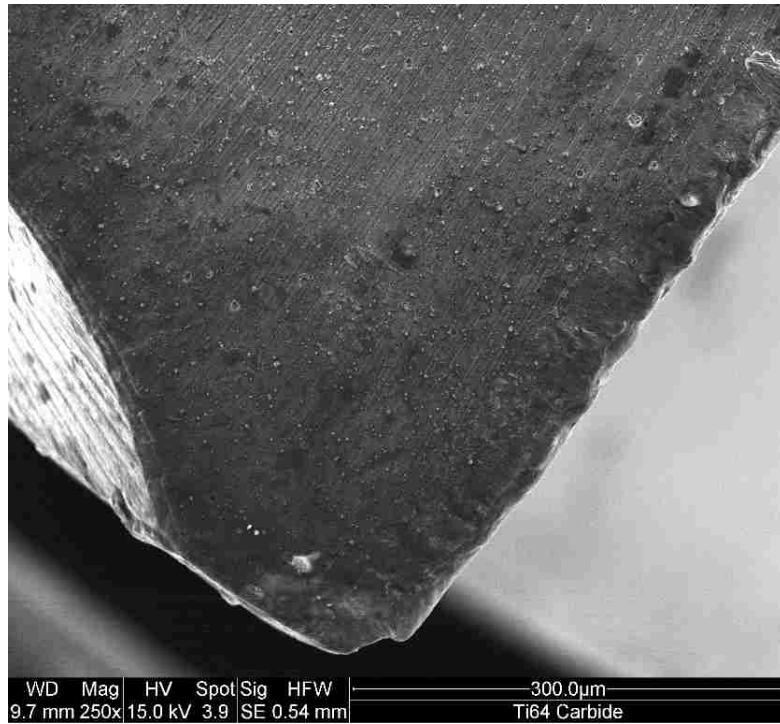
Figure 103. 250x SEM top down view of the carbide drill bit cutting edge after drilling 60 holes in grade 5 titanium (Ti-6Al-4V).
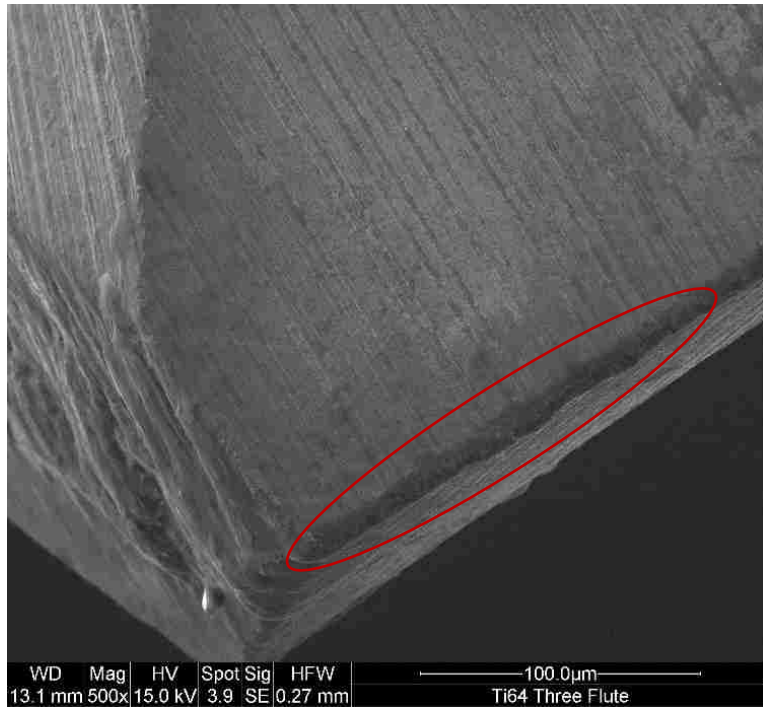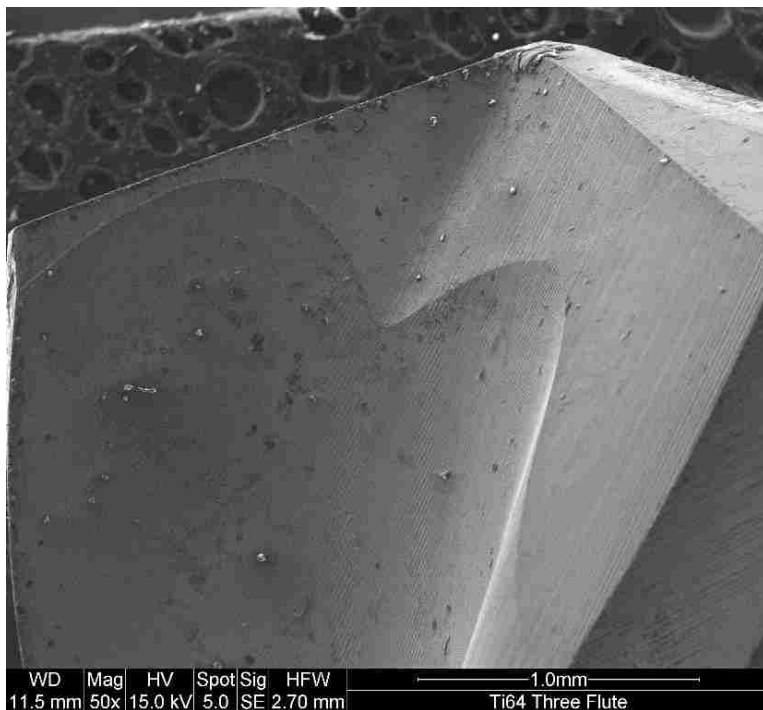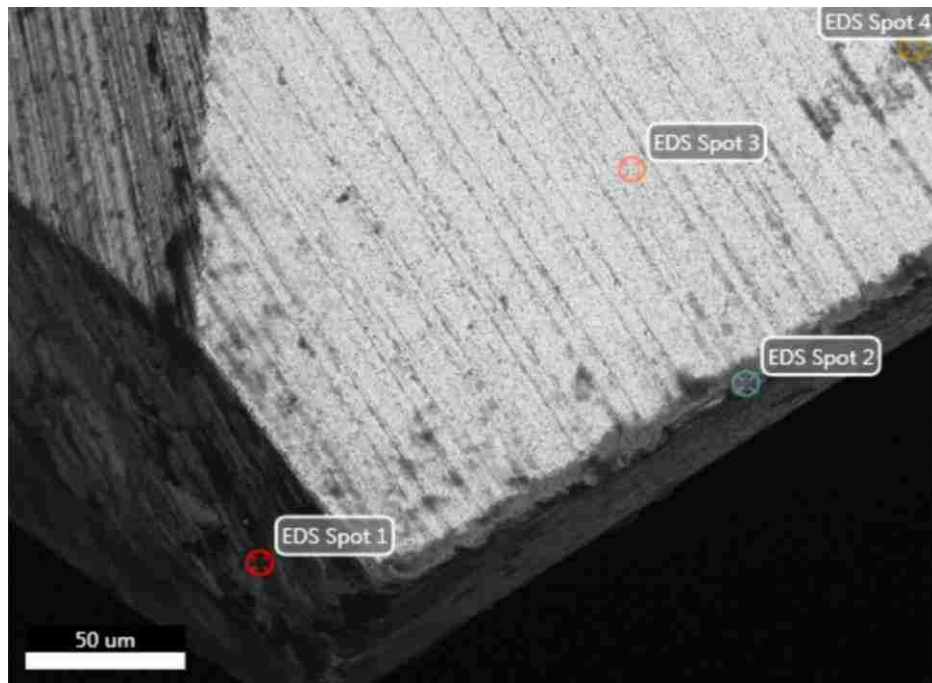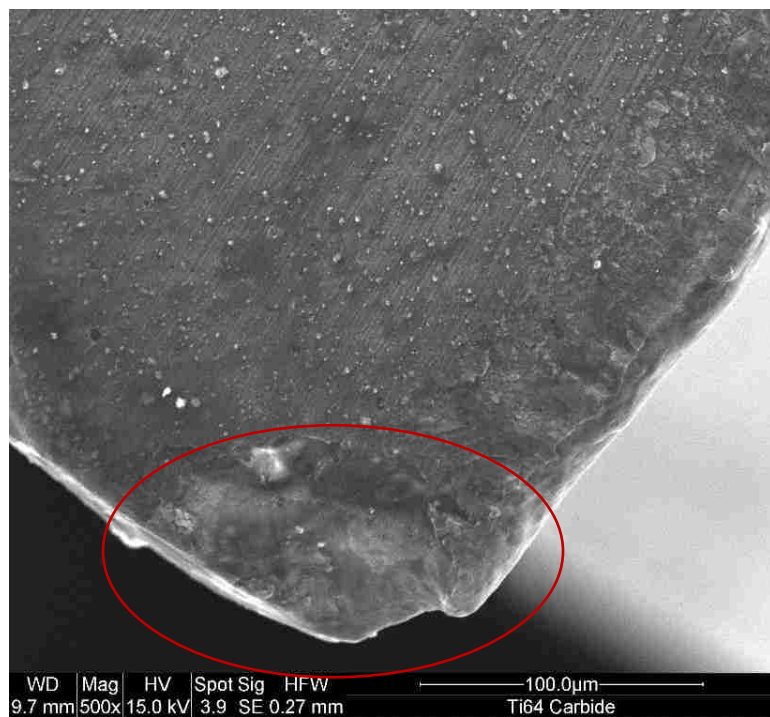

Figure 104. 500x SEM top down view of the carbide drill bit cutting edge after drilling 60 holes in grade 5 titanium (Ti-6Al-4V).
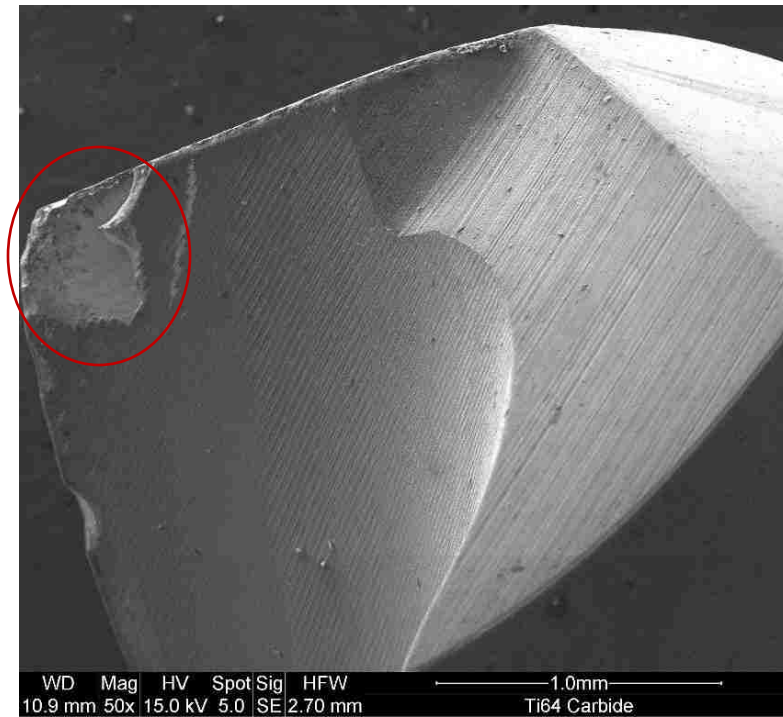
Figure 105. 50x SEM flute view of the carbide drill bit cutting edge after drilling 60 holes in grade 5 titanium (Ti-6Al-4V).
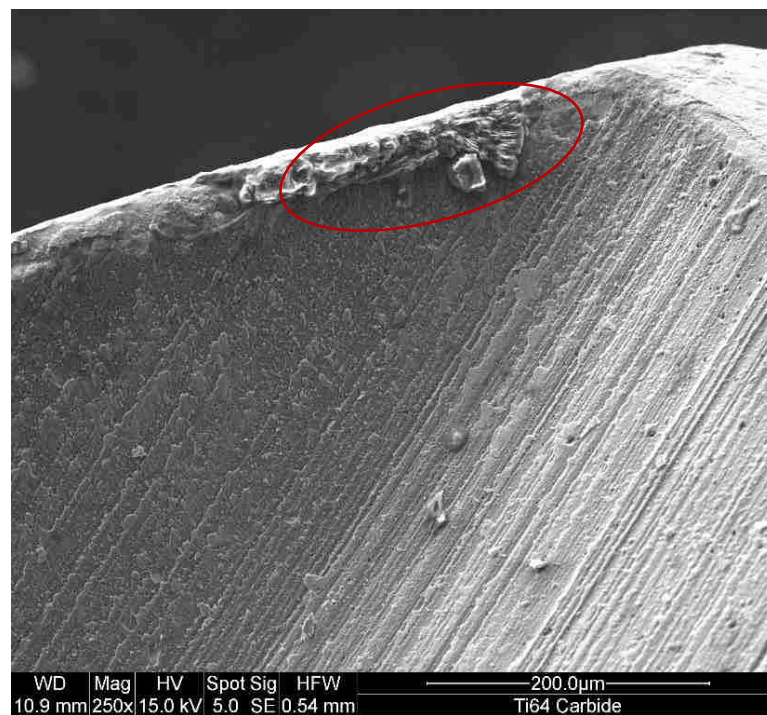
Figure 106. 250x SEM top down view of the carbide drill bit cutting edge after drilling 60 holes in grade 5 titanium (Ti-6Al-4V).
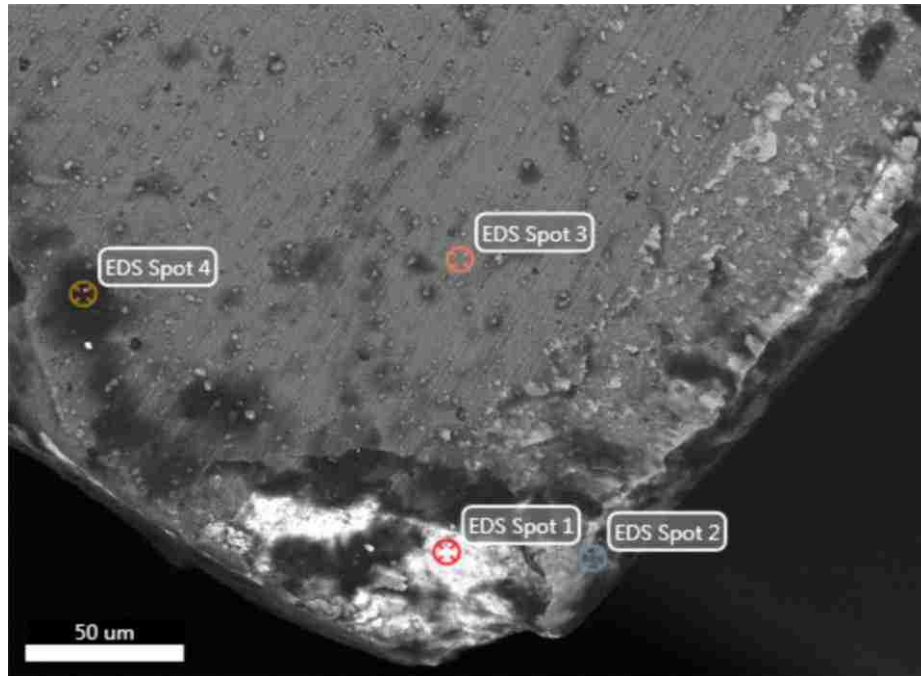
Figure 107. EDS spot analysis of the carbide drill bit cutting edge after drilling 60 holes in grade 5 titanium (Ti-6Al-4V).

Figure 107 and Figure 108 show the EDS spot analysis of the drill bit. Since the coating and the workpiece material both consists of titanium it is hard to confirm which part is adhesion and which part is the coating. To resolve this problem, the wear of the coating is examined. Referring to Figure 108 (A), spot 1 shows the base material of the cutting edge, while spot 3 from Figure 108 (C), shows titanium, aluminum and nitrogen which are components of the coating. Referring to Figure 109, it is known that this drill bit was coated with AlTiN. By overlaying the titanium map and tungsten map, the results showed the cutting edge as the uncoated tungsten material. Meanwhile, the rest of the image was the titanium map which showed possible adhesion and the coating on the drill bit.
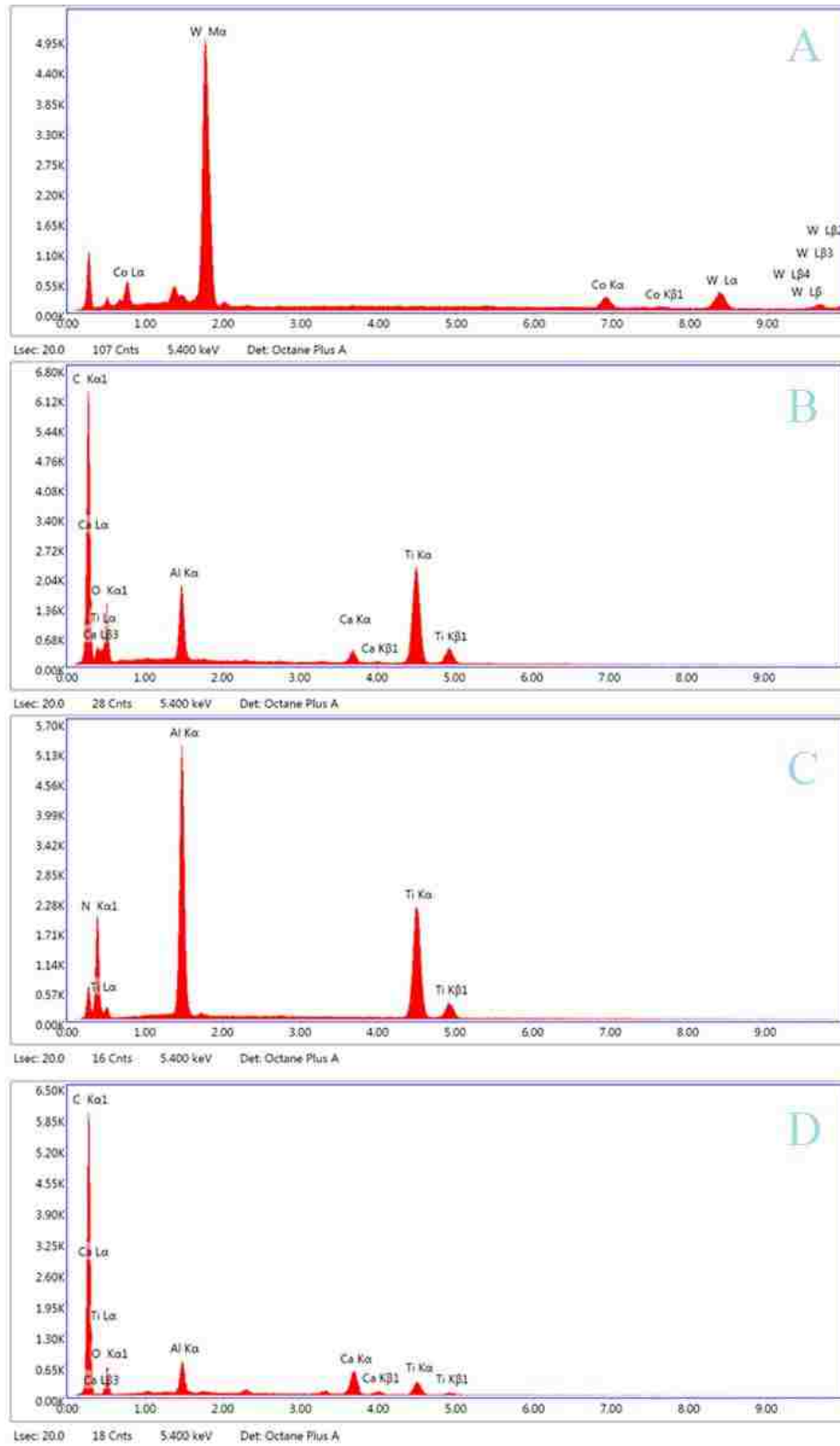
Figure 108. EDS spot analysis of the carbide drill bit after drilling 60 holes in grade 5 titanium (Ti-6Al-4V) where, (A) is Spot 1, (B) is Spot 2, (C) is Spot 3, (D) is Spot 4.
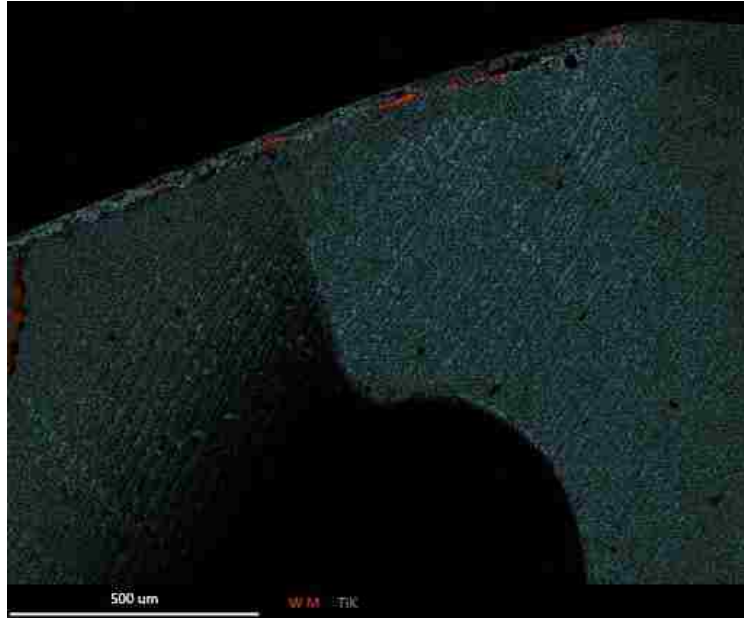
Figure 109. EDS mapping of the carbide drill bit cutting edge after drilling 60 holes in grade 5 titanium (Ti-6Al-4V).

4.3.2 Powder Metallurgy Titanium

After drilling 60 holes in the PM titanium the flank wear of the drill bit was measured to have an average of 0.074 ± 0.020 mm. Figure 110 to Figure 116 shows the SEM images taken after drilling 60 holes in PM titanium. The SEM highlights the flank wear and adhesion on the cutting edge at various magnifications from 50x to 500x from the top view and the flute view. Additionally, the chisel edge is shown to further emphasize the adhesion during drilling titanium alloys.
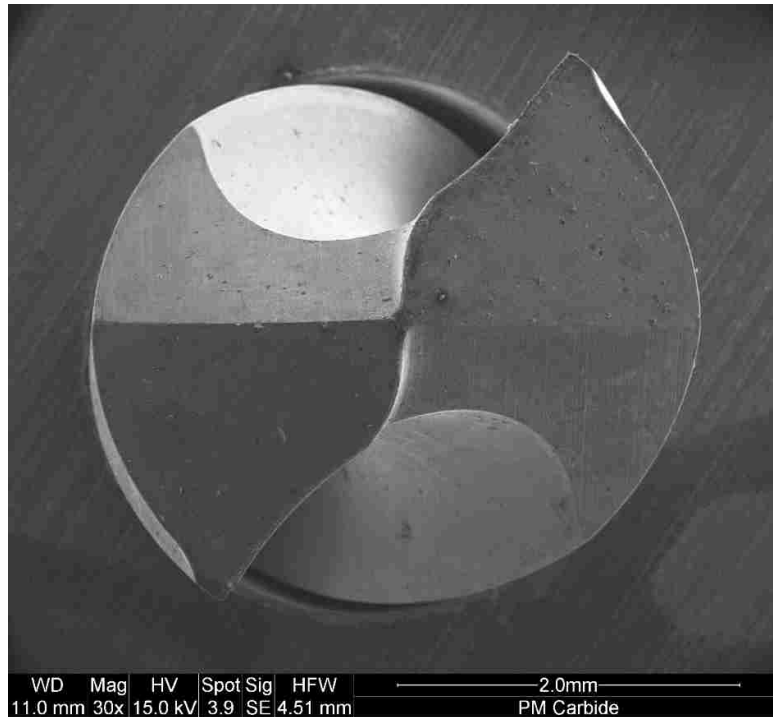
Figure 110. 30x SEM top down view of the carbide drill bit after drilling 60 holes in PM titanium.

Figure 111. 250x SEM top down view of the chisel edge of the carbide drill bit after drilling 60 holes in PM titanium.

98
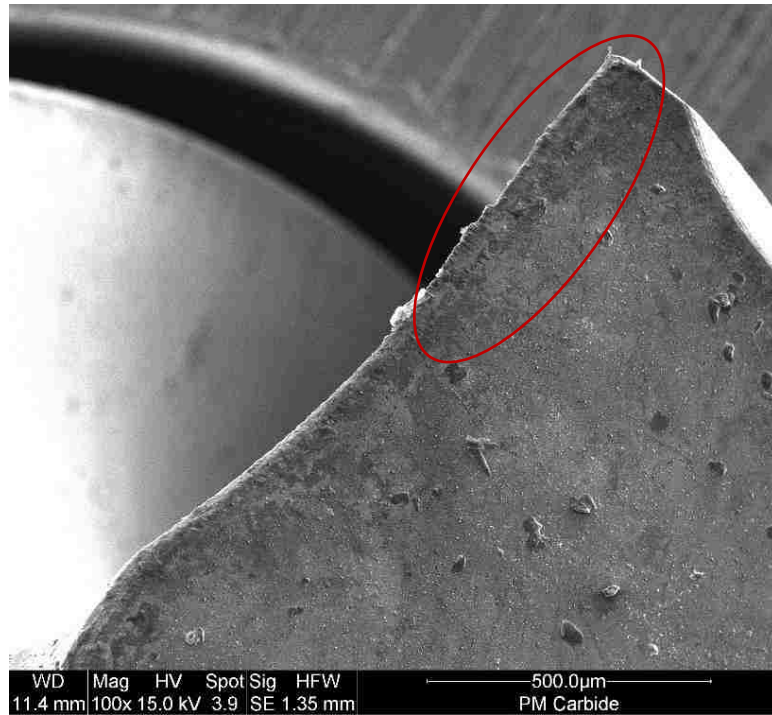
Figure 112. 100x SEM top down view of the cutting edge of the carbide drill bit after drilling 60 holes in PM titanium.
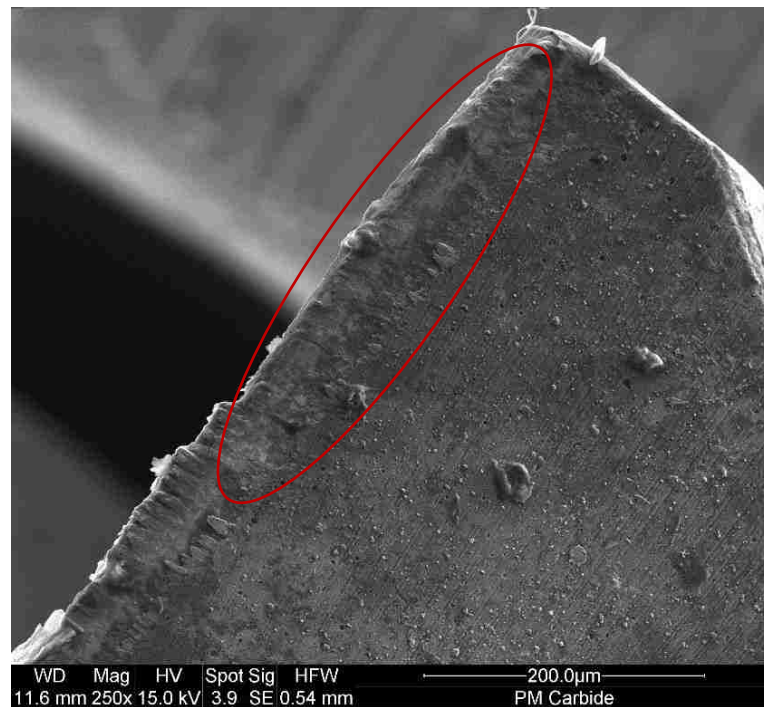
Figure 113. 250x SEM top down view of the cutting edge of the carbide drill bit after drilling 60 holes in PM titanium.
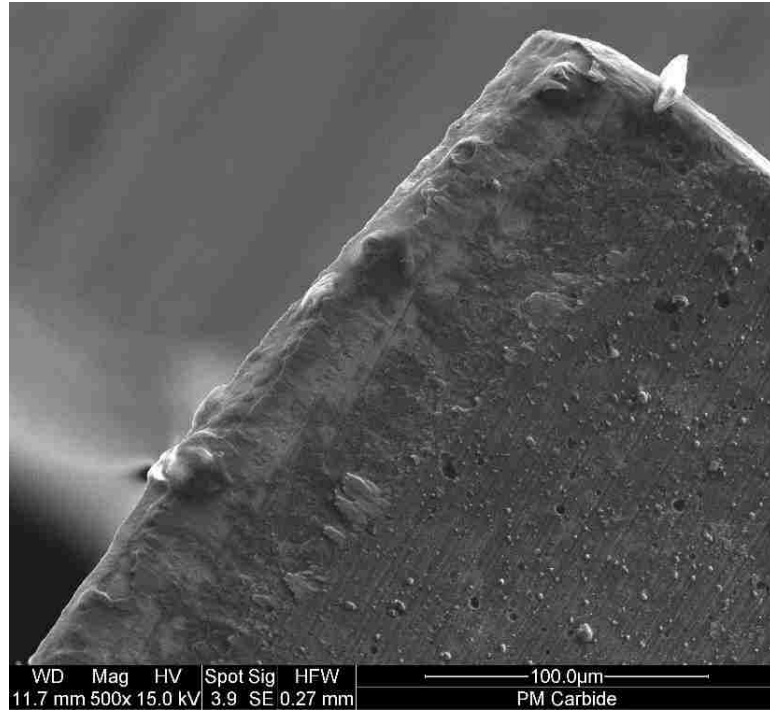
Figure 114. 500x SEM top down view of the cutting edge of the carbide drill bit after drilling 60 holes in PM titanium.
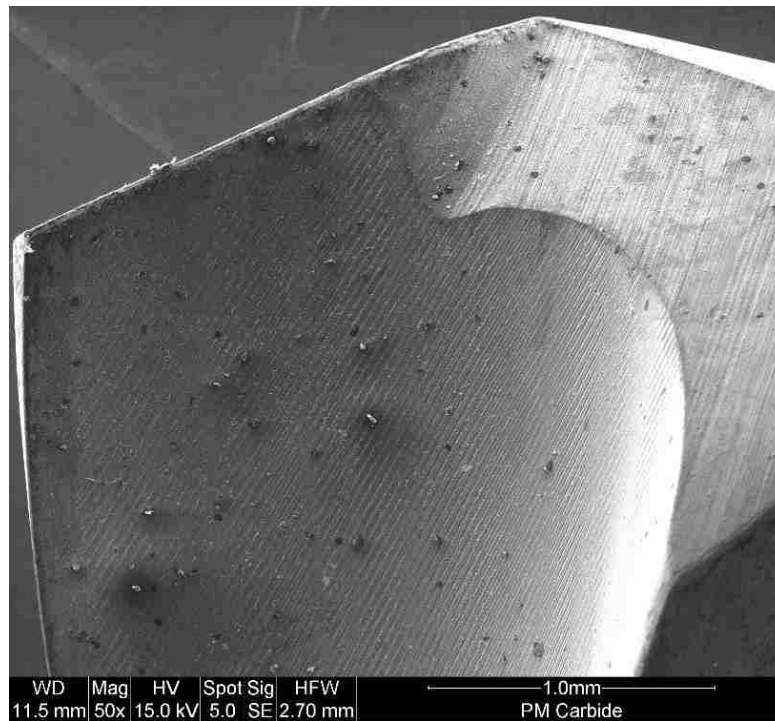
Figure 115. 50x SEM flute view of the cutting edge of the carbide drill bit after drilling 60 holes in PM titanium.

100
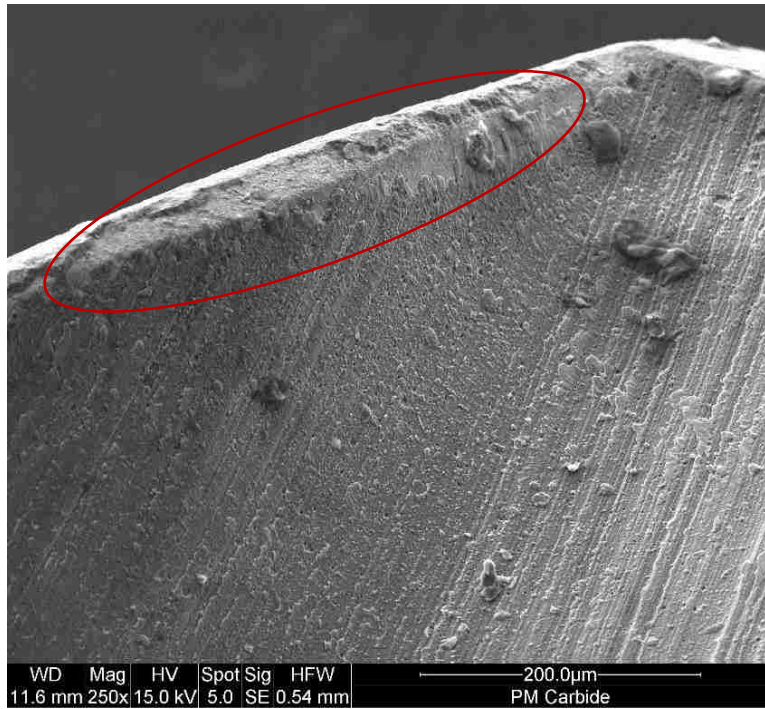
Figure 116. 250x SEM flute view of the cutting edge of the carbide drill bit after drilling 60 holes in PM titanium.
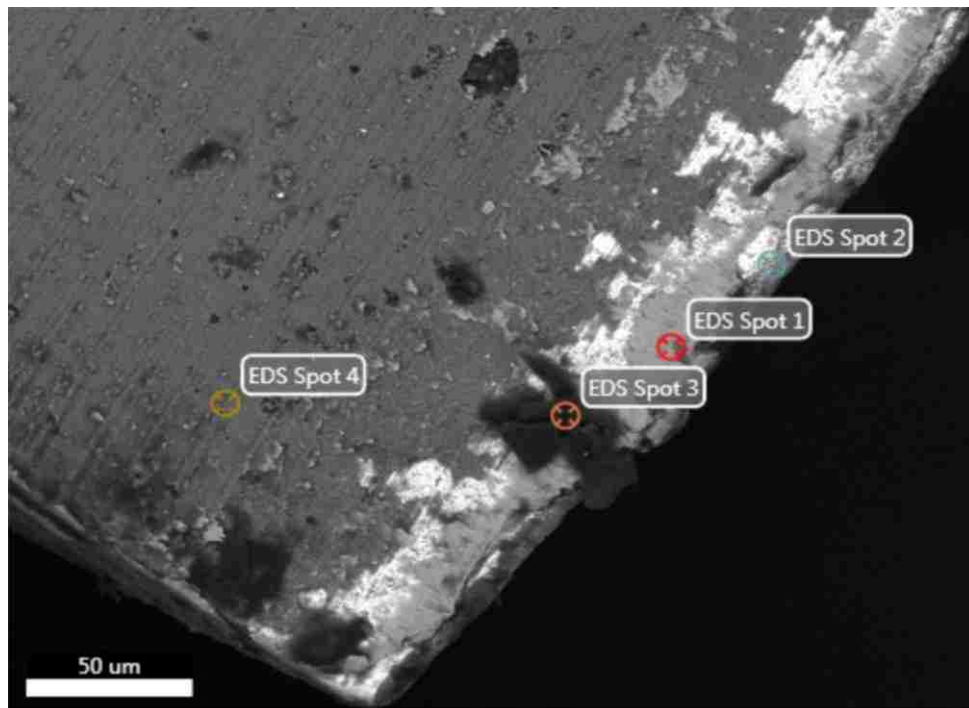
Figure 117. EDS spot analysis of the carbide drill bit cutting edge after drilling 60 holes in PM titanium.

Figure 117 and Figure 119 show the EDS spot analysis of the drill bit. Since the coating and the workpiece material both consists of titanium it is hard to confirm which part is adhesion and which part is the coating. To resolve this problem, the wear of the coating is examined. Referring to Figure 119 (B), spot 2 shows the base material of the cutting edge, while spot 3 from Figure 119 (C), shows titanium, aluminum and nitrogen which are components of the coating. Figure 118 shows the overlay of titanium and tungsten. The EDS overlay map shows the cutting edge as the uncoated tungsten while the titanium is shown as the possible adhesion and the coating on the drill bit.
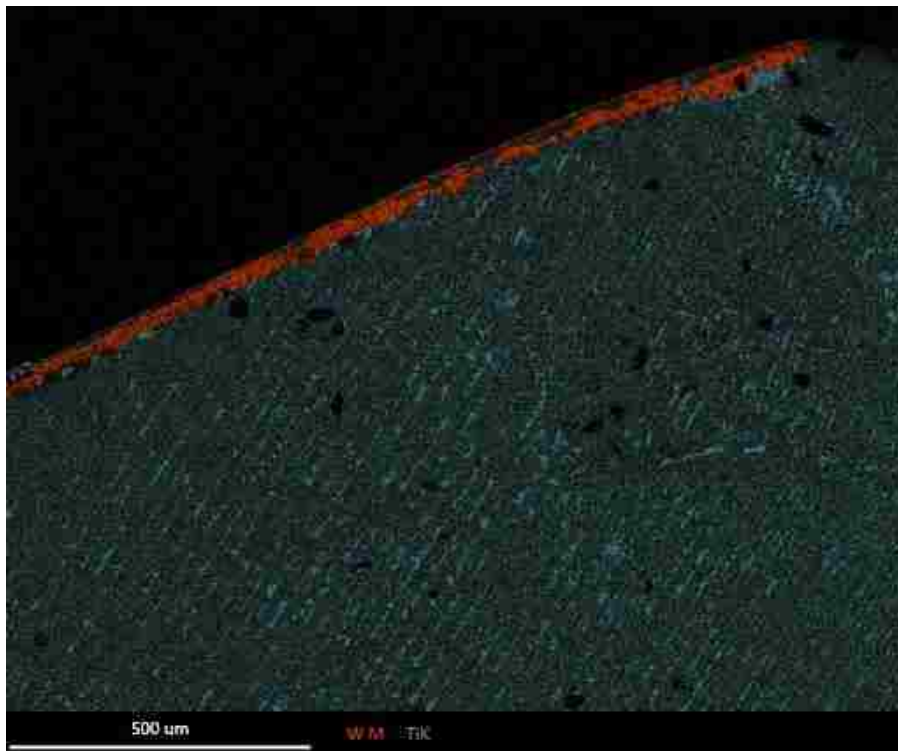
Figure 118. EDS mapping of the carbide drill bit cutting edge after drilling 60 holes in PM titanium.
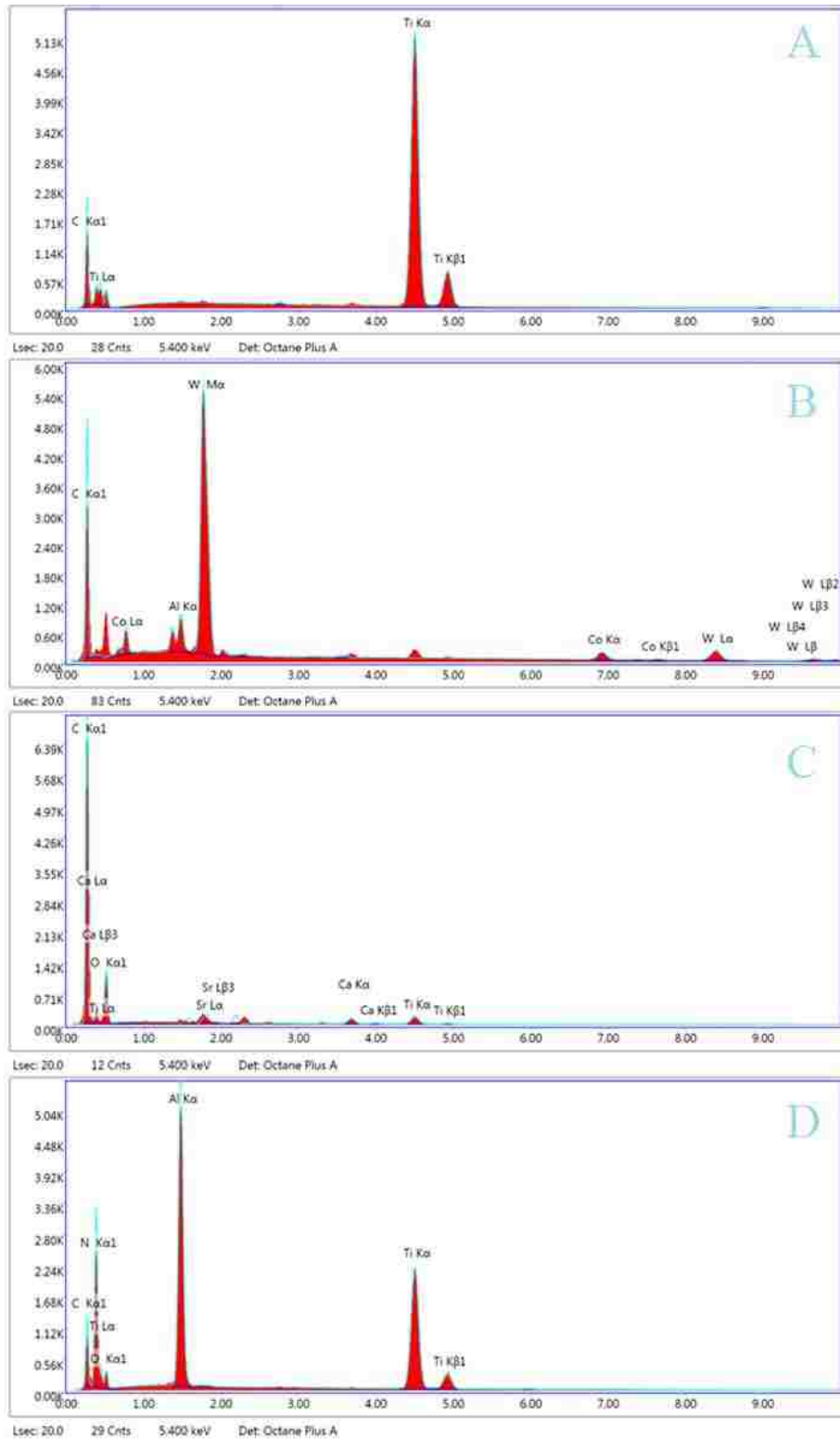
Figure 119. EDS spot analysis of the carbide drill bit after drilling 60 holes in PM titanium where, (A) is Spot 1, (B) is Spot 2, (C) is Spot 3, (D) is Spot 4.

103

4.3.3 Additive Manufactured Titanium

After drilling 60 holes in the AM titanium the flank wear of the drill bit was measured to have an average wear of 0.216 ± 0.044 mm. Figure 120 to Figure 126 shows the SEM images taken after drilling 60 holes in AM titanium. The SEM highlights the flank wear and adhesion on the cutting edge at various magnifications from 50x to 500x from the top view and the flute view. Additionally, the chisel edge is shown to further emphasize the adhesion during drilling titanium alloys.
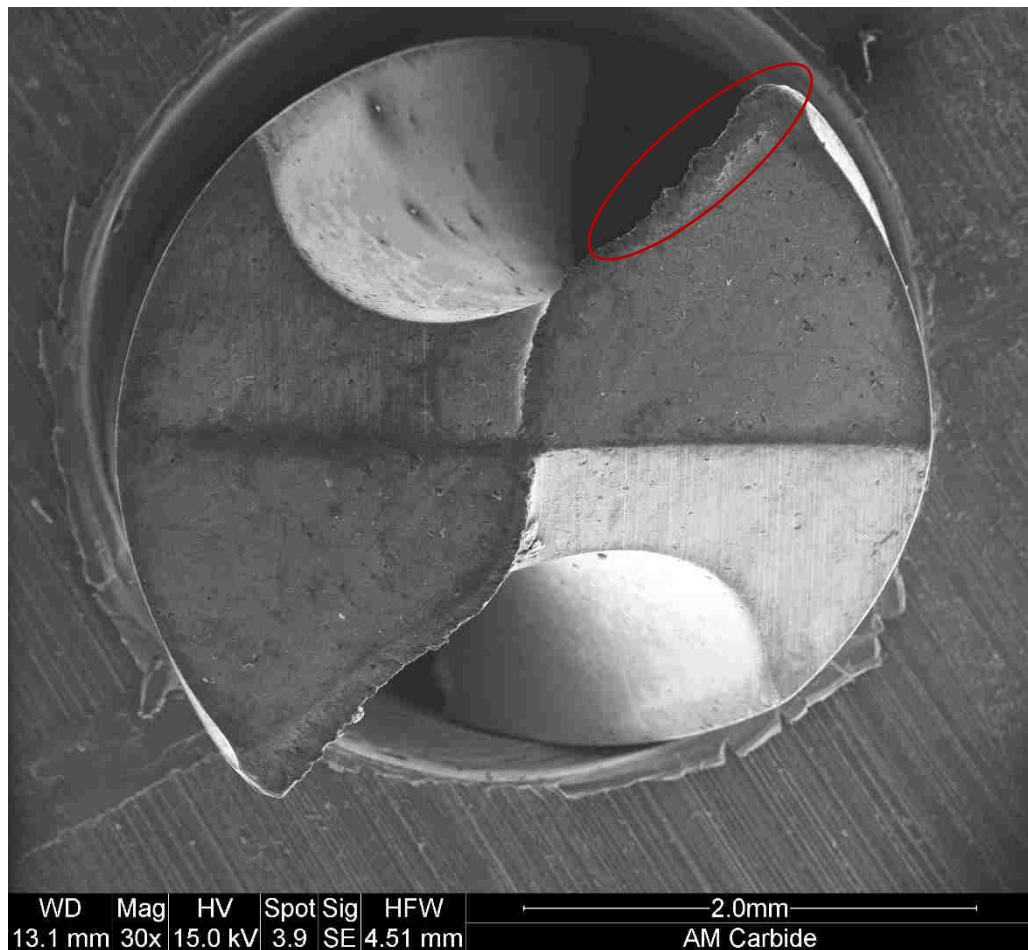

Figure 120. 30x SEM top down view of the carbide drill bit after drilling 60 holes in AM titanium.
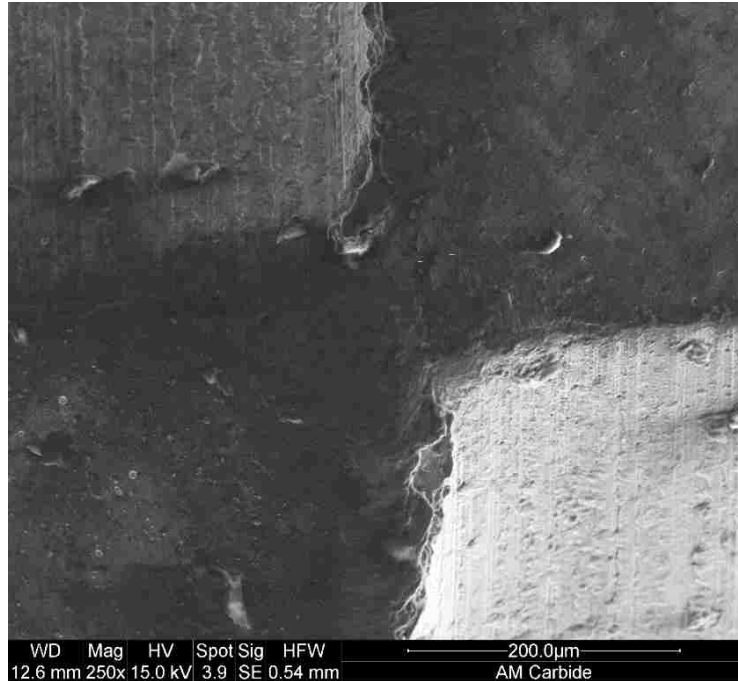
Figure 121. 250x SEM top down view of the carbide drill bit chisel edge after drilling 60 holes in AM titanium.
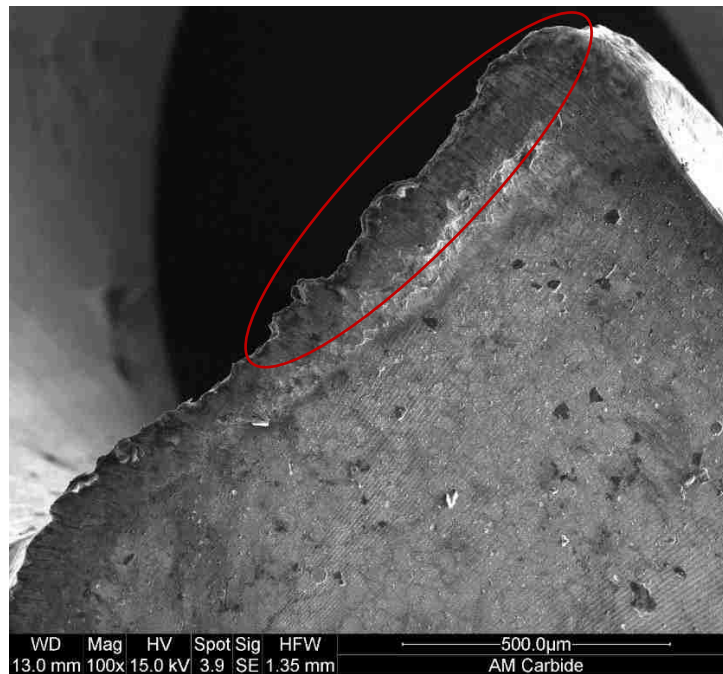
Figure 122. 100x SEM top down view of the carbide drill bit cutting edge after drilling 60 holes in AM titanium.
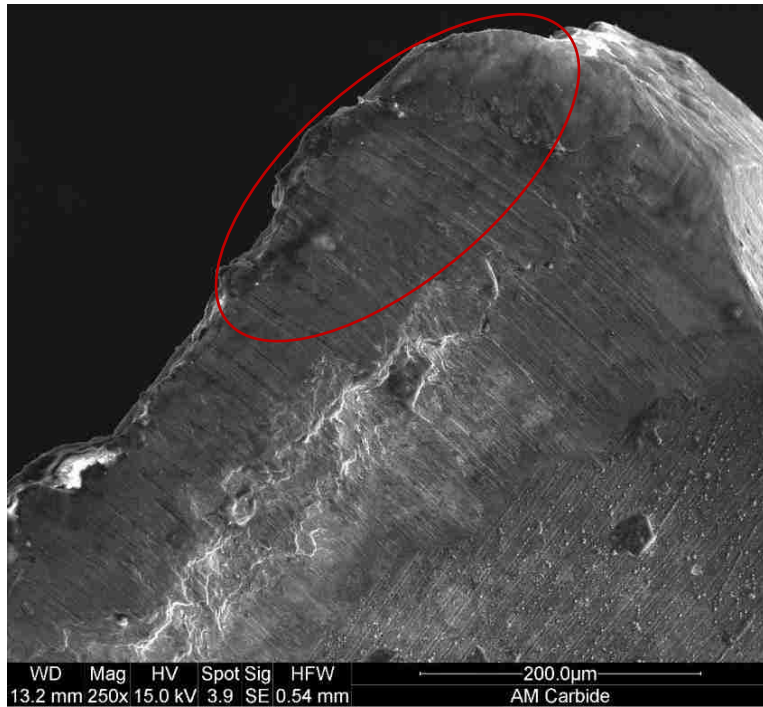
Figure 123. 250x SEM top down view of the carbide drill bit cutting edge after drilling 60 holes in AM titanium.
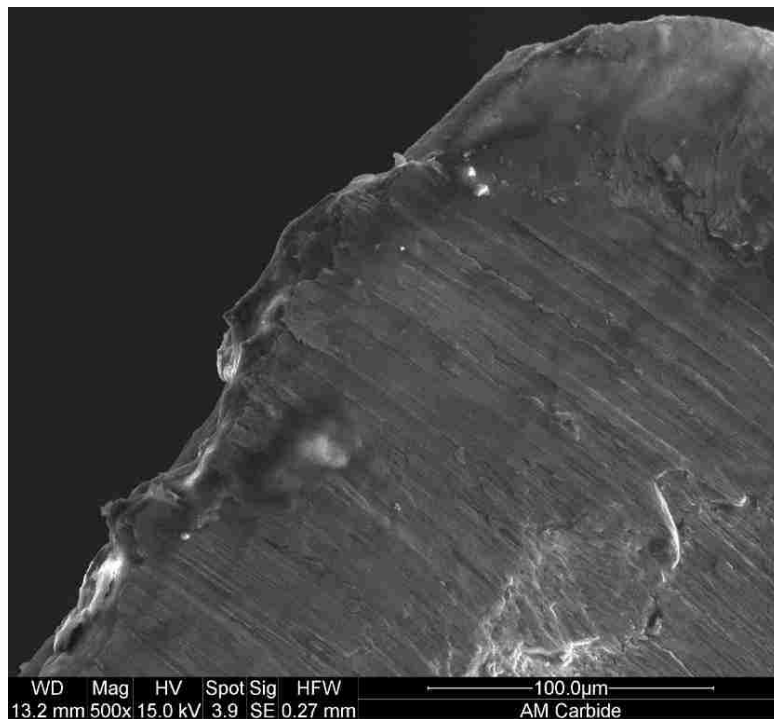
Figure 124. 500x SEM top down view of the carbide drill bit cutting edge after drilling 60 holes in AM titanium.
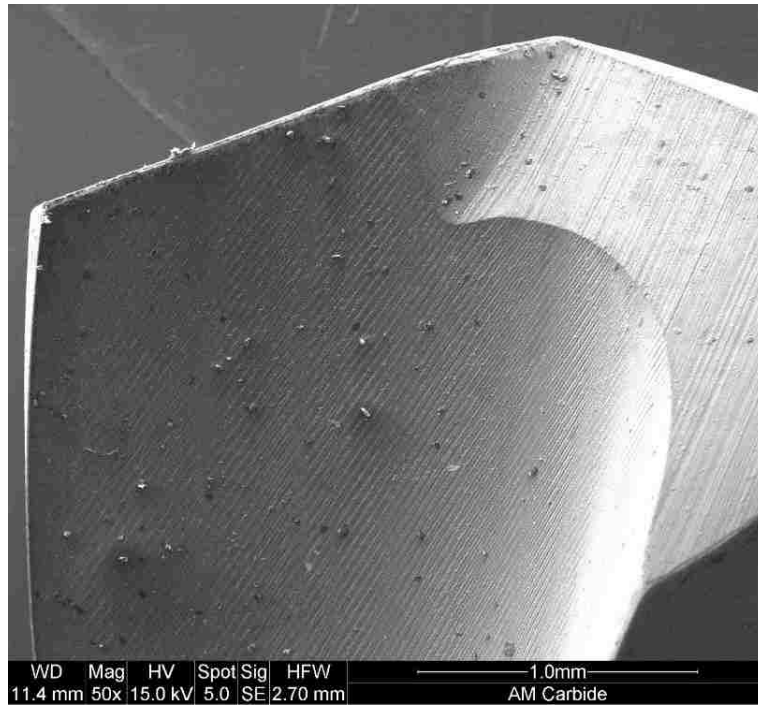
Figure 125. 50x SEM flute view of the carbide drill bit cutting edge after drilling 60 holes in AM titanium.
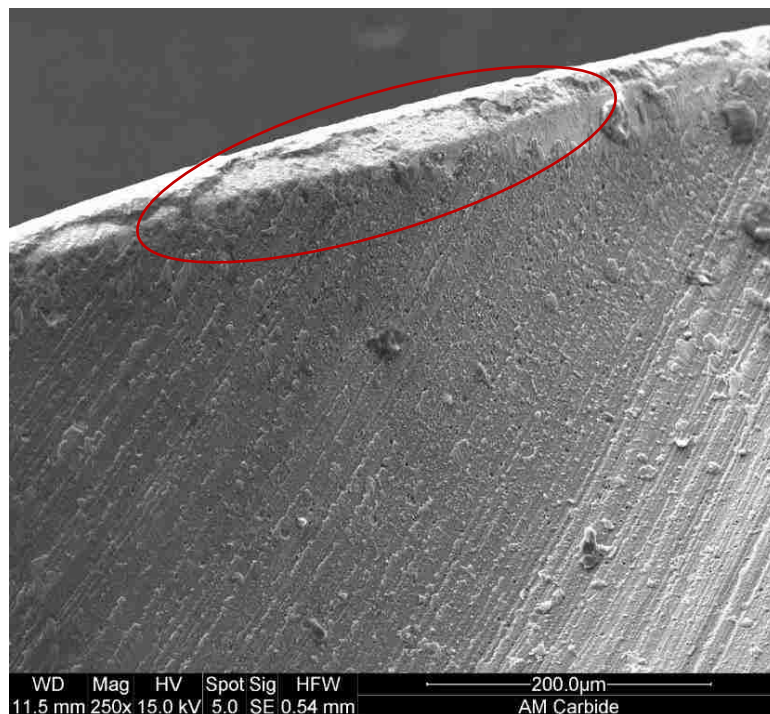
Figure 126. 250x SEM flute view of the carbide drill bit cutting edge after drilling 60 holes in AM titanium.
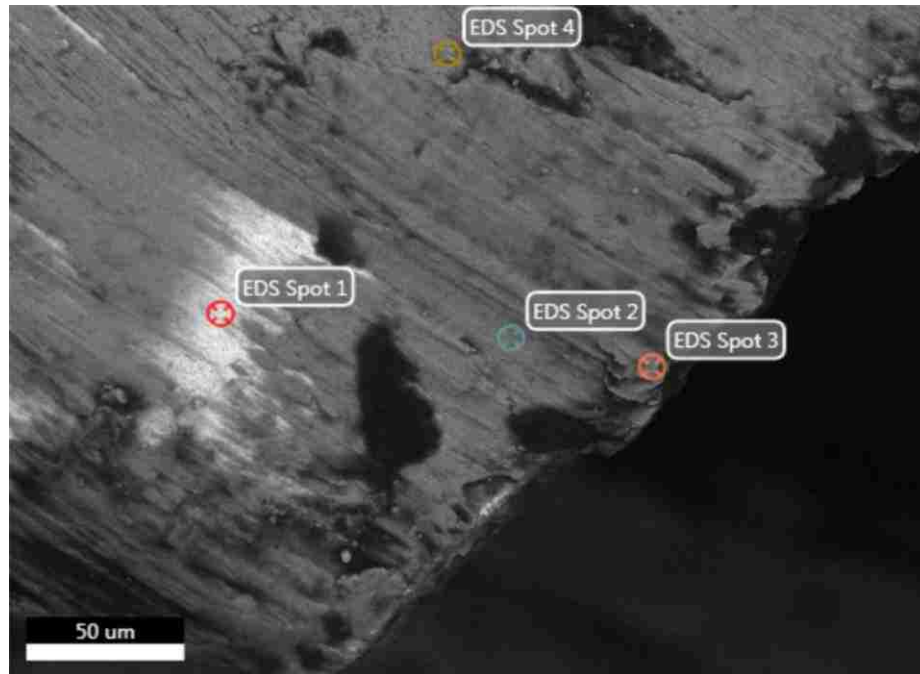
Figure 127. EDS spot analysis of the carbide drill bit cutting edge after drilling 60 holes in AM titanium.

Figure 127 and Figure 128 show the EDS spot analysis of the drill bit. Since the coating and the workpiece material both consists of titanium it is hard to confirm which part is adhesion and which part is the coating. To resolve this problem, the wear of the coating is examined. Referring to Figure 128 (A), spot 1 shows the base material of the cutting edge, while spot 2 and spot 3 from Figure 128 (B, C), shows titanium which can either be the coating or adhesion. Figure 129 shows the overlay of titanium and tungsten. The EDS overlay map shows the cutting edge as the uncoated tungsten while the titanium is shown as the possible adhesion and the coating on the drill bit.
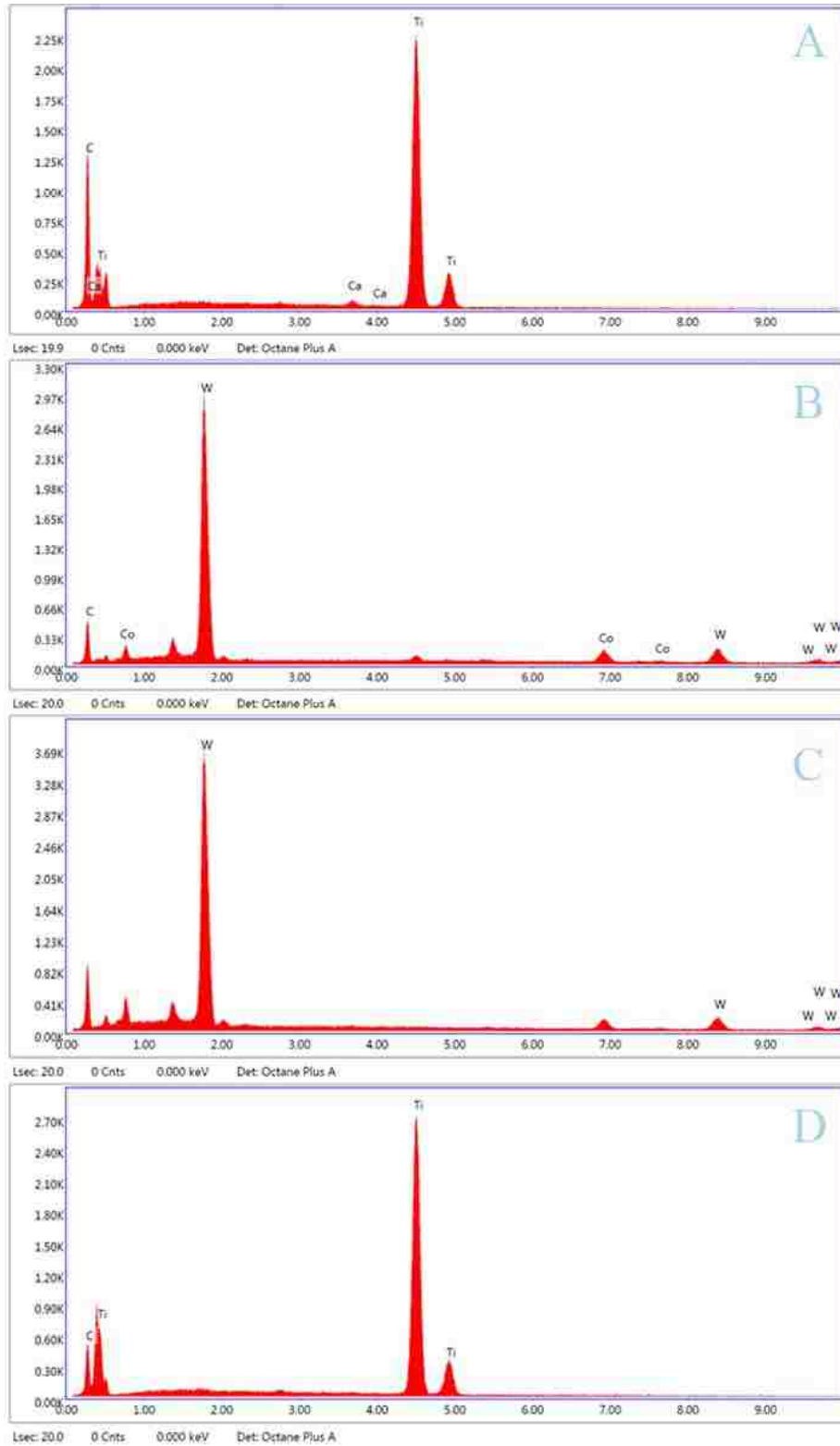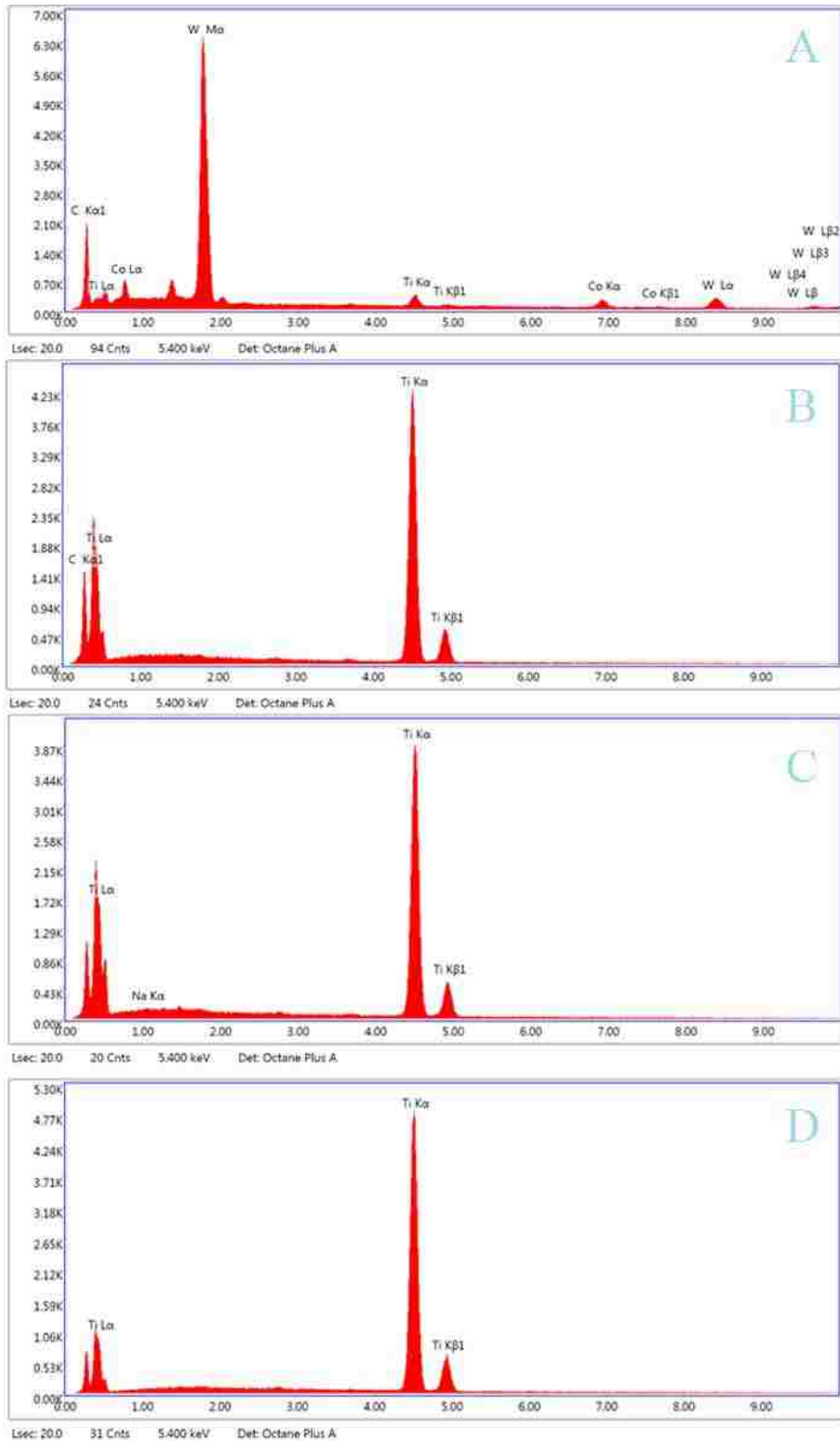
Figure 128. EDS spot analysis of the carbide drill bit after drilling 60 holes in AM titanium where, (A) is Spot 1, (B) is Spot 2, (C) is Spot 3, (D) is Spot 4.

109
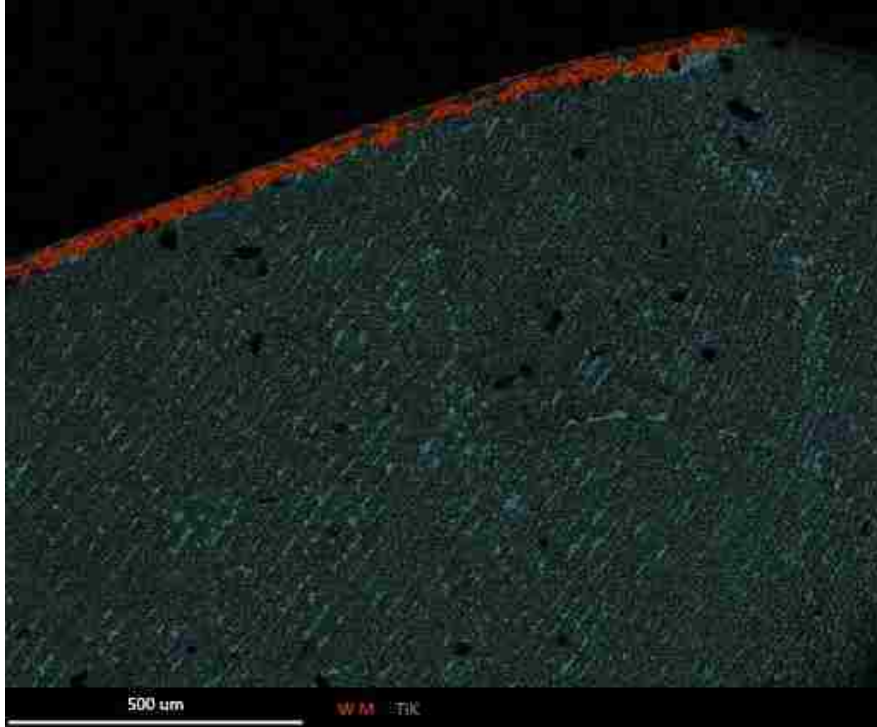
Figure 129. EDS mapping of the carbide drill bit cutting edge after drilling 60 holes in AM titanium.

4.4 Torque

Torque increased as the number of holes increased which may be due to the slipping of the cutting edge. As wear is increased the cutting edge become blunter and duller. The peaks of the torque show the holes drilled and each peak describes how well the holes were created. The experiments include drilling various titanium alloys with various drill bits for 60 holes, 20 holes, 15 holes, 10 holes, 5 holes, and 1 hole. This section is divided into three sections where each section is a different titanium alloy and the subsection are the drill bits which include HSS, three flute drill bit, and carbide drill bit. The average torque is calculated by taking the average torques.

110

4.4.1 Ti-6Al-4V

4.4.1.1 High Speed Steel Twist Drill Bit

The torque data for 1 hole, 5 holes, 10 holes, 15 holes, 20 holes and 60 holes are shown in Figure 130 to Figure 139 showing the initial peaks and the final peaks using the HSS drill bit. The torque for 1 hole is 0.71 Nm when drilling grade 5 titanium (Ti-6Al-4V). The initial average torque for 5 holes is 0.84 Nm, the final average torque of 0.88 Nm and the overall average torque of 0.85 Nm.
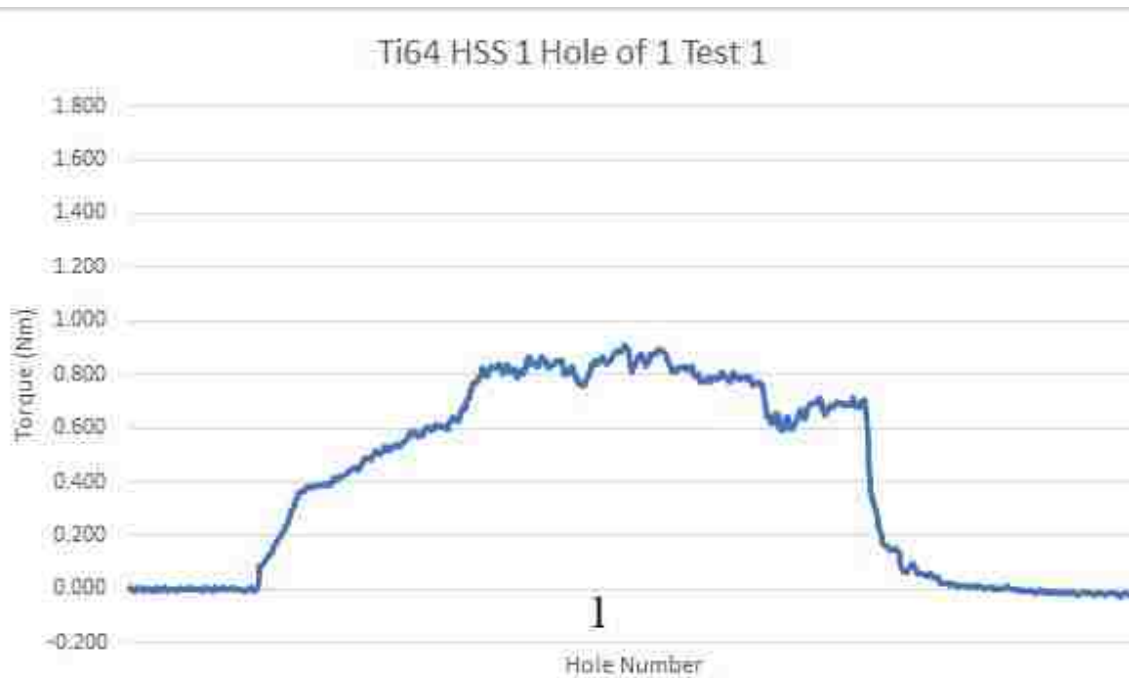
Figure 130. Torque data for drilling 1 hole in grade 5 titanium (Ti-6Al-4V) with the HSS drill bit.
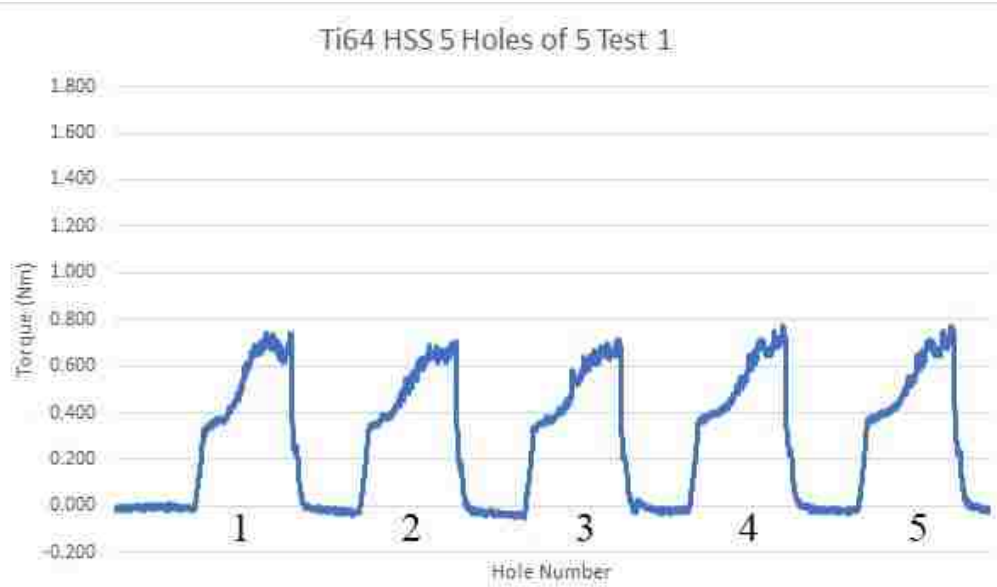
Figure 131. Torque data for drilling 5 holes in grade 5 titanium (Ti-6Al-4V) with the HSS drill bit.

For 10 holes, the initial average torque is 0.97 Nm, the final average torque is 1.05 Nm and the overall average torque is 1.01 Nm.
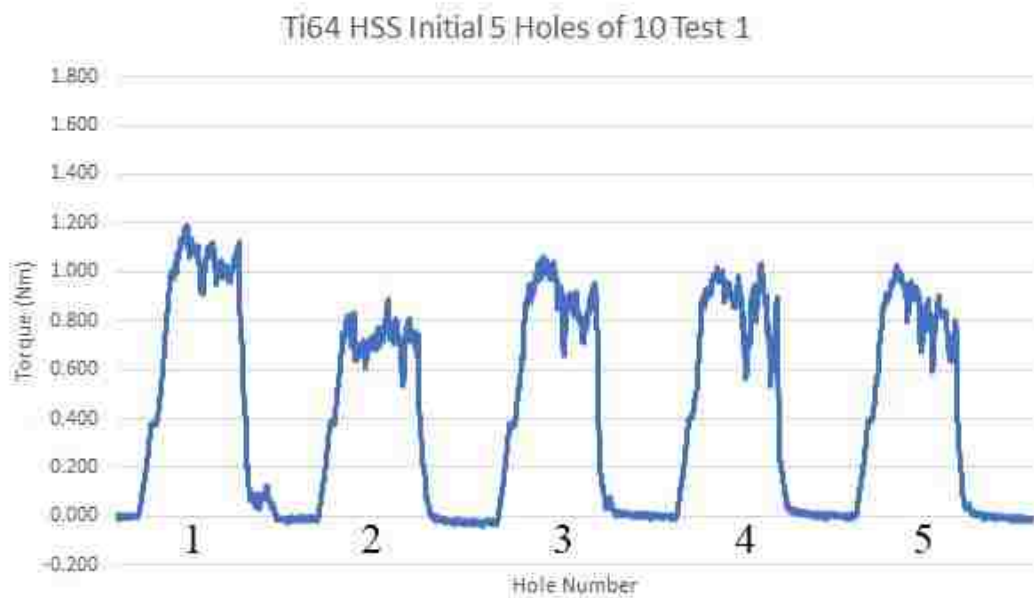
Figure 132. Torque data for the initial 5 holes when drilling 10 holes in grade 5 titanium (Ti-6Al-4V) with the HSS drill bit.

Figure 133. Torque data for the final 5 holes when drilling 10 holes in grade 5 titanium (Ti-6Al-4V) with the HSS drill bit.

For 15 holes, the initial average torque is 1.05 Nm, the final average torque is 1.05 Nm and the overall average torque is 1.05 Nm.
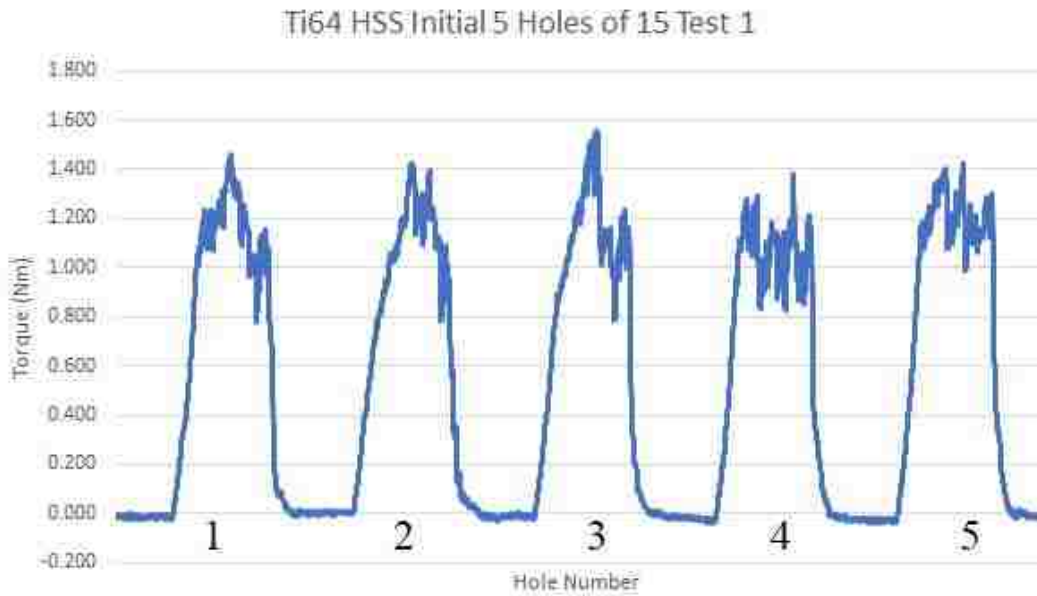
Figure 134. Torque data for the initial 5 holes when drilling 15 holes in grade 5 titanium (Ti-6Al-4V) with the HSS drill bit.

Figure 135. Torque data for the final 5 holes when drilling 15 holes in grade 5 titanium (Ti-6Al-4V) with the HSS drill bit.

For 20 holes, the initial average torque is 1.02 Nm, the final average torque is 1.08 Nm and the overall average torque is 1.05 Nm.
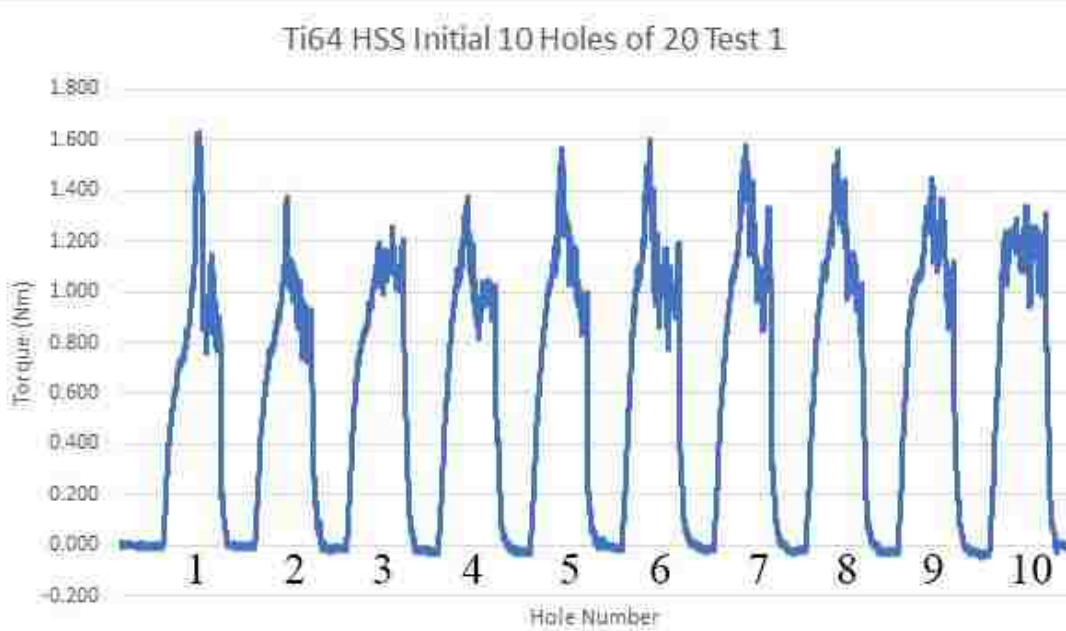
Figure 136. Torque data for the initial 10 holes when drilling 20 holes in grade 5 titanium (Ti-6Al-4V) with the HSS drill bit.

114
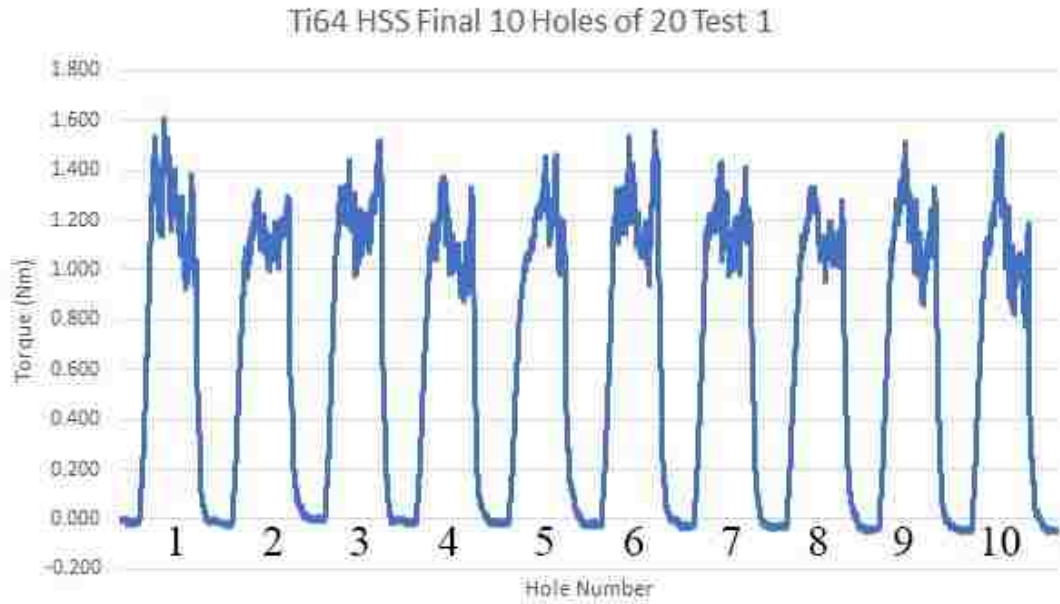
Figure 137. Torque data for the final 10 holes when drilling 20 holes in grade 5 titanium (Ti-6Al-4V) with the HSS drill bit.

For 60 holes, the initial average torque is 1.05 Nm, the final average torque is 1.09

Nm and the overall average torque is 1.07 Nm.
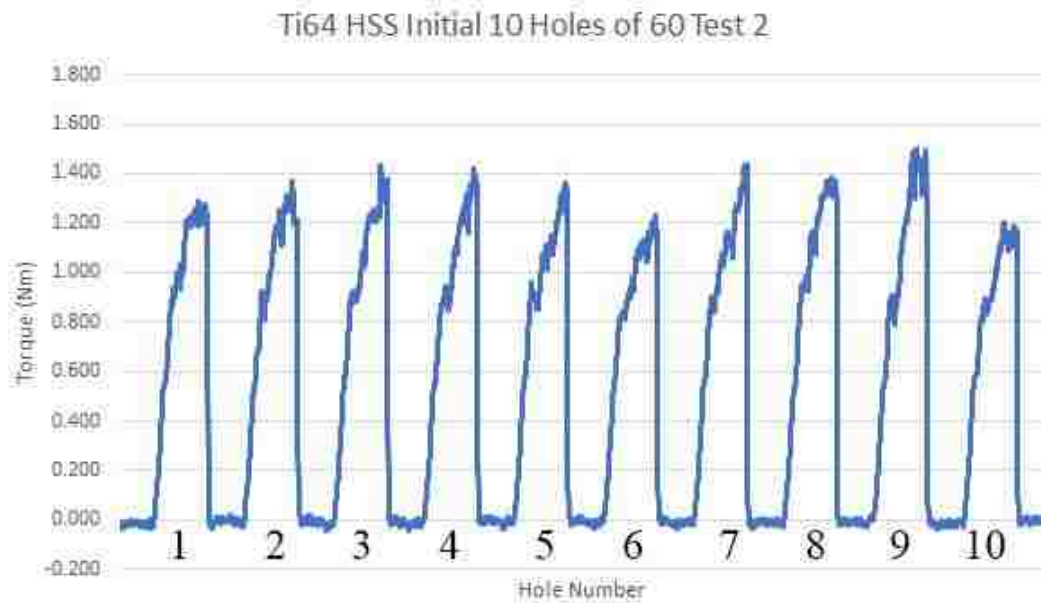
Figure 138. Torque data for the initial 10 holes when drilling 60 holes in grade 5 titanium (Ti-6Al-4V) with the HSS drill bit.

115
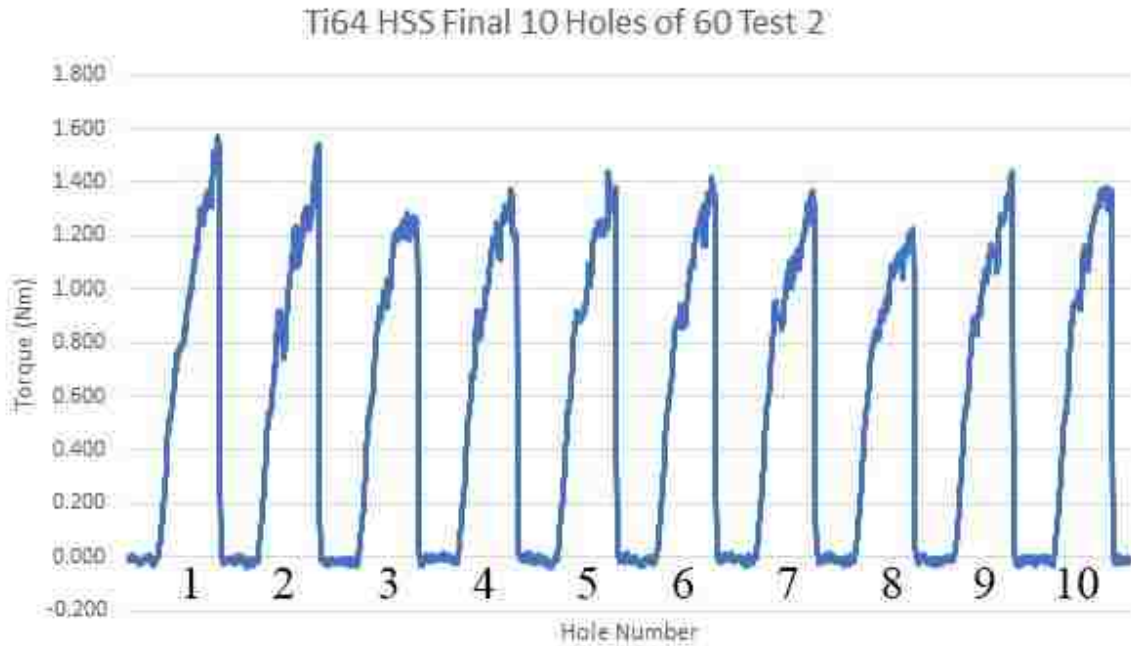
Figure 139. Torque data for the final 10 holes when drilling 60 holes in grade 5 titanium (Ti-6Al-4V) with the HSS drill bit.

4.4.1.2 Three Flute Drill Bit

The torque data for drilling 60 holes with the three flute drill bit holes are shown in Figure 140 and Figure 141 showing the initial peaks and the final peaks. The three flute drill bit is designed for improved chip ejection with an additional flute. The initial average torque is 0.59 Nm, the final average torque is 0.64 Nm and the overall average torque is 0.61 Nm.

Figure 140. Torque data for the initial 10 holes when drilling 60 holes in grade 5 titanium (Ti-6Al-4V) with the three flute drill bit.
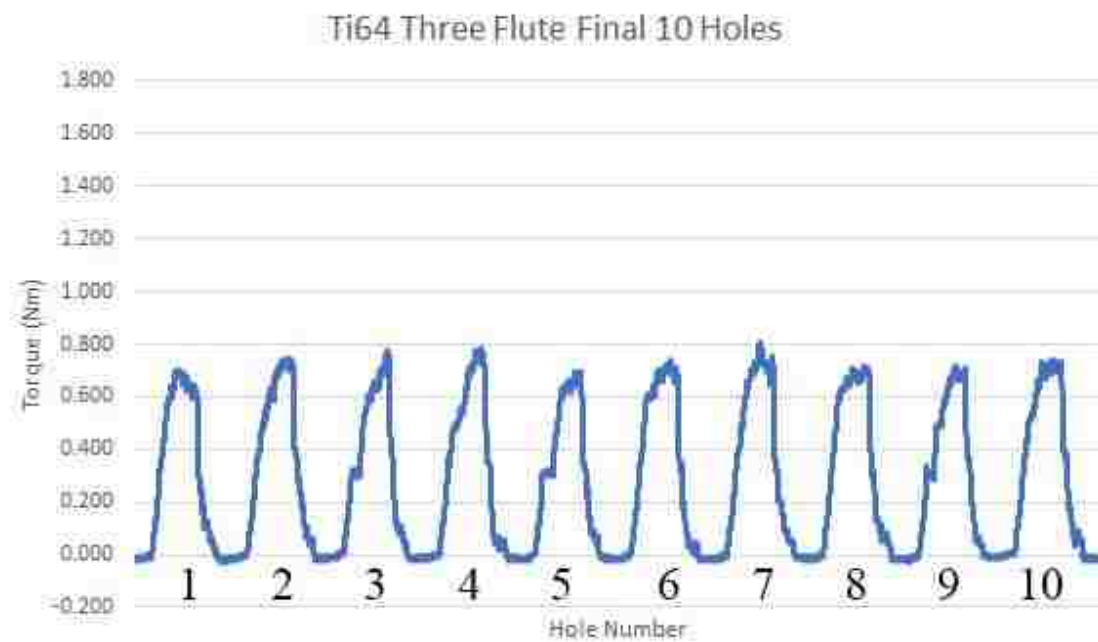
Figure 141. Torque data for the final 10 holes when drilling 60 holes in grade 5 titanium (Ti-6Al-4V) with the three flute drill bit.

117

4.4.1.3 Carbide Drill Bit

The torque data for drilling 60 holes with the carbide drill bit are shown in Figure 142 and Figure 143 showing the initial peaks and the final peaks. The carbide drill bit is coated with AlTiN coating which improves the wear resistance which overall improves tool life. For the carbide drill bit when drilling grade 5 titanium (Ti-6Al-4V), the initial average torque is 0.50 Nm, the final average torque is 0.52 Nm and the overall average torque is 0.51 Nm. The failure was noted when the hole depth was reduced as the number of holes increased.
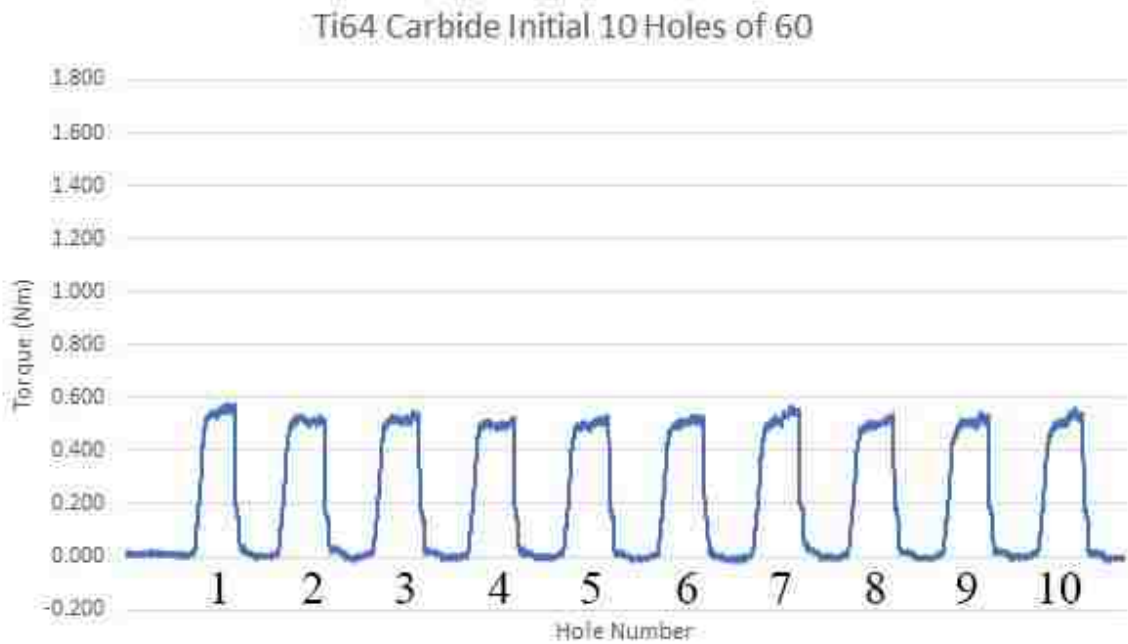
Figure 142. Torque data for the initial 10 holes when drilling 60 holes in grade 5 titanium (Ti-6Al-4V) with the carbide drill bit.
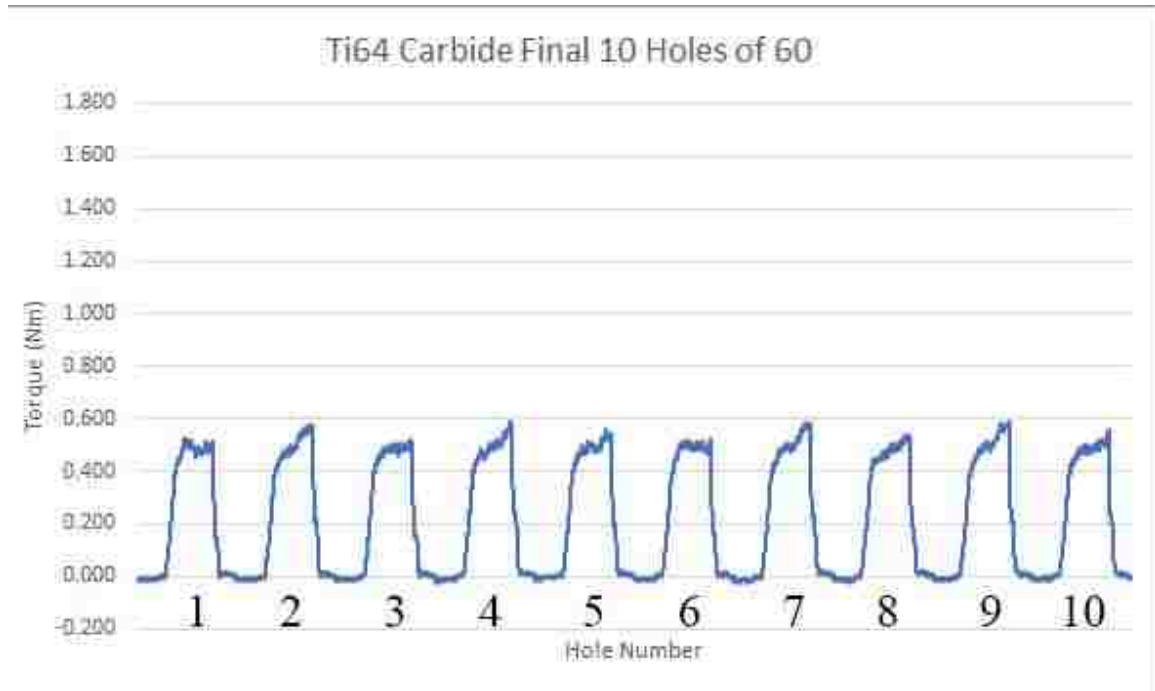
Figure 143. Torque data for the final 10 holes when drilling 60 holes in grade 5 titanium (Ti-6Al-4V) with the carbide drill bit.

4.4.2 Powder Metallurgy Titanium

4.4.2.1 High Speed Steel Twist Drill Bit

Here is the torque data for the PM titanium for 1 hole, 5 holes, 10 holes, 15 holes, 20 holes and 60 holes are shown in Figure 144 to Figure 153 showing the initial peaks and the final peaks using the HSS drill bit. The torque for 1 hole is 0.32 Nm when PM titanium. The initial average torque for 5 holes is 0.36 Nm, the final average torque of 0.36 Nm and the overall average torque of 0.36 Nm.
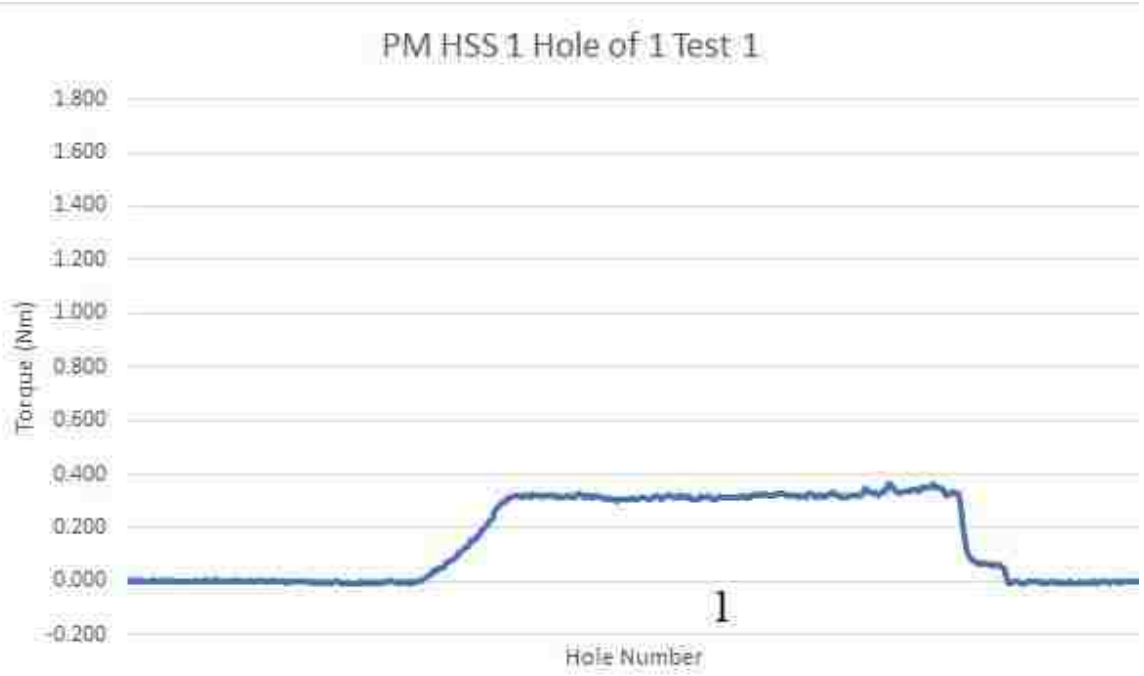
Figure 144. Torque data for drilling 1 hole in PM titanium with the HSS drill bit.
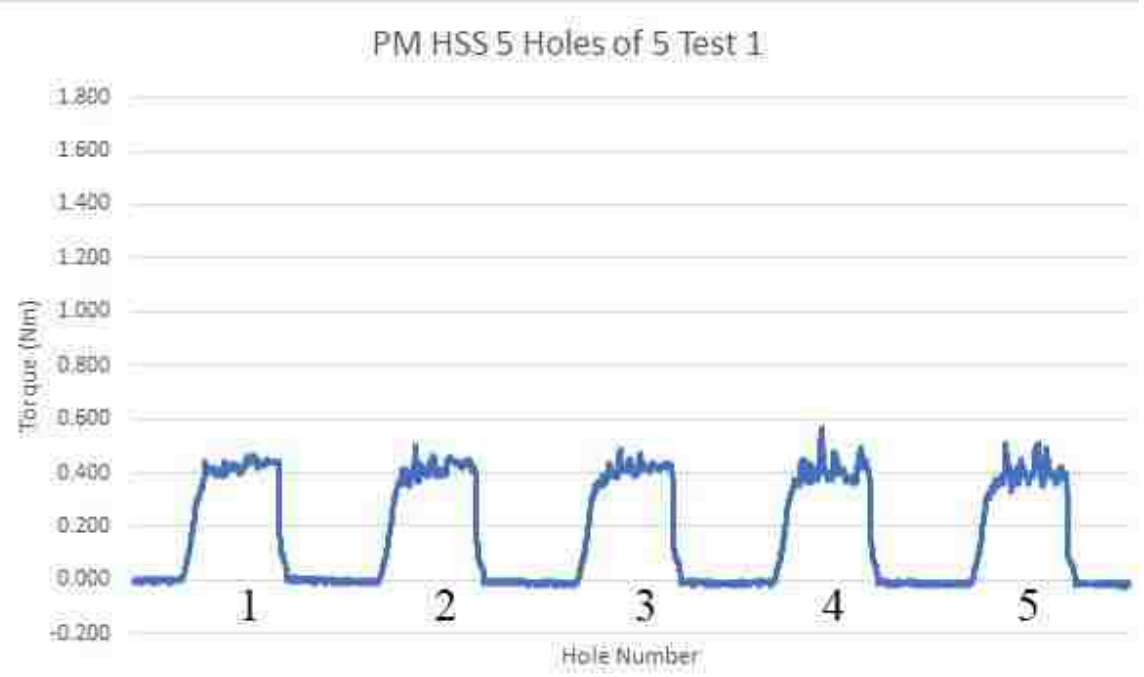
Figure 145. Torque data for drilling 5 holes in PM titanium with the HSS drill bit.

120
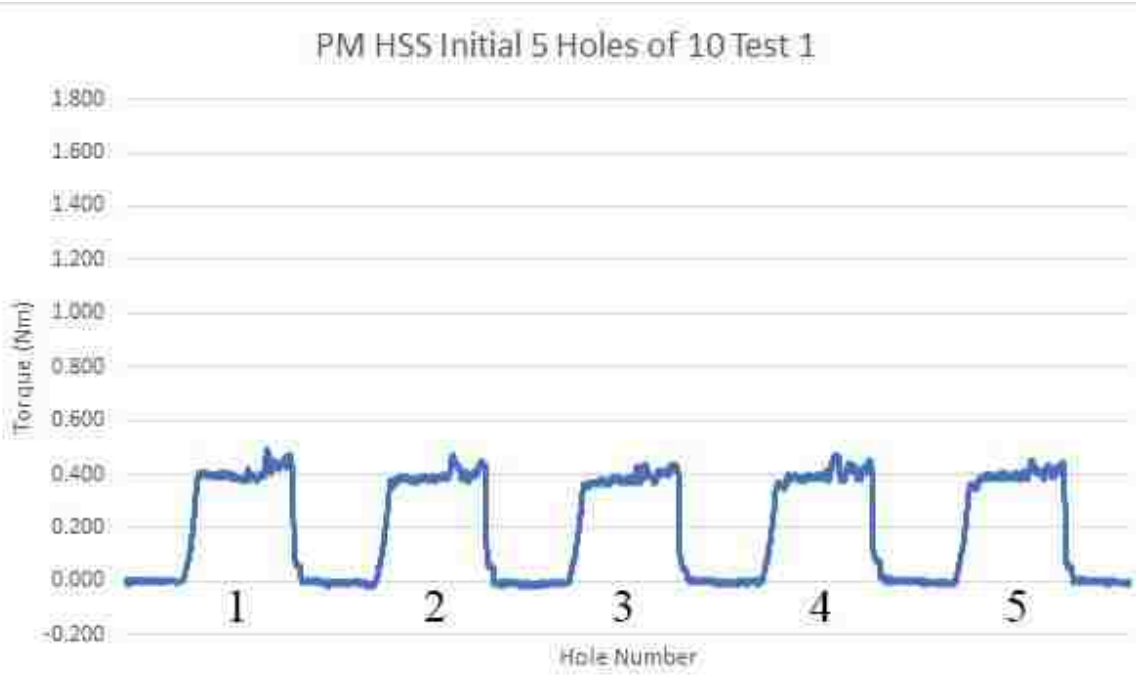
Figure 146. Torque data for the initial 5 holes when drilling 10 holes in PM titanium with the HSS drill bit.
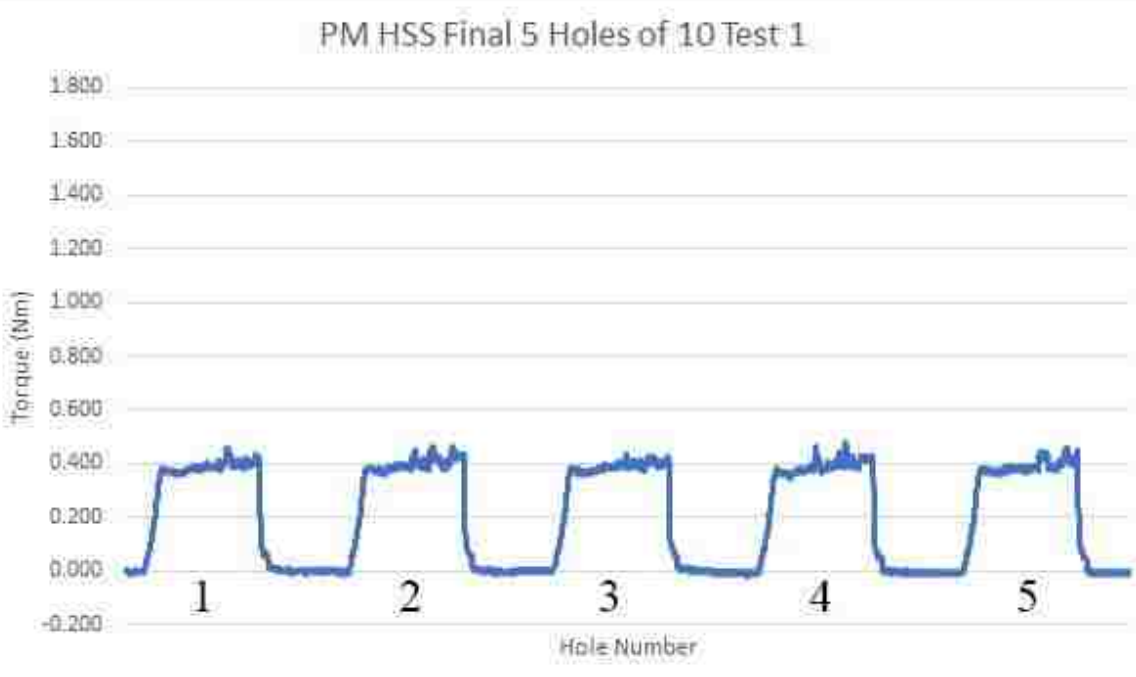
Figure 147. Torque data for the final 5 holes when drilling 10 holes in PM titanium with the HSS drill bit.

121

For 10 holes, the initial average torque is 0.36 Nm, the final average torque is 0.39 Nm and the overall average torque is 0.37 Nm.
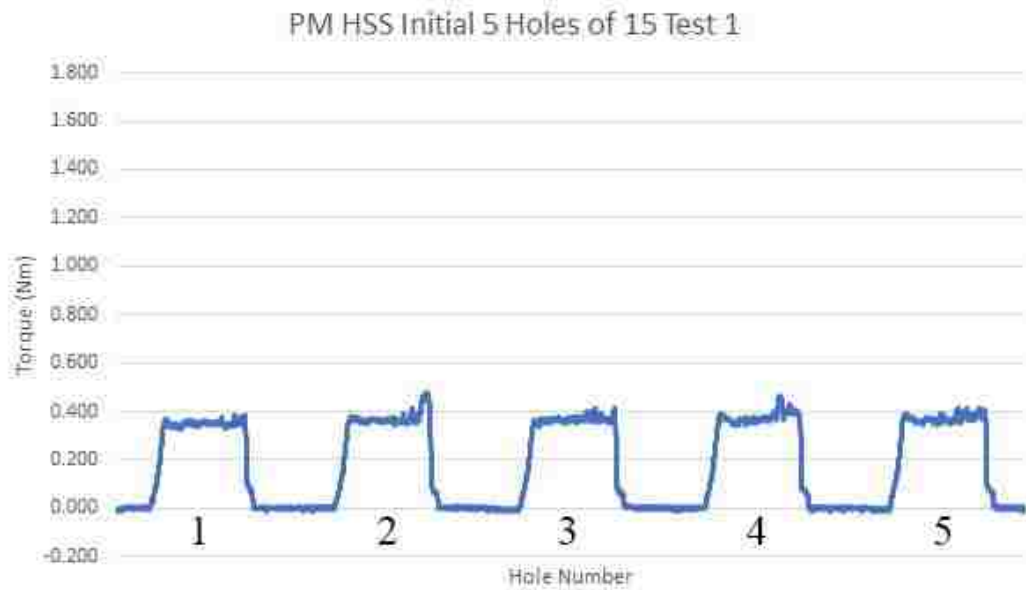
Figure 148. Torque data for the initial 5 holes when drilling 15 holes in PM titanium with the HSS drill bit.
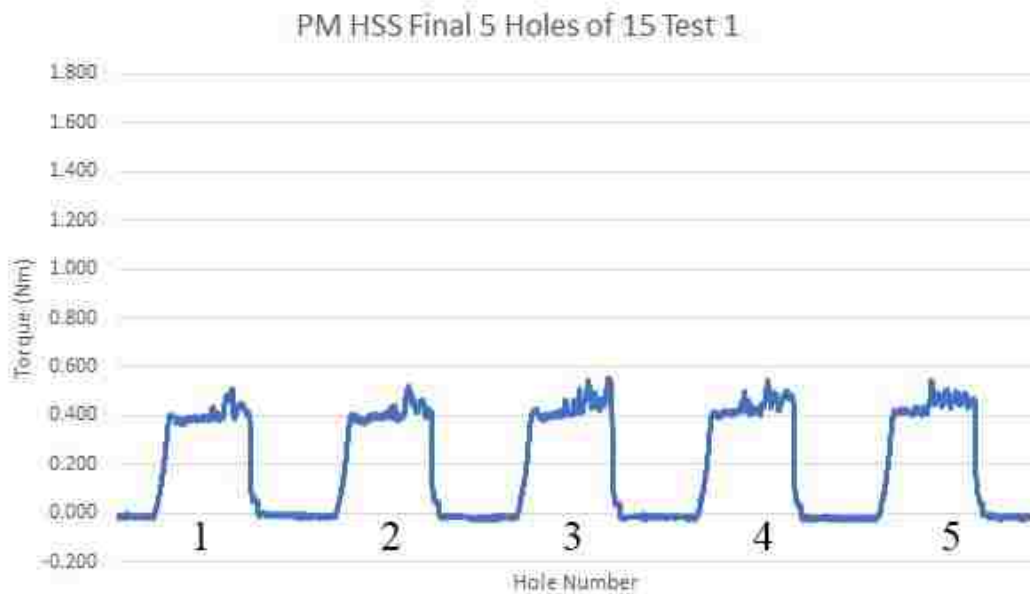
Figure 149. Torque data for the final 5 holes when drilling 10 holes in PM titanium with the HSS drill bit.

For 15 holes, the initial average torque is 0.38 Nm, the final average torque is 0.38

Nm and the overall average torque is 0.38 Nm.
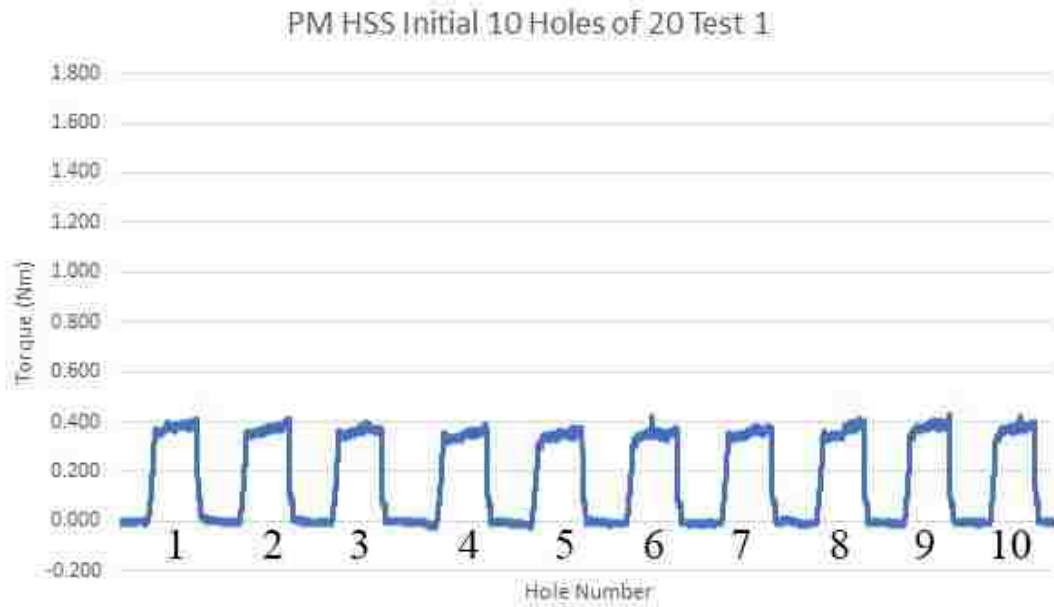
Figure 150. Torque data for the initial 10 holes when drilling 20 holes in PM titanium with the HSS drill bit.
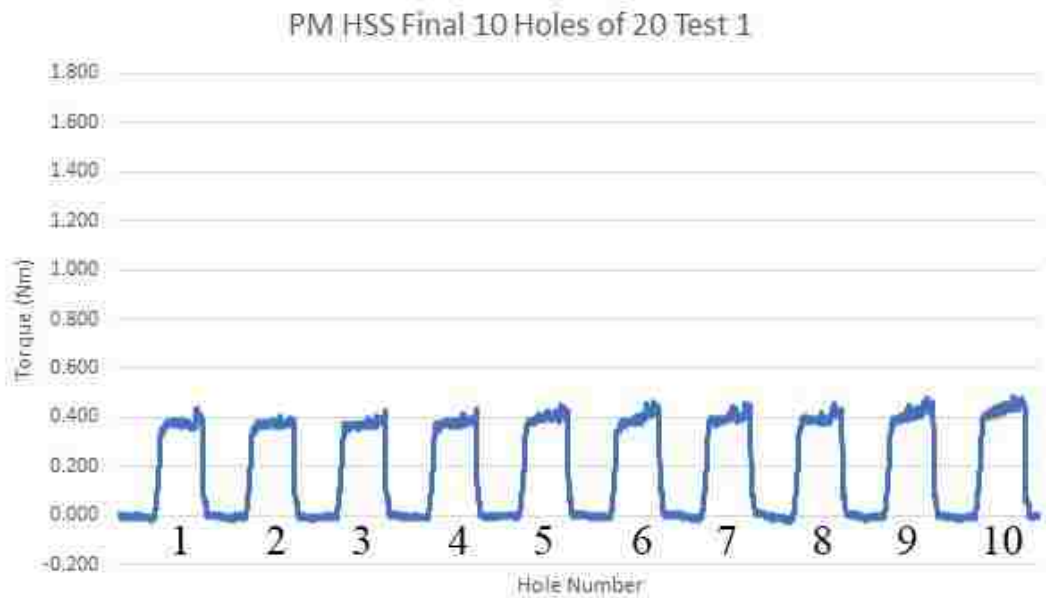
Figure 151. Torque data for the initial 10 holes when drilling 20 holes in PM titanium with the HSS drill bit.

For 20 holes, the initial average torque is 0.37 Nm, the final average torque is 0.41

Nm and the overall average torque is 0.39 Nm.
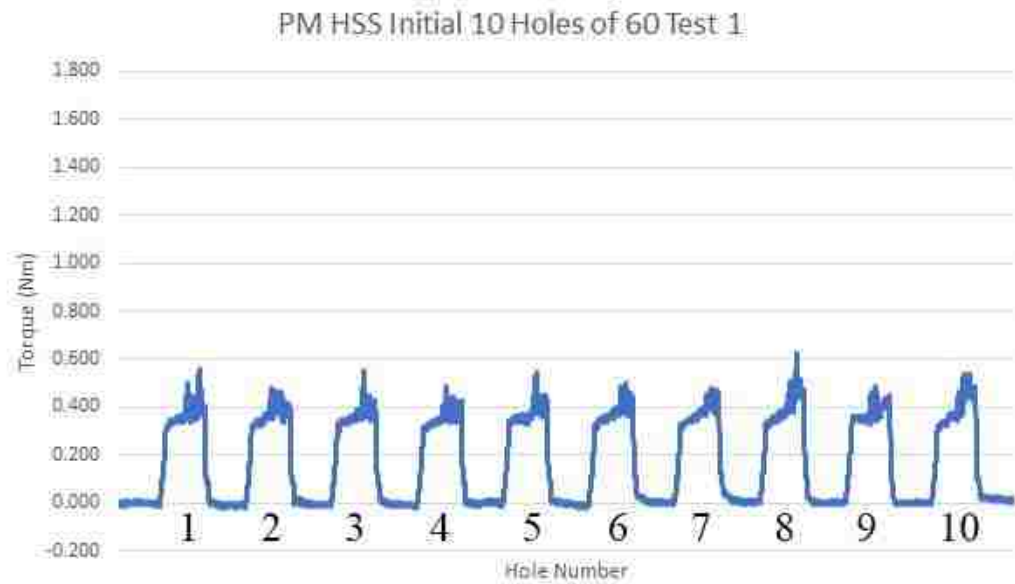
Figure 152. Torque data for the final 10 holes when drilling 60 holes in PM titanium with the HSS drill bit.
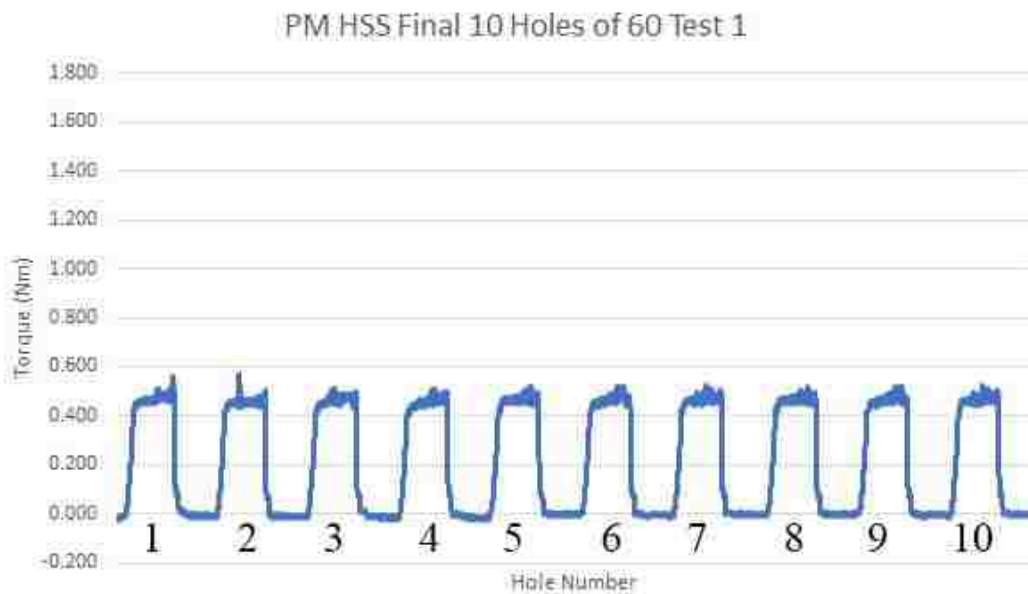
Figure 153. Torque data for the final 10 holes when drilling 60 holes in PM titanium with the HSS drill bit.

For 60 holes, the initial average torque is 0.44 Nm, the final average torque is 0.47 Nm and the overall average torque is 0.46 Nm.

4.4.2.2 Three Flute Drill Bit

The torque data for drilling 60 holes with the three flute drill bit are shown in Figure 154 and Figure 155 showing the initial peaks and the final peaks. The initial average torque is 0.56 Nm, the final average torque is 0.57 Nm and the overall average torque is 0.56 Nm.
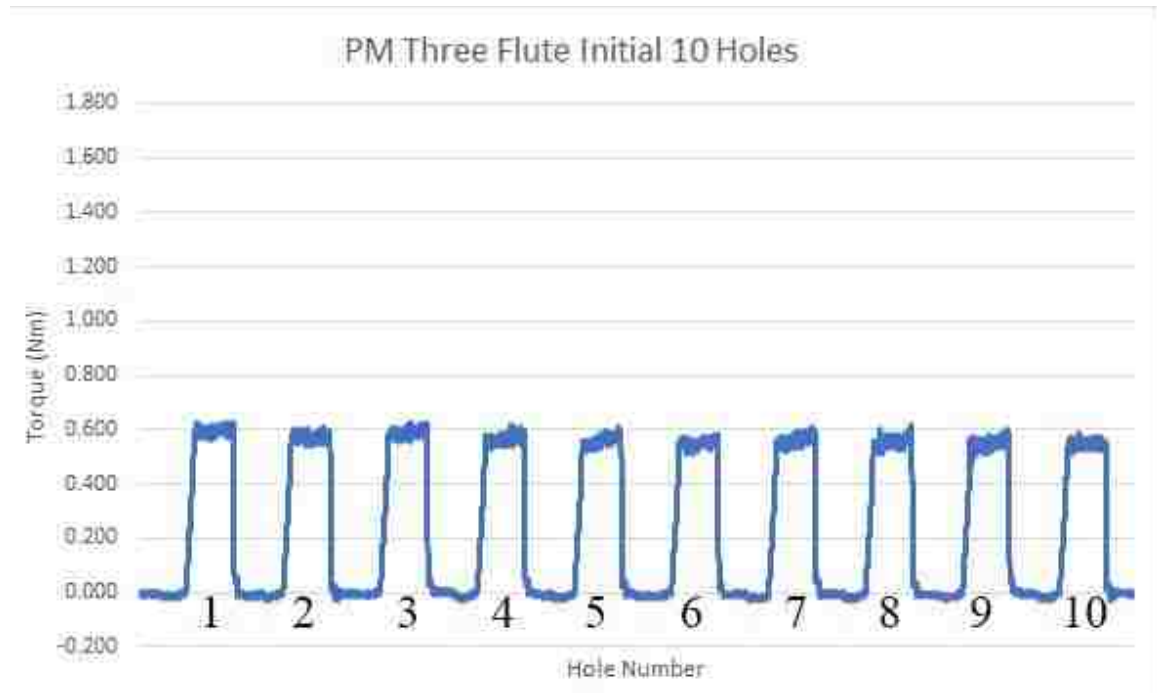
Figure 154. Torque data for the initial 10 holes when drilling 60 holes in PM titanium with the three flute drill bit.
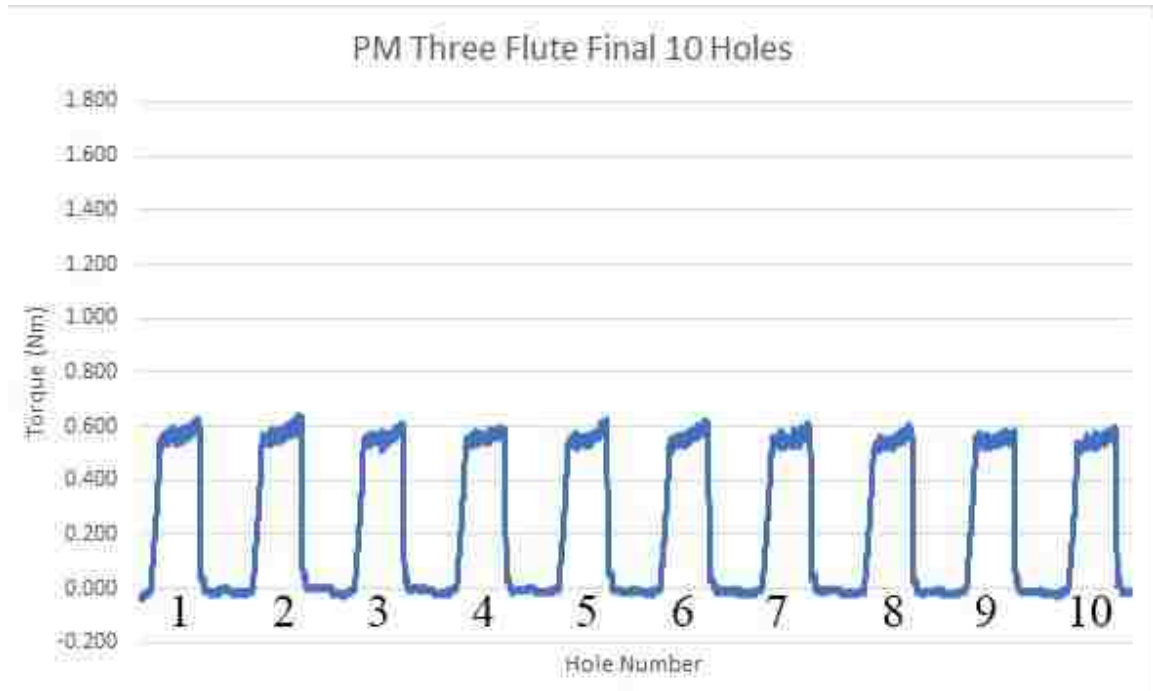
Figure 155. Torque data for the final 10 holes when drilling 60 holes in PM titanium with the three flute drill bit.

4.4.2.3 Carbide Drill Bit

The torque data for drilling 60 holes with the carbide drill bit are shown in Figure 156 and Figure 157 showing the initial peaks and the final peaks. For the carbide drill bit the initial average torque is 0.42 Nm, the final average torque is 0.42 Nm and the overall average torque is 0.42 Nm. The same problem occurred with the three flute drill bit where the drill bit would be shoved into the chuck. The three flute drill bit drilled 24 holes before the drill bit began to shove into the chuck and the depth of the holes began to reduce.
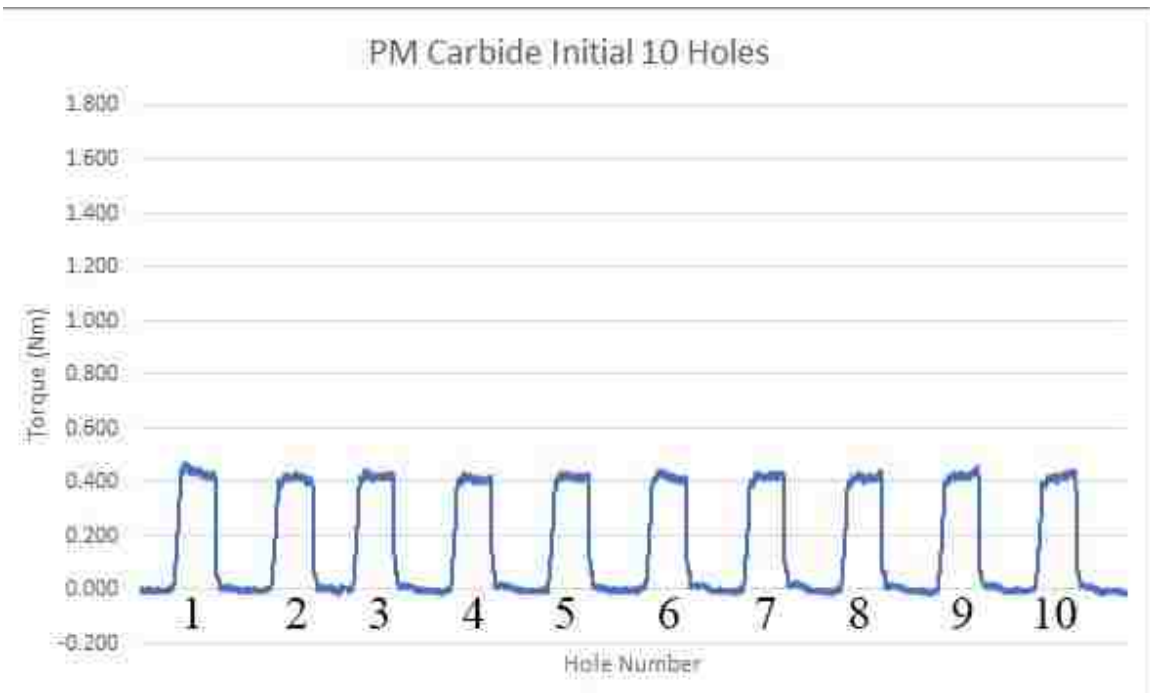
Figure 156. Torque data for the initial 10 holes when drilling 60 holes in PM titanium with the carbide drill bit.
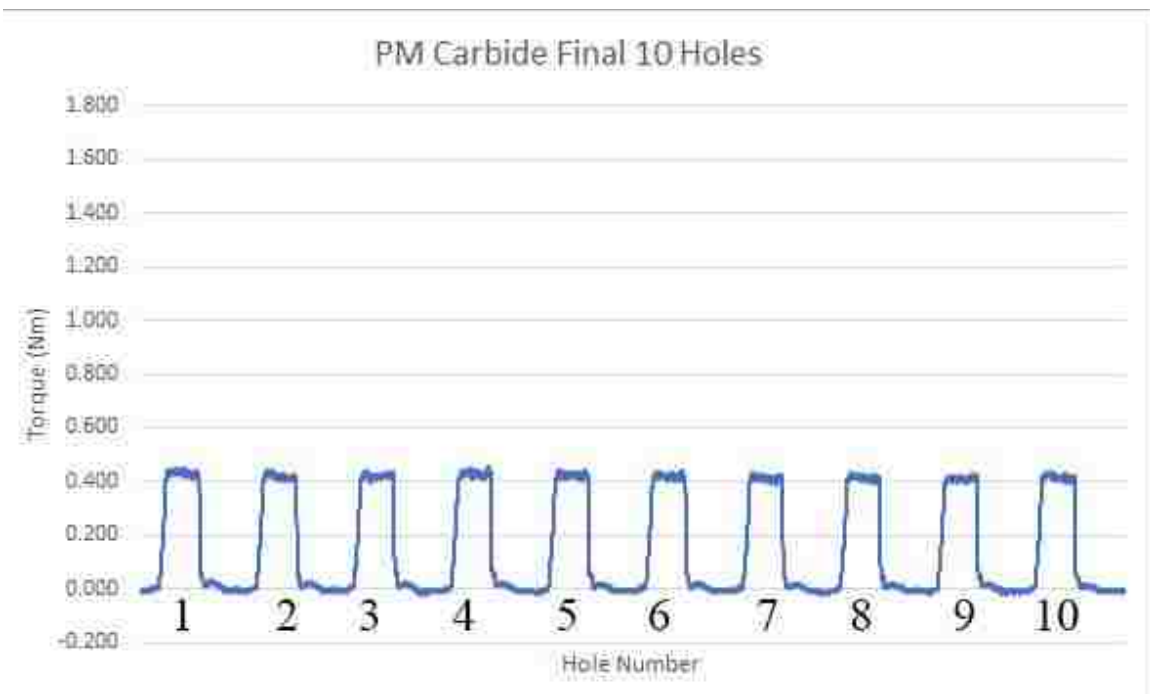
Figure 157. Torque data for the final 10 holes when drilling 60 holes in PM titanium with the carbide drill bit.

4.4.3 Additive Manufactured Titanium

4.4.3.1 High Speed Steel Twist Drill Bit

The HSS drill bit failed to drill 60 holes multiple times, one example is shown in Figure 158 where it failed at 8 holes. The average initial torque is 1.14 Nm, the average final torque is 1.47 Nm and the overall average torque is 1.30 Nm.
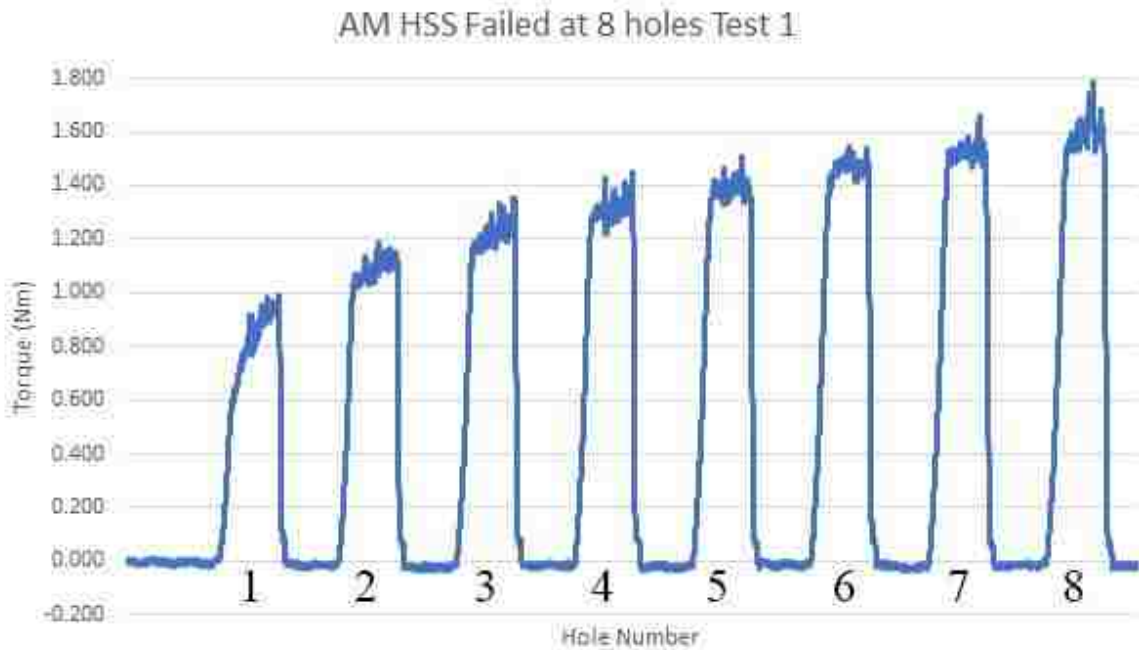
Figure 158. Torque data after it failed at 8 holes when attempting to drill 60 holes in AM titanium with the HSS drill bit.

4.4.3.2 Three Flute Drill Bit

The three flute drill bit failed to drill 60 holes multiple times, the torque collected shows 24 holes drilled in Figure 159 and Figure 160 where the initial torque and final torque are shown respectively. The average initial torque is 1.01 Nm, the average final torque is 1.43 Nm and the overall average torque is 1.22 Nm.
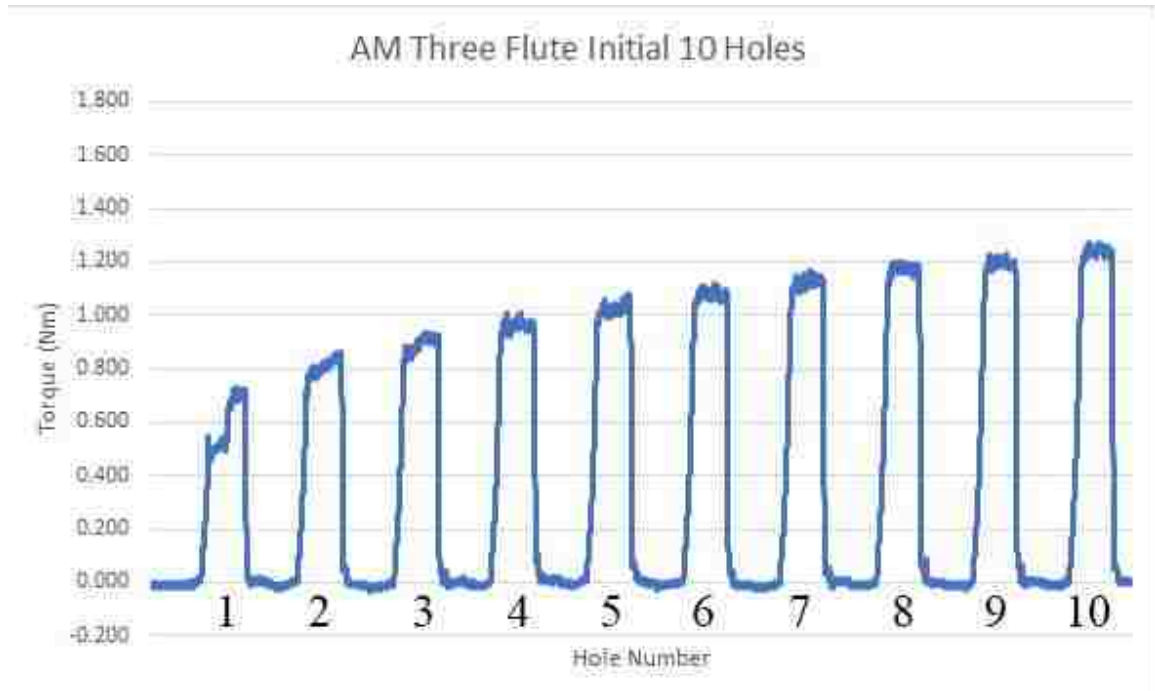
Figure 159. Torque data for the initial 10 holes after it failed at 24 holes when attempting to drill 60 holes in AM titanium with the three flute drill bit.
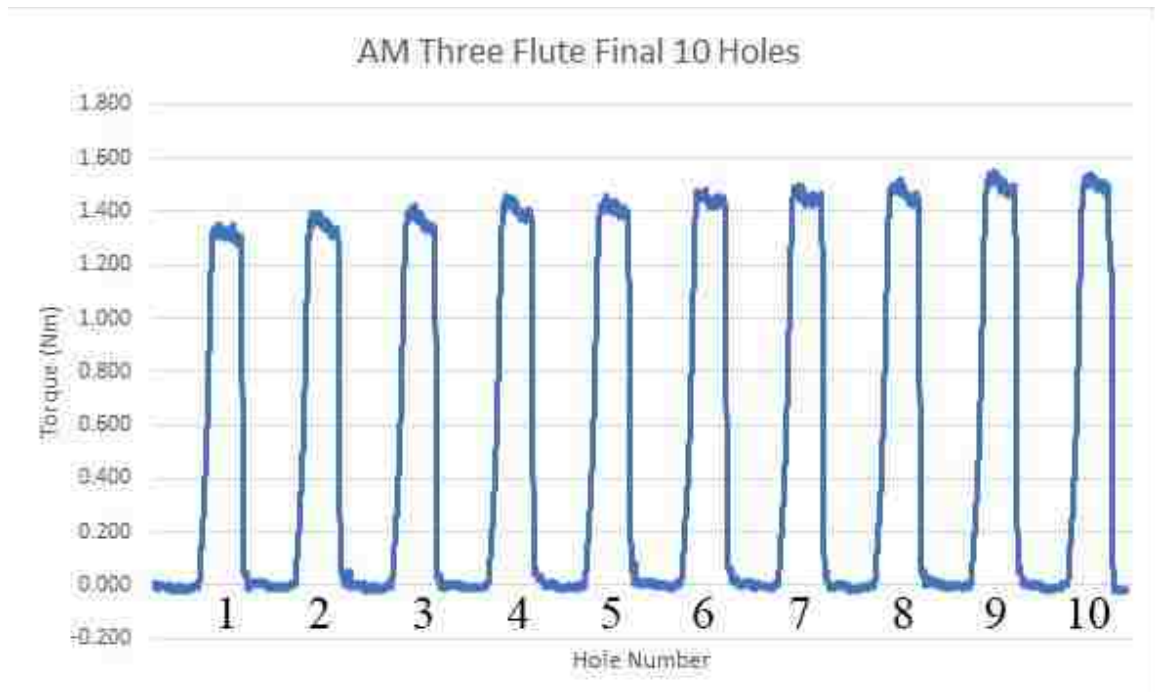
Figure 160. Torque data for the final 10 holes after it failed at 24 holes when attempting to drill 60 holes in AM titanium with the three flute drill bit.

4.4.3.3 Carbide Drill Bit

The carbide drill bit drilled 60 holes, the torque data is shown in Figure 161 and Figure 162 where the initial torque and final torque are shown respectively. The average initial torque is 0.77 Nm, the average final torque is 1.39 Nm and the overall average torque is 1.08 Nm.

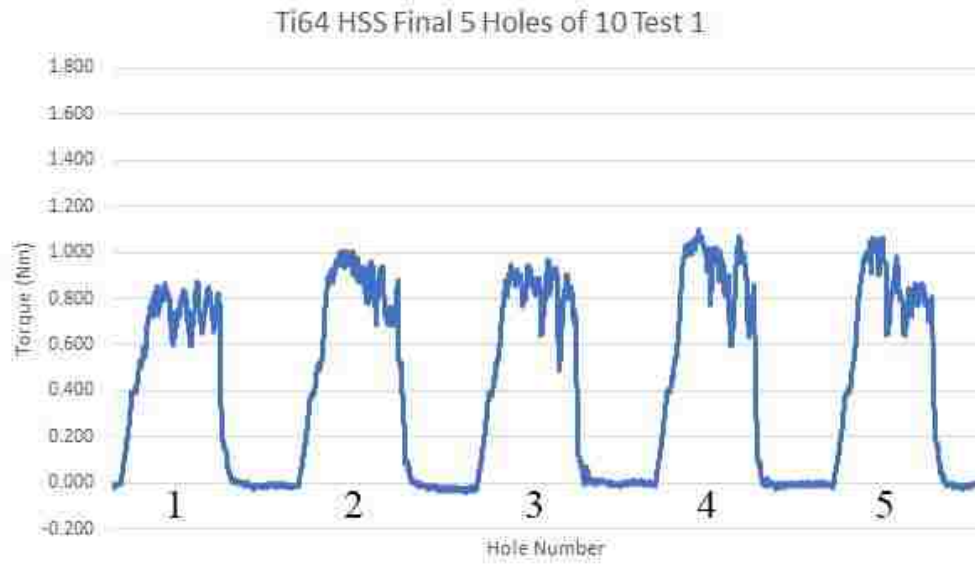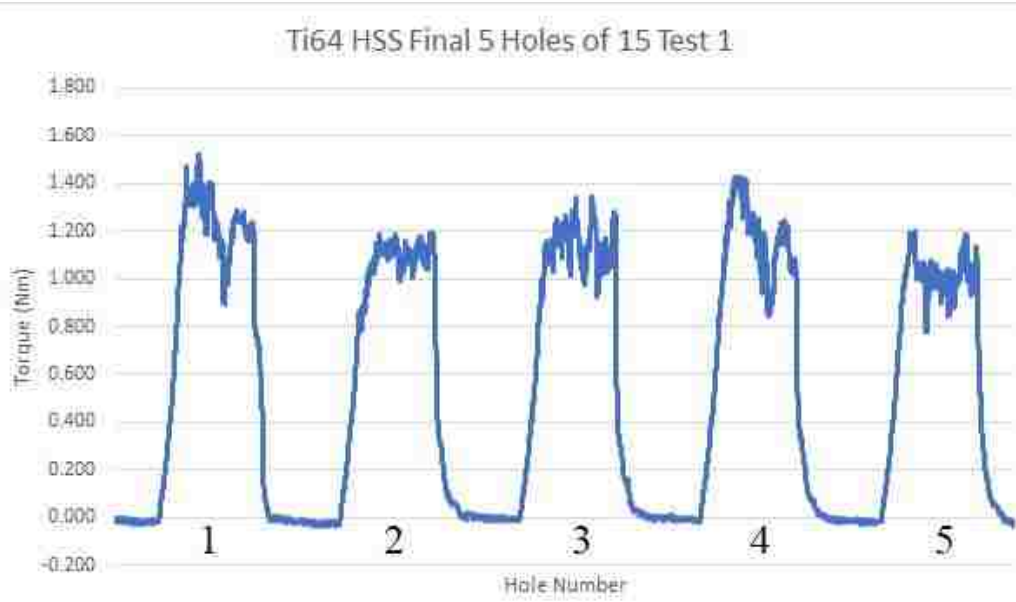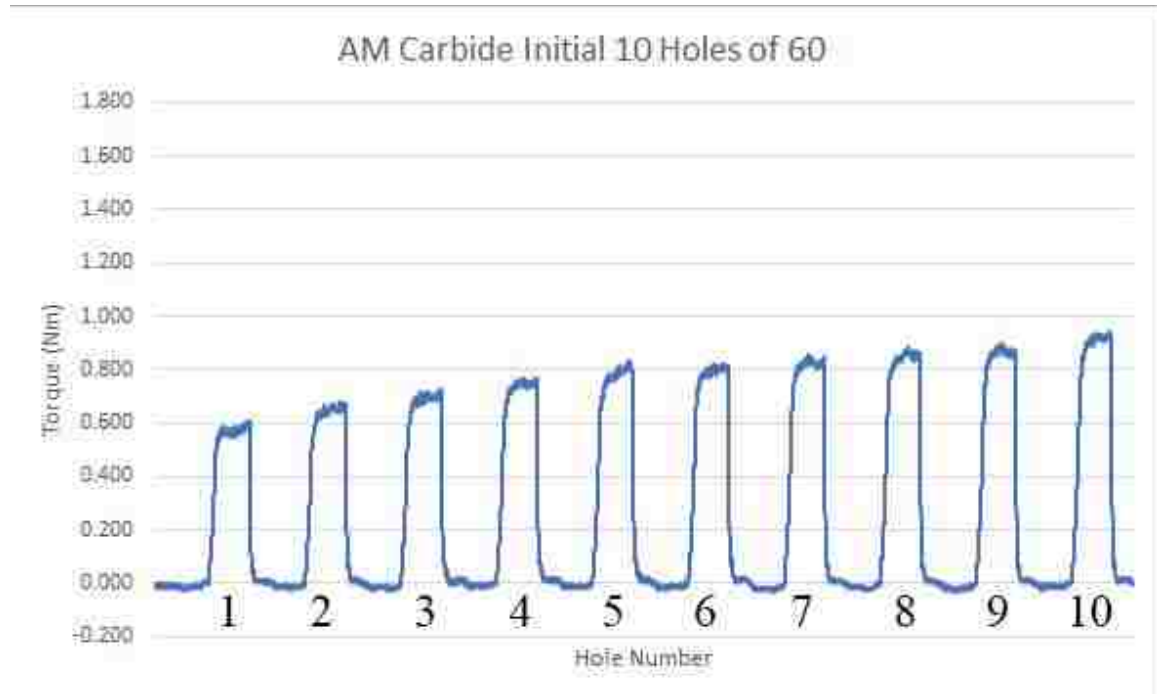*Figure 161. Torque data for the initial 10 holes when drilling 60 holes in AM titanium with the carbide drill bit.*
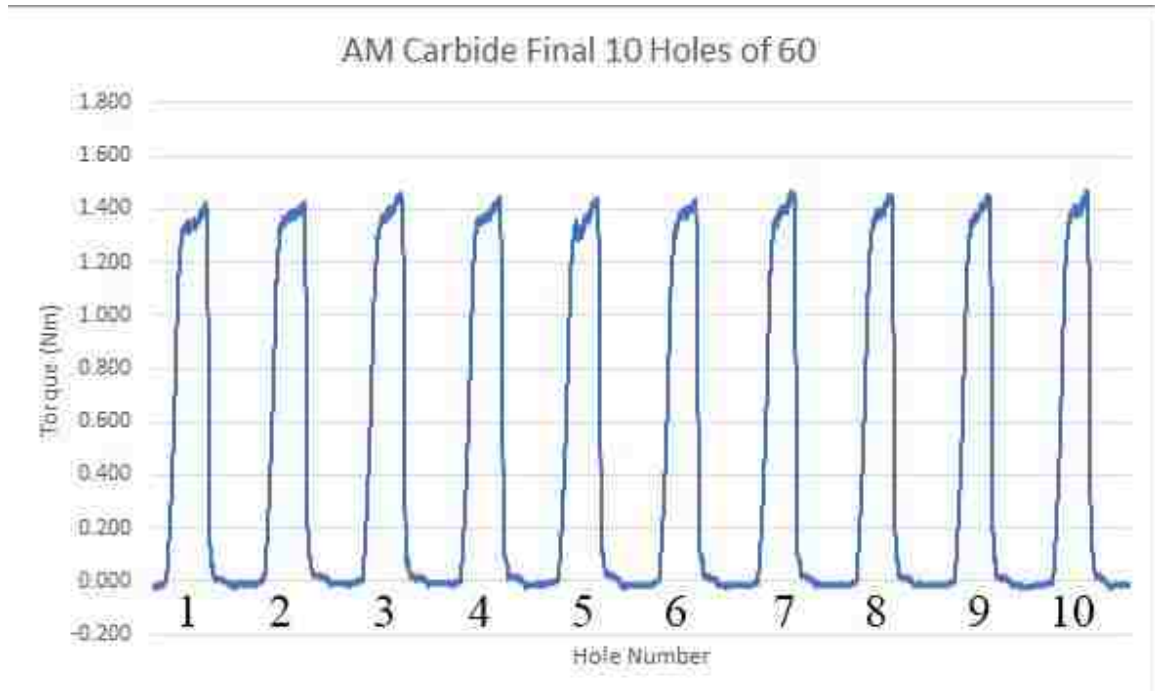
Figure 162. Torque data for the final 10 holes when drilling 60 holes in AM titanium with the carbide drill bit.

4.5 Chip Morphology

The chip morphology of titanium alloys has been a great interest for industry production due to their chip formations and shapes. The feed rate affects the chip length while the cutting speed has no affect. Since the feed rate is constant in this study, the distance between the spirals or the pitch of the chips increase as the number of holes increase.

4.5.1 High Speed Steel Twist Drill Bit

The chip morphology of the HSS drill bit when drilling grade 5 titanium (Ti-6Al-4V), PM titanium and AM titanium is shown in Figure 163, Figure 164 and Figure 165, respectively.

131
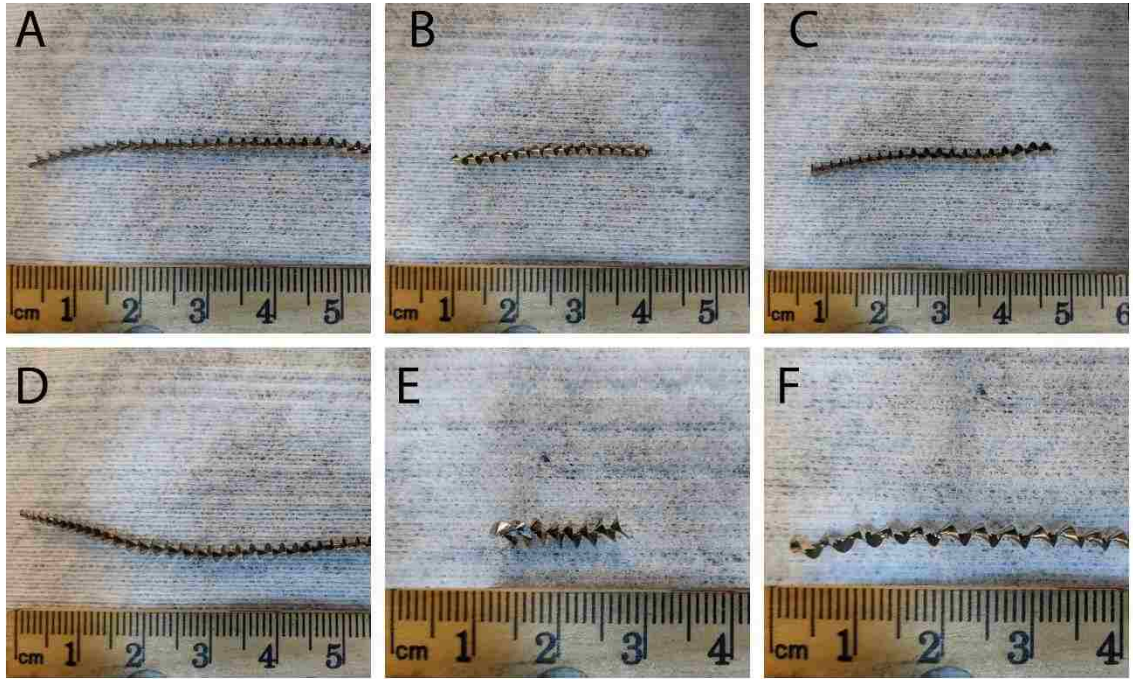
Figure 163. Chip morphology of grade 5 titanium (Ti-6Al-4V) using an HSS drill bit for (A) 1 hole, (B) 5 holes, (C) 10 holes, (D), 15 holes, (E) 20 holes, (F) 60 holes.
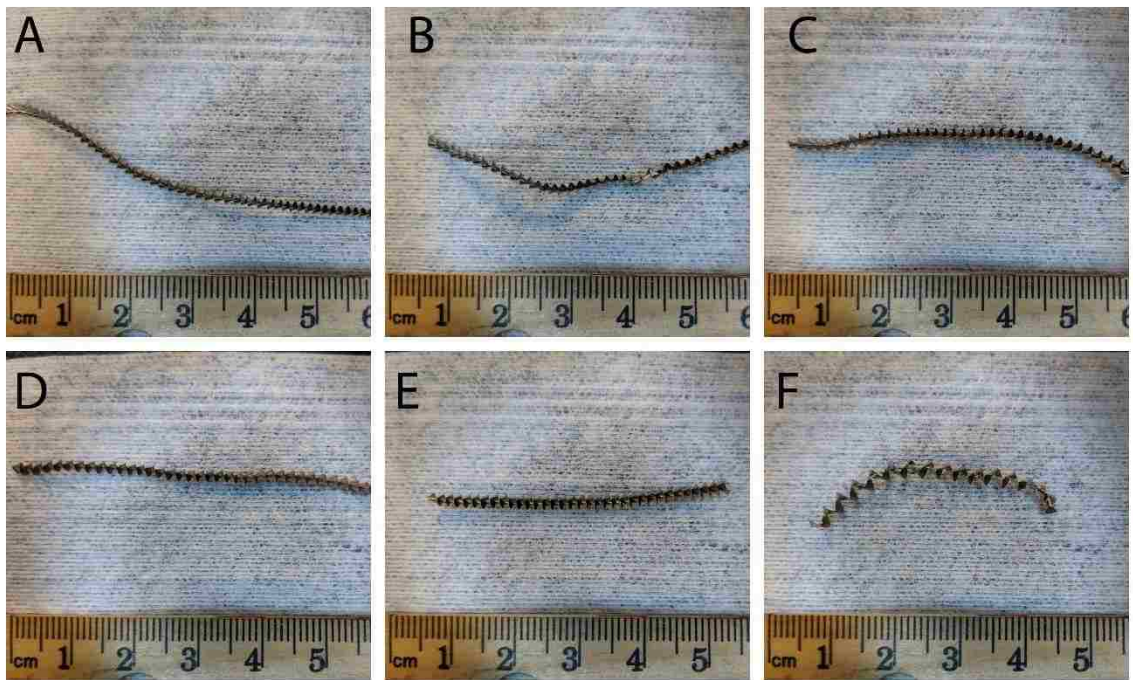
Figure 164. Chip morphology of PM titanium using an HSS drill bit for (A) 1 hole, (B) 5 holes, (C) 10 holes, (D), 15 holes, (E) 20 holes, (F) 60 holes.

Figure 165. Chip morphology of AM titanium using an HSS drill bit after drilling and failing at 8 holes.

4.5.2 Three Flute Drill Bit

The three flute drill bit was designed to improve chip ejection by adding an additional drilling flute to the drill bit. The chip morphology of the three flute drill bit when drilling grade 5 titanium (Ti-6Al-4V), PM titanium and AM titanium is shown in Figure 166 (A), Figure 166 (B), Figure 166 (C), respectively.

Figure 166. Chip morphology after drilling (A) grade 5 titanium (Ti-6Al-4V) for 60 holes, (B) PM titanium for 60 holes, and (C) AM titanium for 23 holes using a three flute drill bit.

4.5.3 Carbide Drill Bit

The carbide drill bit is coated with an AlTiN coating which helps improve wear resistance. The chip morphology of the carbide drill bit when drilling grade 5 titanium (Ti-

133

6Al-4V), PM titanium and AM titanium is shown in Figure 167 (A), Figure 167 (B), Figure

167 (C), respectively.
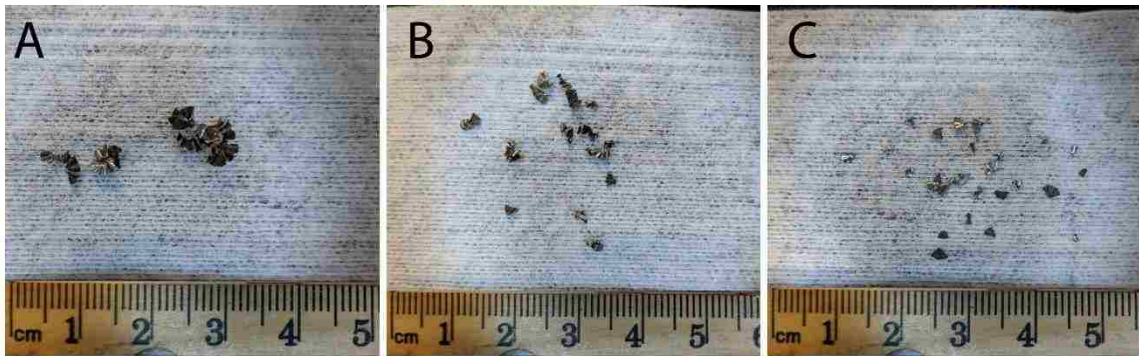
Figure 167. Chip morphology after drilling 60 holes for (A) grade 5 titanium (Ti-6Al-4V), (B) PM titanium, and (C) AM titanium using a carbide drill bit.

Chapter 5: Discussion

The following section discusses the results obtained during this study which is divided into three sections. The first section consists of the wear mechanisms of the drill bits, and comparison of flank wear. The second section discusses the torque analysis of the drill bit, correlating wear with torque and explaining the peaks in the torque data. The third section explains the chip morphology after prolonged drilling with various titanium alloys and the effect of various drill bits.

5.1 Wear

The purpose of studying the wear was to determine the drill bit with the least amount of damage and adhesion to the tool during machining the various manufactured titanium alloys. The image of the HSS drill bit before drilling is shown in Figure 30 to Figure 32. The wear measurements of the HSS drill bit after drilling grade 5 titanium (Ti-6Al-4V) is shown in Table 7. The wear from hole 1 to hole 60 gradually rises from 0.03 mm to 0.05 mm which overall shows a small amount of wear change of 0.01 mm. The EDS analysis confirmed the adhesion on the cutting edge shown in Figure 48 and Figure 49. Figure 48 shows the titanium peak is present, confirming the adhesion on the cutting edge. Additionally, using the EDS mapping feature, Figure 49 shows the titanium adhesion on the HSS drill bit. To calculate the amount of adhesion present on the cutting edge of an imaging software was used. The percentage of area covered in adhered material on the HSS drill bit after drilling grade 5 titanium (Ti-6Al-4V) was 27.57%. The wear measurements of the HSS drill bit for PM titanium are summarized in Table 8. The wear of the HSS drill bit was 0.05 mm and rose to 0.07 mm from hole 1 to hole 60, respectively. EDS was used to confirm the adhesion on the cutting edge shown in Figure 57 where spot 2 is the

adhesion. Referring to Figure 58 (B), titanium is present which confirmed the adhesion on the cutting edge. As shown in Figure 59, the titanium is adhered to the cutting edge. The amount of titanium adhesion on the cutting edge was 20.32%. The post image of drilling with the HSS drill bit and additive manufactured titanium is shown in Figure 60. The drill failed at 8 holes twice and a third attempted showed the drill failed at 3 holes. The wear after drilling just 8 holes is 0.37 mm. The EDS analysis is shown in Figure 67 and Figure 68 where the adhesion is shown at spot 1,2 and 3. The titanium adhesion is shown with the EDS mapping overlay in Figure 69. The percentage area of adhesion on the cutting edge was calculated as 13.72%. Comparing the HSS drill bits, the least amount of wear is present when drilling grade 5 titanium (Ti-6Al-4V) with 0.05 mm of wear, followed by PM titanium with 0.07 mm of wear, and lastly, AM titanium with 0.37 mm of wear. Based on

Table 9, AM titanium has the least percentage of adhesion on the cutting edge with 13.72%. The failure of the HSS drill bit may be due to the TiB particles in the AM titanium as circled in Figure 168. Since the HSS drill bit failed at 8 holes when drilling AM titanium, the least amount of adhesion when drilling with the HSS drill bit would go to the PM titanium at 20.32%. This showed that AM titanium was difficult to machine using the HSS drill bit, the PM titanium was the easiest to machine in terms of torque with the HSS drill bit. The HSS drill bit is not ideal for drilling titanium alloys due to the high amount of wear and adhesion.
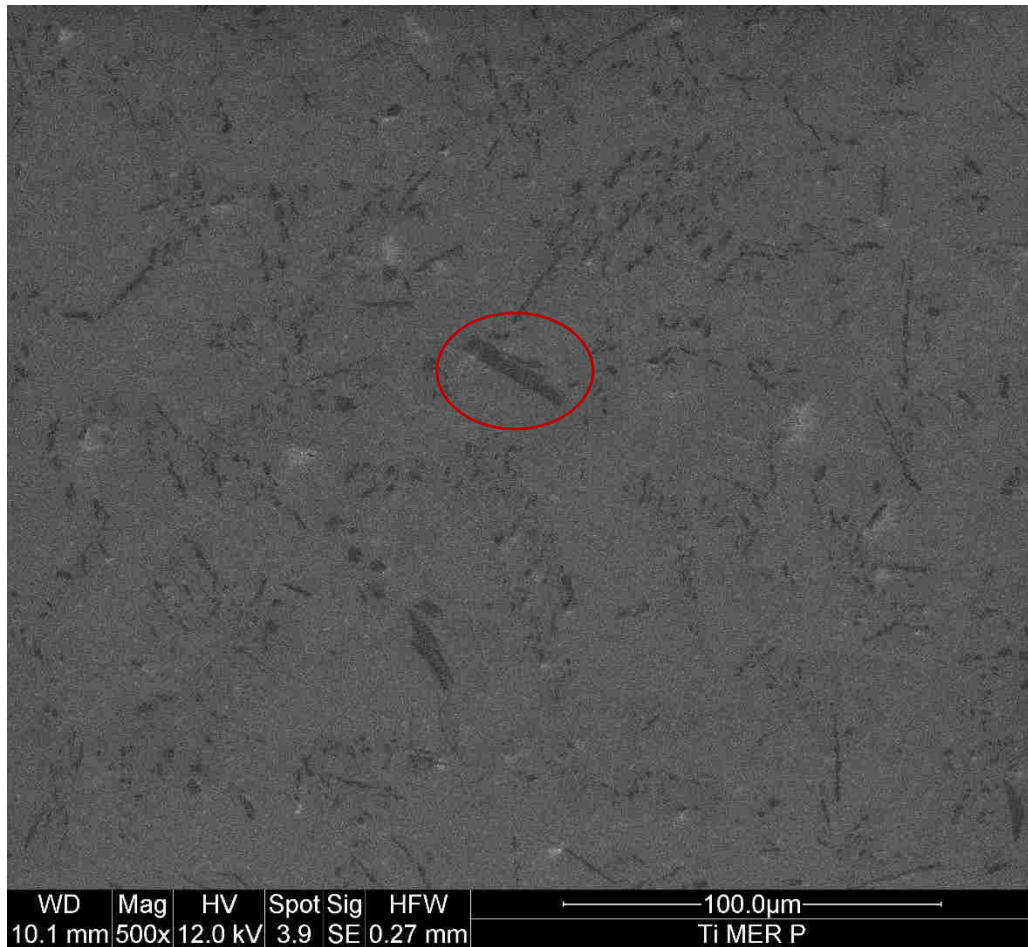
Figure 168. AM titanium cross section at 500x magnification displaying the TiB.

The three flute drill bit was designed for improved chip ejection by using tungsten carbide as the base material with an additional flute as shown in Figure 70. Drilling the grade 5 titanium (Ti-6Al-4V), the wear on the cutting edge of the three flute drill bit is shown in Figure 70. The amount of wear for the three flute drill bit when drilling grade 5 titanium (Ti-6Al-4V) is 0.17 mm. The EDS spot analysis is shown in Figure 77 and Figure 78 (A), where spot 1 is the adhesion on the cutting edge. Referring to Figure 79, the EDS overlay map is shown where titanium is the cyan and tungsten is the brown. The area covered with adhesion was calculated to a percentage area of 6.53%. Next, the PM titanium was drilled with the three flute drill, the result is shown in Figure 80. The amount of wear

137

calculated was 0.08 mm. The EDS analysis of the cutting edge is shown in Figure 87 and Figure 89 where spot 1 shows the base material of tungsten and spot 3 shows the adhesion on the cutting edge. Furthermore, the EDS map is shown in Figure 88 and used to calculate the percentage of area of adhesion. The calculated area of adhesion was 19.39%. The AM titanium is drilled next with the three flute drill bit shown in Figure 90 with a calculated wear of 0.21 mm of wear. Referring to Figure 97 and Figure 99, the adhesion is confirmed on spot 1 and spot 4. Spot 2 shows the base material of the drill bit of tungsten. An adhesion percentage area of 44.23% was calculated. Overall, drilling PM titanium shows the least amount of wear of 0.08 mm, and drilling grade 5 titanium (Ti-6Al-4V) provides the least amount of percentage area of adhesion with 6.53% as shown in

Table 9. This showed that AM titanium was difficult to machine using the three flute drill bit after failing at 24 holes. The difficulty in drilling the AM titanium may be due to the TiB particles as circled in Figure 168. The three flute drill bit displayed lower wear and adhesion than the HSS drill bit when drilling wrought titanium and PM titanium. In terms of torque the HSS drill bit showed a lower value than the three flute when drilling PM titanium but when drilling wrought titanium, the three flute drill bit resulted in a lower torque value. The three flute may yield a higher torque value since it is experimented at a lower recommended cutting speed by the manufacturer.

Lastly, the carbide drill bit is composed of tungsten carbide coated with an AlTiN coating to improve wear resistance. It is noted when examining the adhesion of the carbide

drill bit, there is no way to confirm the titanium adhesion since the coating is composed of titanium as well. Rather than examining the adhesion, a workaround is to examine the wear of coating on the cutting edge. The carbide drill bit top down view before drill is shown in Figure 100. After drilling grade 5 titanium (Ti-6Al-4V) for 60 holes, the wear was 0.08 mm. Referring to the EDS spot analysis in Figure 107 where the base material of tungsten is shown at spot 1. Spot 3 in Figure 108 (C) shows the coating of the drill bit composing of aluminum, titanium and nitrogen. The percentage area of wear is 2.45%. The wear on the carbide drill bit after drilling 60 holes in the PM titanium is shown in Figure 110 and the wear measured to be 0.07 mm. Referring to Figure 117 and Figure 119, the EDS analysis on the cutting edge shows that in spot 2 the coating was removed. Furthermore, the percentage area of worn coating was calculated which resulted in 14.01%. The drill bit in Figure 120 shows the wear after drilling 60 holes in the AM titanium. The wear of the carbide drill bit is 0.22 mm. Figure 127 and Figure 128 shows the EDS spot analysis of the carbide cutting edge after drilling AM titanium for 60 holes. Spot 1 shows the base material, confirming the external coating is removed on the cutting edge. Calculation of the percentage area of the coating that was worn is 20.19%. Overall, the least amount of wear measured after drilling various manufactured titanium for 60 holes is the PM titanium with 0.07 mm. It is noted that the grade 5 titanium (Ti-6Al-4V) had 0.08 mm of wear, similar to the PM titanium. Referring to the results in

Table 9, the least amount of percentage area was the grade 5 titanium (Ti-6Al-4V) with 2.45% when drilling with the carbide drill bit. The carbide drill bit can be used to drill all the tested titanium alloys due to low wear and adhesion. It was the best tool for AM titanium since it was the only drill to finish 60 holes.

Table 9. ImageJ Percent Adhesion & Wear for each Material with Various Drill Bits.

	Ti-6Al-4V	PM Titanium	AM Titanium
HSS	27.57%	20.32%	13.72%
Three Flute	6.53%	19.39%	44.23%
Carbide	2.45%	14.01%	20.19%

5.2 Torque

Torque data displays the results of the experiments in terms of how well each hole was drilled. The average torque for drilling into the grade 5 titanium (Ti-6Al-4V) with the HSS drill gradually increased from 0.71 Nm to 1.09 Nm with hole 1 to hole 60. With the three flute drill bit, the initial average torque is 0.59 Nm and the final average torque is 0.64 Nm. Additionally, the torque for the carbide drill bit rises from 0.50 Nm to 0.52 Nm. The torque data for drilling grade 5 titanium (Ti-6Al-4V) with various drill bits is shown in

Table 10. Comparing the 60 holes of each of the drill bit, the carbide drill bit shows the lowest amount overall average torque at 0.51 Nm, followed by the three flute drill bit at 0.61 Nm and the HSS drill bit at 1.07 Nm. The trend of an increase in number of holes correlates to the increase of torque. As the amount of drilled holes increased the wear also increased which showed an increase in wear on the cutting edge. Referring to Figure 135,

hole 2 shows a general flat peak which signifies a hole being formed without difficulty. Referring to Figure 138, holes 4 shows the peak slowly increases upwards then drops down immediately which shows the difficulty in chip ejection. Referring to Figure 136, hole 2 shows an initial spike is shown then the peak slopes downwards, this shows material transfer to the drill bit. Difficulty in material ejection begins on the 4th hole For the HSS drill bit, the three flute drill bit showed difficulty ejecting the material from hole 1 but as it progressed the difficulty fluctuated and the carbide drill bit showed little to no difficulty in chip ejection. So, in summary, the carbide had the lowest torque making it and the three flute drill bit preferable for drilling grade 5 titanium (Ti-6Al-4V).

Table 10. Torque Data Summary Table for Grade 5 Titanium (Ti-6Al-4V) with Various Drill Bits.

	Initial Average Torque (Nm)	Final Average Torque (Nm)	Average Torque (Nm)
HSS - 60 Holes	1.05	1.09	1.07
HSS - 20 Holes	1.01	1.08	1.05
HSS - 15 Holes	1.04	1.05	1.05
HSS - 10 Holes	0.97	1.04	1.01
HSS - 5 Holes	0.84	0.88	0.85
HSS - 1 Hole	0.70	0.70	0.70
Three Flute - 60 Holes	0.59	0.63	0.61
Carbide - 60 Holes	0.50	0.52	0.51

Referring to the PM titanium, they share the same trends as the other torque data. Referring to Figure 144, hole 1 shows a flat peak which shows a hole being formed without difficulty in chip ejection. Referring to Figure 152, hole 8 shows an upwards slope to a peak and an immediate drop which signifies difficulty in chip ejection. Material adhesion is shown in the PM experiments shown in Figure 156 hole 1 and hole 6. The torque data for drilling PM titanium with various drill bits is shown in

Table 11. Comparing the 60 holes of each of the drill bit, the carbide drill bit shows the least amount of torque at 0.42 Nm, followed by the HSS drill bit at 0.46 Nm and the three flute drill bit at 0.56 Nm. The chip ejection and adhesion observed for the HSS drill bit showed some difficulty in chip ejection for the first 10 holes but as it progressed the difficulty was reduced. Additionally, the three flute drill bit showed no difficulty in chip ejection at the beginning but towards the end, the difficulty in chip ejection rose. Overall, the carbide drill bit displayed the best performance for drilling PM titanium.

Table 11. Torque Data Summary Table for PM Titanium with Various Drill Bits.

	Initial Torque (Nm)	End Torque (Nm)	Average Torque (Nm)
HSS - 60 Holes	0.44	0.47	0.46
HSS - 20 Holes	0.37	0.41	0.39
HSS - 15 Holes	0.38	0.38	0.38
HSS - 10 Holes	0.36	0.39	0.37
HSS - 5 Holes	0.35	0.36	0.36
HSS - 1 Hole	0.32	0.32	0.32
Three Flute - 60 Holes	0.56	0.57	0.56
Carbide - 60 Holes	0.42	0.42	0.42

The AM titanium was more difficult to machine as shown by the torque data shown in Table 12 and by the failure of the tests. Comparing the drill bits, the carbide drill bit shows the least amount of torque at 1.08 Nm, followed by the three flute drill bit at 1.22 Nm and the HSS drill bit at 1.30 Nm. The HSS drill bit drilled at most 8 holes before failing. The three tests consisted of drilling 8 holes, 8 holes and 3 holes. The trends are present in drilling AM titanium where material adherence is shown in Figure 160 in hole 3, and difficulty in chip ejection is shown in Figure 161 hole 5.

Table 12. Torque Data Summary Table for AM Titanium with Various Drill Bits.

	Initial Torque (Nm)	End Torque (Nm)	Average Torque (Nm)
HSS - 8 Holes	1.14	1.47	1.30
Three Flute - 24 Holes	1.01	1.43	1.22
Carbide - 60 Holes	0.77	1.39	1.08

Overall, the carbide drill bit remains dominant being the best drill bit showing the least amount of torque when drilling the various titanium alloys. The least amount of wear is shown when drilling the PM titanium with the carbide drill bit. To make the drill bits comparable, the first hole of each drill bit was observed. The HSS resulted in a torque value of 0.99 Nm, the three flute resulted in 0.88 Nm and the carbide resulted in 0.57 Nm. In summary, despite the torque values being unable to compare, the carbide drill bit was ideal

for drilling AM titanium since it was the only to drill 60 holes. The HSS drill bit was not ideal since it only drill 8 holes with a high torque.

5.3 Chip Morphology

Chip morphology is a topic of interest since it plays a predominant role in determining the machinability and tool wear during machining. Segmented chips are the preferred types of chip since they are easily ejected from the hole and pushed away with flood cooling. The typical chips found in drilling titanium alloys are spiral chips with an initial state, a steady state, and a transition state to string chips. The chips change states as the number of holes increase. Additionally, after a certain depth the spiral chips are ejected and segmented chips are created. This is due to the friction force between the drill flute and the hole generated by drilling. Referring to Figure 163 and Figure 164, the chip length is variant, but the distance between the spirals or the pitch is increased over the number of holes drilled. From hole 1, the spiral formation is tightly wound and referring to hole 60, the spiral formation is becoming loose. If the drilling continued further with more holes, it is likely that the spirals would become more unwound and turn into string chips as noted by Ke [34]. Referring to the chip morphology in Figure 166, the chips show an odd formation, this is due to the extra cutting edge. With the extra cutting edge, the metal removal rate is increased but with an inadequate flow of chips, the risk of the chips jamming is imminent. The chip jamming may affect the performance of the three flute drill bit. A solution to this may be to increase the cutting speed. The cutting speed used was too slow to utilize the third cutting edge, therefore the chips are jammed together as shown in Figure 166 (A), (B). The performance of the carbide drill bill could be attributed in part to

144

the production of segmented chips which are easily ejected from the cutting zone shown in

Figure 167.

Chapter 6: Conclusions

The final chapter is a concise restatement of the significant conclusions resulting from this research, as well as recommendations for future work which could further compare the machinability of various titanium alloys.

6.1 Conclusions

- Drilling the powder metallurgy titanium showed the lowest wear and torque when drilling with all three types of drill bits. The high speed steel drill bit had 0.072 mm of wear and an average torque of 0.459Nm. The three flute drill bit had 0.075 mm of wear and an average torque of 0.562 Nm. The carbide drill bit had 0.074 mm of wear and an average torque of 0.421 Nm.

- Additive manufactured titanium showed the highest torque and wear with the high speed steel drill bit with a torque of 1.300 Nm and wear of 0.372 mm and the drill bit failed at 8 holes, while, the carbide drill bit had the lowest torque (1.078 Nm) and wear (0.216 mm).

- The carbide drill bit had the least amount of adhesion on the cutting edge when drilling titanium alloy Ti-6Al-4V (2.45% of surface area) and powder metallurgy titanium (14.01%). When drilling additive manufactured titanium the high speed steel drill bit had the least percent adhesion at 13.72%. Since the high speed steel drill bit failed at 8 holes and the carbide drill bit completed the 60 holes, it would be considered to have less percent adhesion with 20.19%.

- The carbide drill bit had the lowest wear when drilling all three various titanium alloys compared to the HSS drill bit and the three flute drill bit.

146

- As the number of holes increase the chips shape change from spiral chips to string chips

6.2 Recommendations

To further compare the machinability of various titanium alloys, the investigation of fluctuating feed rate and cutting speed should be conducted. Additionally, more tests should be conducted with the three flute and carbide drill bit to confirm the reliability of the drill bit. By varying the feed rate, the length of the chip morphology can be studied more in depth. Additionally, the feed rate may affect the rate of material ejection. By varying the cutting speed, a study of change in torque can be observed. An increase of cutting speed may improve the performance of the three flute drill bit. Furthermore, the length of the chip morphology can be further studied based on the different ranges on the feed rate and cutting speeds.

References

[1] W. D. Brewer, R. K. Bird, and T. A. Wallace, "Titanium alloys and processing for high speed aircraft," *Mater. Sci. Eng. A*, vol. 243, no. 1–2, pp. 299–304, 1998.

[2] R. Li and A. J. Shih, "Tool Temperature in Titanium Drilling," *J. Manuf. Sci. Eng.*, vol. 129, no. 4, p. 740, 2007.

[3] K. A. Al-Ghamdi and A. Iqbal, "A sustainability comparison between conventional and high-speed machining," *J. Clean. Prod.*, vol. 108, pp. 192–206, 2015.

[4] M. Qian and F. H. Froes, *Titanium Powder Metallurgy: Science, Technology and Applications*, 1st ed. 2015.

[5] Y. Liu, L. F. Chen, H. P. Tang, C. T. Liu, B. Liu, and B. Y. Huang, "Design of powder metallurgy titanium alloys and composites," *Mater. Sci. Eng. A*, vol. 418, no. 1–2, pp. 25–35, 2006.

[6] W. E. Frazier, "Metal additive manufacturing: A review," *J. Mater. Eng. Perform.*, vol. 23, no. 6, pp. 1917–1928, 2014.

[7] J. W. Sutherland, "Traditional Machining," 2004. [Online]. Available: http://www.mfg.mtu.edu/cyberman/machining.html.

[8] P. J. Arrazola, A. Garay, L. M. Iriarte, M. Armendia, S. Marya, and F. Le Maître, "Machinability of titanium alloys (Ti6Al4V and Ti555.3)," *J. Mater. Process. Technol.*, vol. 209, no. 5, pp. 2223–2230, 2009.

[9] A. Jawaid, S. Sharif, and S. Koksal, "Evaluation of wear mechanisms of coated carbide tools when face milling titanium alloy," *J. Mater. Process. Technol.*, vol. 99, no. 1, pp. 266–274, 2000.

[10] S. A. Abbasi and F. Pingfa, "Evaluating the effectiveness of various coating layers

applied on k-grade cemented carbide cutting tools on machinability of titanium alloy Ti-6Al-4V in high speed end milling," *Proc. 2015 12th Int. Bhurban Conf. Appl. Sci. Technol. IBCAST 2015*, pp. 14–19, 2015.

[11] D. Kim and V. K. Hall, "Machinability of titanium / graphite hybrid composites in drilling," *Transactions of the North American Manufacturing Research Institute of SME.*, vol. 33, pp. 445-452, 2005.

[12] P. F. Zhang, N. J. Churi, Z. J. Pei, and C. Treadwell, "Mechanical drilling processes for titanium alloys: A literature review," *Mach. Sci. Technol.*, vol. 12, no. 4, pp. 417–444, 2008.

[13] W. Zhao, N. He, and L. Li, "High Speed Milling of Ti6Al4V Alloy with Minimal Quantity Lubrication," *Key Eng. Mater.*, vol. 329, pp. 663–668, 2007.

[14] Z. Zhu, S. Sui, J. Sun, J. Li, and Y. Li, "Investigation on performance characteristics in drilling of Ti6Al4V alloy," pp. 1–17, 2017.

[15] M. Czampa, S. Markos, and T. Szalay, "Improvement of drilling possibilities for machining powder metallurgy materials," *Procedia CIRP*, vol. 7, pp. 288–293, 2013.

[16] A. Bordin, S. Bruschi, A. Ghiotti, and P. F. Bariani, "Analysis of tool wear in cryogenic machining of additive manufactured Ti6Al4V alloy," *Wear*, vol. 328–329, pp. 89–99, 2015.

[17] L. S. Ahmed and M. P. Kumar, "Cryogenic Drilling of Ti-6Al-4V Alloy Under Liquid Nitrogen Cooling," *Mater. Manuf. Process.*, vol. 31, no. 7, pp. 951–959, 2016.

[18] L. S. Ahmed, N. Govindaraju, and M. P. Kumar, "Experimental Investigations on

Cryogenic Cooling in the Drilling of Aluminum Alloy," *Mater. Manuf. Process.*, vol. 31, no. 5, pp. 603–607, 2016.

[19] S. Hong and Y. Ding, "Cooling Approach and Cutting Temperature in Cryogenic Machining of Ti-6 Al-4V," *Int. J. Mach. tool Manuf.*, vol. 41, pp. 1417–1437, 2001.

[20] E. Bagci and B. Ozcelik, "Effects of different cooling conditions on twist drill temperature," *Int. J. Adv. Manuf. Technol.*, vol. 34, no. 9–10, pp. 867–877, 2007.

[21] E. A. Rahim and S. Sharif, "Evaluation of tool wear mechanism of TiAlN coated tools when drilling Ti-6Al-4V," *Int. J. Manuf. Technol. Manag.*, vol. 17, no. 4, p. 327, 2009.

[22] S. Sharif, E. A. Rahim, S. Ahmad, A. Mohruni, and I. Syed, "Machinability Investigation when Drilling Titanium Alloys," *Proceedings of International Conference on Leading Edge Manufacturing in 21st Century.*, vol. 2005.2, pp. 553-557, 2005.

[23] S. Sharif and E. A. Rahim, "Performance of coated- and uncoated-carbide tools when drilling titanium alloy-Ti-6Al4V," *J. Mater. Process. Technol.*, vol. 185, no. 1–3, pp. 72–76, 2007.

[24] S. Dolinšek, B. Šuštaršič, and J. Kopač, "Wear mechanisms of cutting tools in high-speed cutting processes," *Wear*, vol. 250–251, no. 1–12, pp. 349–356, 2001.

[25] J. Samuel, J. Rafiee, P. Dhiman, Z. Z. Yu, and N. Koratkar, "Graphene colloidal suspensions as high performance semi-synthetic metal-working fluids," *J. Phys. Chem. C*, vol. 115, no. 8, pp. 3410–3415, 2011.

[26] P. J. Smith, B. Chu, E. Singh, P. Chow, J. Samuel, and N. Koratkar, "Graphene oxide colloidal suspensions mitigate carbon diffusion during diamond turning of

steel," *J. Manuf. Process.*, vol. 17, pp. 41–47, 2015.

[27] H. D. Huang, J. P. Tu, L. P. Gan, and C. Z. Li, "An investigation on tribological properties of graphite nanosheets as oil additive," *Wear*, vol. 261, no. 2, pp. 140–144, 2006.

[28] C. G. Lee, Y. J. Hwang, Y. M. Choi, J. K. Lee, C. Choi, and J. M. Oh, "A study on the tribological characteristics of graphite nano lubricants," *Int. J. Precis. Eng. Manuf.*, vol. 10, no. 1, pp. 85–90, 2009.

[29] E. A. Rahim and H. Sasahara, "Investigation of tool wear and surface integrity on MQL machining of Ti-6AL-4V using biodegradable oil," *Proc. Inst. Mech. Eng. Part B J. Eng. Manuf.*, vol. 225, no. 9, pp. 1505–1511, 2011.

[30] R. P. Zeilmann and W. L. Weingaertner, "Analysis of temperature during drilling of Ti6Al4V with minimal quantity of lubricant," *J. Mater. Process. Technol.*, vol. 179, no. 1–3, pp. 124–127, 2006.

[31] S. Yi, G. Li, S. Ding, and J. Mo, "Performance and mechanisms of graphene oxide suspended cutting fluid in the drilling of titanium alloy Ti-6Al-4V," *J. Manuf. Process.*, vol. 29, pp. 182–193, 2017.

[32] Z. Zhu, S. Sui, J. Sun, J. Li, and Y. Li, "Investigation on performance characteristics in drilling of Ti6Al4V alloy," *Int. J. Adv. Manuf. Technol.*, pp. 651–660, 2017.

[33] D. B. Boudreau, "Characterization of Powder Metallurgy Lightweight Alloys," 2017.

[34] F. Ke, J. Ni, and D. A. Stephenson, "Continuous chip formation in drilling," *Int. J. Mach. Tools Manuf.*, vol. 45, no. 15, pp. 1652–1658, 2005.

Vita Auctoris

NAME: Tanny Tran

PLACE OF BIRTH: Mississauga, ON

YEAR OF BIRTH: 1994

EDUCATION: St. Peter's Catholic Secondary School, Barrie, ON,

2008 – 2012

University of Windsor, Windsor, ON,

2012 – 2016 B.A.Sc.

University of Windsor, Windsor, ON,

2016 – 2018 M.A.Sc.